UNIVERSITÀ DEGLI STUDI DI TRIESTE

UNIVERSITÀ DEGLI STUDI DI TRIESTE

XXXIV CICLO DEL DOTTORATO DI RICERCA IN

AMBIENTE E VITA

ALGAL TOXINS IN MEDITERRANEAN SEA: ECOTOXICOLOGICAL AND POTENTIAL EFFECTS ON HUMAN HEALTH

Settore scientifico-disciplinare: BIO-14

DOTTORANDA
FEDERICA CAVION

COORDINATORE
PROF. GIORGIO ALBERTI

SUPERVISORE DI TESI
PROF.SSA AURELIA TUBARO

CO-SUPERVISORE DI TESI
DOTT. MARCO PELIN

CO-SUPERVISORE DI TESI
PROF.SSA FRANCESCA MALFATTI

ANNO ACCADEMICO 2020/2021

RIASSUNTO

Il fenomeno noto con il termine "Harmful Algal Bloom" (HAB) è in espansione in termini di incidenza, frequenza e distribuzione geografica, con conseguenze negative a livello di ecosistema, oltre che sulla salute umana e a livello socioeconomico. Per questo motivo è importante analizzare l'impatto ecotossicologico e gli effetti tossici sull'uomo di queste tossine i cui produttori si stanno diffondendo in diverse aree geografiche. Questa tesi si concentra su due principali tossine frequentemente rilevate negli ultimi decenni anche nel Mar Mediterraneo: la palitossina (PLTX) e l'acido okadaico (OA) insieme ai suoi analoghi. La PLTX è stata associata a fioriture algali di dinoflagellati del genere *Ostreopsis*, ma è stata ritrovata anche in altri organismi marini come i coralli molli del genere *Palythoa* e i cianobatteri marini del genere *Trichodesmium*, mentre l'OA è stato associato principalmente a dinoflagellati del genere *Dinophysis*.

Per indagare il loro potenziale impatto ecotossicologico, nella prima parte della tesi è stato analizzato l'effetto tossico della PLTX, dell'OA e di due analoghi, la dinofisistossina (DTX)-1 e -2, sull'organismo *Artemia franciscana*. Questo micro-crostaceo è considerato un organismo modello per studi di ecotossicologia soprattutto a livello di ecosistema marino, essendo rappresentativo dello zooplancton, alla base della rete trofica. Per tale motivo, gli effetti negativi sulla popolazione di *Artemia* spp. potrebbero compromettere organismi a livelli trofici più elevati e più in generale avere un effetto negativo a livello di ecosistema. Gli effetti tossici indotti da queste tossine sono stati inizialmente analizzati in termini di % di schiusa delle cisti di *A. franciscana* e mortalità degli organismi a due stadi di sviluppo: il primo stadio larvale (nauplii Instar I) e lo stadio adulto. Le quattro tossine, ovvero PLTX, OA, DTX1 e DTX2, testate in un range di concentrazioni che includevano quelle ambientali rilevate o stimate, hanno indotto una maggiore mortalità in *Artemia* allo stadio adulto rispetto ai nauplii. Nello specifico, la PLTX ($1.0x10^{-10}$-$1.0x10^{-8}$ M) è risultata il composto più tossico, inducendo una mortalità significativa negli adulti a partire da 12 h di esposizione con una concentrazione che causa il 50% di letalità negli organismi trattati (LC_{50}) pari a $2.3x10^{-9}$ M (C.I. 95%=1.2–$4.7x10^{-9}$ M). Al contrario, per OA e DTXs ($1.0x10^{-10}$-$1.0x10^{-7}$ M) la tossicità è risultata minore, registrando mortalità degli organismi adulti solo alla massima concentrazione testata ($1.0x10^{-7}$ M), a partire da 24 h per DTX1, 48 h per OA e 72 h per DTX2. Nel complesso, la tossina DSP più tossica è la DTX1, seguita da OA e DTX2 con LC_{50} a 72 h pari a $17.3x10^{-9}$ M (C.I. 95%= 1.7–$171.1x10^{-9}$ M), $48.5x10^{-9}$ M (C.I. 95%=25.9-$91.0x10^{-9}$ M) e $49.7x10^{-9}$ M (C.I. 95%= 35.9–$68.6x10^{-9}$ M), rispettivamente. Il possibile meccanismo di tossicità indotto su *A. franciscana* è stato quindi analizzato in termini di induzione dello stress ossidativo, valutando gli effetti sulla produzione di specie reattive dell'ossigeno (ROS) e sull'attività dei tre principali enzimi antiossidanti (glutatione S-transferasi, superossido dismutasi e catalasi) nello stadio di sviluppo più

sensibile (adulti). Le quattro tossine hanno indotto effetti diversi in *A. franciscana*: un aumento della produzione di ROS è stato registrato solo per PLTX e DTX2. Allo stesso modo, le quattro tossine hanno indotto diverse variazioni nell'attività degli enzimi antiossidanti, suggerendo diversi meccanismi di tossicità. In generale, questi risultati indicano un potenziale effetto negativo di queste tossine sulla popolazione di *Artemia* con potenziali conseguenze a livello di ecosistema. Tuttavia, è importante sottolineare come, gli effetti tossici su *Artemia* di tutte queste tossine sono stati indotti a concentrazioni superiori a quelle finora rilevate a livello ambientale ($<1.0x10^{-8}$ M, $\leq1.0x10^{-9}$ M, $\leq1.0x10^{-11}$ M, $\leq1.0x10^{-12}$ M, rispettivamente per la PLTX, l'OA, la DTX1 e la DTX2). Ciò nonostante, va considerato che l'incidenza e la frequenza delle HAB, come anche la loro espansione geografica, sono in costante aumento ed in futuro potrebbero portare ad un aumentato rilascio delle relative tossine, le cui concentrazioni ambientali potrebbero superare quelle attuali. Nella seconda parte della tesi, sono stati analizzati i potenziali effetti tossici della PLTX nell'uomo, soffermandosi sul suo potenziale embriotossico, aspetto poco considerato in letteratura. A tal fine, le cellule staminali pluripotenti indotte umane (iPSC) sono state utilizzate come modello *in vitro* delle prime fasi dello sviluppo embrionale. La PLTX ha indotto un effetto citotossico inferiore sulle iPSC rispetto a una linea di cellule somatiche non staminali (cheratinociti HaCaT): le concentrazioni che inducevano il 50% dell'effetto (EC_{50}) dopo 4 h di esposizione sono risultate pari a $1.3x10^{-8}$ M (C.I. 95%= 0.5-3.8x10^{-8} M) e $8.3x10^{-11}$ M (C.I. 95%= 0.4–1.9x10^{-10} M), rispettivamente. La diversa sensibilità sembra essere correlata con una diversa affinità di legame della PLTX per queste due linee cellulari. Questo fenomeno sembra essere dovuto a diversi *pattern* di espressione genica delle isoforme delle subunità α e β della Na^+/K^+ ATPasi, il bersaglio molecolare della tossina. Anche se le iPSC sembrano essere meno sensibili agli effetti citotossici della tossina rispetto a una linea cellulare somatica, la citotossicità della PLTX è risultata significativa, concentrazione- e tempo- dipendente e irreversibile, come dimostrato dall'analisi di *recovery*. Inoltre, l'analisi dell'espressione genica di 13 *marker* (cinque *marker* delle cellule staminali: *OCT4*, *C-MYC*, *KLF4*, *SOX2*, *NANOG*; tre *marker* dell'endoderma: *SOX17*, *AFP* e *FOXA2*; tre *marker* del mesoderma: *ACTA2*, *BRACHYURY*, *CXCR4*; due *marker* di ectoderma: *SOX1* e *PAX6*) e l'espressione proteica dei *marker* più rappresentativi di staminalità (OCT4), endoderma (SOX17), mesoderma (BRACHYURY) ed ectoderma (PAX6), suggeriscono che la tossina non sembra influenzare la staminalità della linea di iPSC. Tuttavia, analizzando l'impatto della PLTX sul differenziamento delle iPSC nei tre foglietti embrionali (cioè, esponendo le cellule a $1.0x10^{-11}$ M di PLTX durante il differenziamento delle iPSC in endoderma, mesoderma ed ectoderma), la tossina ha indotto una perturbazione del differenziamento delle iPSC verso l'endoderma come dimostrato dall'espressione genica e proteica di *marker* di staminalità e differenziamento. Inoltre, gli effetti citotossici della PLTX su iPSC differenziate a endoderma, mesoderma o

ectoderma dopo 24 h di esposizione hanno dimostrato un maggiore effetto proprio sul foglietto embrionale endoderma (EC_{50} = 5.1x10^{-8} M; C.I. 95%= 0.2-1.1x10^{-7} M) oltre che sull'ectoderma (EC_{50}= 2.2x10^{-8} M; C.I. 95%= 0.7-7.4x10^{-8} M); al contrario, il mesoderma è risultato quasi insensibile agli effetti della tossina. Questi effetti sono stati osservati a concentrazioni di tossina inferiori a quelle rilasciate dagli organismi produttori, a cui l'uomo potrebbe essere esposto attraverso diverse vie. Tuttavia, la mancanza di dati di tossicocinetica sulla PLTX e di esposizione umana non permette di stimare l'entità di una potenziale esposizione embrionale. Complessivamente, però, questi risultati hanno evidenziato un potenziale effetto embriotossico della PLTX durante le prime fasi dello sviluppo embrionale, sul corretto differenziamento dell'endoderma.

ABSTRACT

Harmful Algal Bloom (HAB) is an expanding phenomenon in terms of incidence, frequency and geographical distribution, with negative consequences at the ecosystem level, in addition to human health and at the socio-economic level. For this reason, it is important to analyse the ecotoxicological impact and the toxic effects on humans associated with these toxins, whose producers are expanding in different geographical areas. This thesis focuses on two main toxins frequently identified in last decades also in the Mediterranean Sea: palytoxin (PLTX) and okadaic acid (OA), together with its analogues. PLTX has been associated with algal blooms of *Ostreopsis* dinoflagellates, even though it has been found also in other marine organisms such as *Palythoa* soft corals and *Trichodesmium* marine cyanobacteria, while OA has been associated mainly with *Dinophysis* dinoflagellates.

To investigate their potential ecotoxicological impact, the toxic effect of PLTX, OA and two analogues, dinophysistoxin (DTX)-1 and -2, on the organism *Artemia franciscana* was analysed in the first part of the thesis. This micro-crustacean is considered a model organism for ecotoxicology studies especially at the marine ecosystem level, representing part of the marine zooplankton, at the base of the marine food web. In this scenario, negative effects on *Artemia* spp. population could compromise organisms at higher trophic levels and more generally at the ecosystem level. The toxic effects were initially analysed in terms of % of hatching of *A. franciscana* cysts and mortality at two developmental stages: the first larval stage (nauplii Instar I) and the adult one. The four toxins, namely PLTX, OA, DTX1 and DTX2, tested in a range of concentrations that included the detected or estimated environmental ones, induced a higher mortality in the adult stage of *Artemia* with respect to nauplii. Specifically, PLTX ($1.0x10^{-10}$-$1.0x10^{-8}$ M) turned out to be the most toxic compound, inducing a significant mortality in adults already starting from 12 h of exposure, with a concentration inducing 50% of lethality in the treated organisms (LC_{50}) of $2.3x10^{-9}$ M (C.I. 95%=1.2–$4.7x10^{-9}$ M). On the contrary, OA and DTXs ($1.0x10^{-10}$-$1.0x10^{-7}$ M) were less toxic, recording mortality in adult organisms only at the highest concentration tested ($1.0x10^{-7}$ M) starting from 24 h for DTX1, 48 h for OA, and 72 h for DTX2. Overall, the most toxic DSP-toxin was DTX1, followed by OA and DTX2, with LC_{50} at 72 h of exposure of $17.3x10^{-9}$ M (C.I. 95%= 1.7–$171.1x10^{-9}$ M), $48.5x10^{-9}$ M (C.I. 95%= 25.9-$91.0x10^{-9}$ M) and $49.7x10^{-9}$ M (C.I. 95%= 35.9–$68.6x10^{-9}$ M), respectively. The possible toxicity mechanism induced on *A. franciscana* was then analysed in terms of oxidative stress induction evaluating the effects on reactive oxygen species (ROS) production and activity of three main antioxidant enzymes (glutathione S-transferase, superoxide dismutase and catalase) in the most sensitive developmental stage (adult). The four toxins induced different effects in *A. franciscana*: an increase of ROS production

was recorded only for PLTX and DTX2. Similarly, the four toxins induced different patterns of variations of antioxidant enzymes activity, suggesting different toxicity mechanisms. In general, these results indicate a potential negative effect of these toxins on *Artemia* population with potential consequences at the ecosystem level. However, it has to be underlined that the toxic effects of each toxin on *Artemia* were recorded at concentrations higher than those detected at the environmental level, so far ($<1.0x10^{-8}$ M, $\leq 1.0x10^{-9}$ M, $\leq 1.0x10^{-11}$ M, $\leq 1.0x10^{-12}$ M, for PLTX, OA, DTX1 and DTX2, respectively). Nevertheless, the constant increase of the incidence and frequency of HABs together with the geographical expansion of harmful algae, could lead to an increased release of their toxins, which could lead to their environmental concentrations higher than current ones.

In the second part of the thesis, the toxic effects of PLTX in humans were assessed focusing on its potential embryotoxicity, an aspect scarcely considered in literature. To this aim, human induced pluripotent stem cells (iPSC) were used as an *in vitro* model of the early stages of the embryonic development. PLTX induced a lower cytotoxic effect on iPSC as compared to a somatic non-stem cell line (HaCaT keratinocytes): the concentrations giving the 50% of the effect (EC_{50}) after 4 h exposure were equal to $1.3x10^{-8}$ M (C.I. 95%= 0.5-3.8x10^{-8} M) and $8.3x10^{-11}$ M (C.I. 95%= 0.4-1.9x10^{-10} M), respectively. The different sensitivity appeared to be correlated with a different binding affinity of PLTX for these two cell lines. This phenomenon appeared to be due to different gene expression patterns of the isoforms of α and β subunits of Na^+/K^+ ATPase, the molecular target of the toxin. Even though iPSC seems to be less sensitive to the toxin effects in comparison to a somatic cell line, PLTX cytotoxicity was still significant, concentration- and time-dependent up to 96 h exposure and irreversible, as demonstrated by recovery analysis. In addition, the analysis of gene expression of 13 markers (five markers of stem cells: *OCT4*, *C-MYC*, *KLF4*, *SOX2*, *NANOG*; three markers of endoderm: *SOX17*, *AFP* and *FOXA2*; three markers of the mesoderm: *ACTA2*, *BRACHYURY*, *CXCR4;* two markers of ectoderm: *SOX1* and *PAX6*) and the protein expression of the most representative markers of stemness (OCT4), endoderm (SOX17), mesoderm (BRACHYURY) and ectoderm (PAX6), suggest that the toxin does not affect iPSC stemness. However, analysing the impact of PLTX on iPSC differentiation into the three germ layers (i.e., exposing the cells to $1.0x10^{-11}$ M PLTX during iPSC differentiation into endoderm, mesoderm and ectoderm), the toxin induced a perturbation of iPSC differentiation towards endoderm as assessed by gene and protein expression of stemness and differentiation markers. Intriguingly, cytotoxic effect of PLTX on differentiated iPSC to endoderm, mesoderm or ectoderm cells after 24 h of exposure, demonstrated a higher effect right in the endoderm (EC_{50} =5.1x10^{-8} M; C.I. 95%= 0.2-1.1x10^{-7} M) other than in the ectoderm (EC_{50} =2.2x10^{-8} M; C.I. 95%= 0.7-7.4x10^{-8} M), while mesoderm was almost insensitive to the toxin effects. These effects were recorded at toxin concentrations lower than those released by the

producing organisms, to which humans could be exposed through various pathways. However, the lack of toxicokinetic data on PLTX and of human exposure does not allow to estimate the entity of the potential embryo exposure. Notwithstanding, these results highlighted a potential embryotoxic effect of PLTX during the early phases of embryo development, in particular affecting the correct differentiation process towards endoderm.

Index

Introduction

1 Harmful Algal Bloom (HABs) 2

1.1 The HABs phenomenon and its occurrence 2
1.2 Toxigenic algae and biotoxins 5

2 Palytoxin (PLTX) 7

2.1 Producing organisms 7
2.2 Chemical structure of PLTXs 8
2.3 Mechanism of action 10
2.4 Effects of PLTX on humans 12
2.5 Effects of PLTX on aquatic organisms 14

3 Okadaic acid (OA) and its analogous, dynophysistoxins (DTXs) 16

3.1 Producing organisms 16
3.2 Chemical structure of OA and DTXs 16
3.3 Mechanism of action 17
3.4 Effects of OA and DTXs on humans 18
3.5 Effects of OA and DTXs on aquatic organisms 20

Section A

Introduction 23

1 *Artemia* spp. 23
1.1 Life cycle 24
1.2 *Artemia* spp. morphology 25
1.3 Ecology and distribution 26
1.4 *Artemia* spp. as a model organism 27

Aim 28

Materials and methods 30

1 Toxins 30

2 *Artemia franciscana* 30

3 Hatching and breeding of *Artemia franciscana* 30

4 Toxicity tests 31
4.1 Hatching test 31
4.2 Mortality test on nauplii Instar I 31
4.3 Mortality test on adults 32

5 Sample preparation for ROS production measurement and antioxidant enzymes activity assays 32

6 Reactive oxygen species (ROS) production 32

7 Antioxidant enzymes activity assay 34

7.1 Glutathione S-transferase activity 34
7.2 Superoxide dismutase activity 35
7.3 Catalase activity 35
7.4 Cholinesterase activity 36
7.5 Enzyme's activity calculation 37

8 Protein content 37

9 Statistical analysis 37

Results 38

1 Effects of PLTX on *Artemia* cysts hatching and mortality 38

2 Effects of PLTX on ROS production and antioxidant enzymes activity 40

3 Effects of PLTX on mobility 41

4 Effects of OA on *Artemia* cysts hatching and mortality 42

5 Effects of OA on ROS production and antioxidant enzymes activity 44

6 Effects of DTX1 on *Artemia* cysts hatching and mortality 46

7 Effects of DTX1 on ROS production and antioxidant enzymes activity 47

8 Effects of DTX2 on *Artemia* cysts hatching and mortality 49

9 Effects of DTX2 on ROS production and antioxidant enzymes activity 50

Discussion and conclusion 53

Section B

Introduction 59

1 Human stem cells 59

2 Potential uses of iPSC 61

Aim 65

Materials and methods 67

1 Cell culture 67

1.1 Induced pluripotent stem cell (iPSC) 67
1.2 HaCaT cell line 68

2 MTT reduction assay 69

3 Binding assay 69

4 Protein lysates 71

5 Gene expression analysis 71

5.1 RNA extraction 73
5.2 Reverse transcription PCR (RT-PCR) 74
5.3 Real time-PCR (q-PCR) 74

6 Protein expression level (western blot assay) 76

7 Differentiation kit 78

8 Statistical analysis **78**

Results **79**

1 Evaluation of the cytotoxic effect of PLTX on iPSC **79**

2 Evaluation of binding affinity of PLTX on iPSC **80**

3 Evaluation of Na^+/K^+ ATPase genes expression in iPSC **81**

4 Evaluation of the cytotoxic effect of PLTX on iPSC up to 96 h **83**

5 Evaluation of the effect of PLTX on iPSC stemness **85**

5.1 Gene expression levels 85
5.2 Protein expression levels 86

6 Evaluation of PLTX effects on iPSC differentiation **88**

6.1 Gene expression levels 88
6.2 Protein expression levels 89

7 PLTX effects on iPSC viability during differentiation **91**

8 PLTX cytotoxicity on the three germ layers **92**

9 Evaluation of Na^+/K^+ ATPase genes expression in the three germ layers **94**

Discussion and conclusion **97**

General conclusions **101**

References **103**

Appendices **124**

Introduction

1 Harmful Algal Bloom (HABs)

1.1 The HABs phenomenon and its occurrence

The term Harmful Algal Bloom (HAB) was introduced by the scientific community to define the proliferation of toxic or harmful algae species. HABs can result into (i) the formation of "red tide", a macroscopic phenomenon correlated with discolouring of seawater due to the pigments contained into algal cells, when their concentration is extremely high; (ii) mucillages, constituted by macroaggregates of organic matter; (iii) high toxin concentrations, produced by the relevant algal cells[1] (fig. 1). HABs occur worldwide in marine, estuarine, and freshwater environment and can have significant impacts on aquatic ecosystems and on human health. HABs can cause negative impacts via three primary routes: oxygen depletion, damage or clog fish gills and toxins production. The first one is due to the decomposition of blooms and the reduction of aquatic vegetation, phenomenon often observed during blooms and due to light attenuation, resulting in the death of fish and other vertebrate whose decomposition exacerbates oxygen depletion. The damage or clog of gills can be caused by the presence of projections in the algal cells (e.g., spines) or production of haemolytic substances. Numerous algal species are also associated with the presence or the production of toxins that can cause direct lethal effects on water organisms or can be accumulated into different individuals and, therefore, be transferred along the food web with negative effects at higher trophic levels with a potential impact also on humans[2]. In humans, a mortality rate of 1.5 % is recorded with 60 000 cases/years of intoxication primarily due to consumption of seafood and/or respiratory exposure to aerosolized toxins[3]. The HABs phenomenon is also associated with significant socio-economic consequences, correlated with public health costs after human intoxication and the repercussion on both the seafood industry and the tourism sector[4]. The real economic impact, especially as regards the cost incurred for public health, is difficult to estimate for many reasons, such as unreported illnesses, misleading symptoms induced by harmful algae and the chronic long-term effects that are difficult to highlight[5]. However, in 2016 the European Commission drafted the Joint Research Center (JRC) technical report about the algal bloom and its economical impact[6], reporting the socio-economic effects caused by HABs, grouped in four main impacts: (1) human health impacts; (2) fishery impacts; (3) tourism and recreational impacts; (4) monitoring and management costs. The cost depends on the country considered: for instance, the currently known socio-economic costs for public health are $670 000/year for Canada[7], £29-118 000/year for commercial fishery in the United Kingdom[8] and $43 million/year in Maryland[9]; $1.16 billion/year in USA tourism/recreation sector[10] and

for the monitoring and management the costs are $300 000, $500 000, $500 000, $800 000 and $1 114 000 for Norway, Denmark, Portugal, France and Spain, respectivily[11].

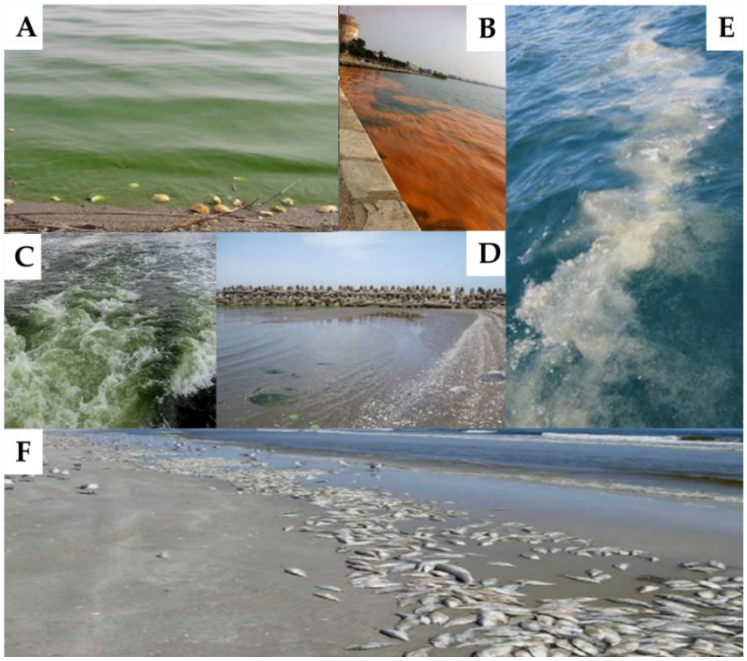

Figure 1. Examples of HABs: A) discoloration of water[6]; B) Bloom of Noctiluca scintillans[12]; C) Discoloration caused by Euglena viridis[12]; D) Shellfish mortality due to the proliferation of N. scintillans and consequent oxygen depletion[12]; E) Pelagic mucilages[12] F) Fish kill caused by a bloom episode[6].

HABs events are collected in the Harmful Algal Events Dataset (HAEDAT), that contains records of marine harmful algal events worldwide from the International Council for the Exploration of the Sea (ICES) area (North Atlantic) since 1985, and from the North Pacific Marine Science Organization (PICES) area (North Pacific) since 2000. In the last three decades, HABs are increased in various coastal regions around the globe (fig. 2). The main reasons are correlated with natural dispersion of species by currents and winds and by direct anthropogenic activities, including the large eutrophication of coastal areas and leakage of species through ships ballast waters[13]. Also, climate changes play a key role in the expansion of algal species with the ocean acidification, alterations of temperature, stratification entry of nutrient induced by precipitation and light[14].

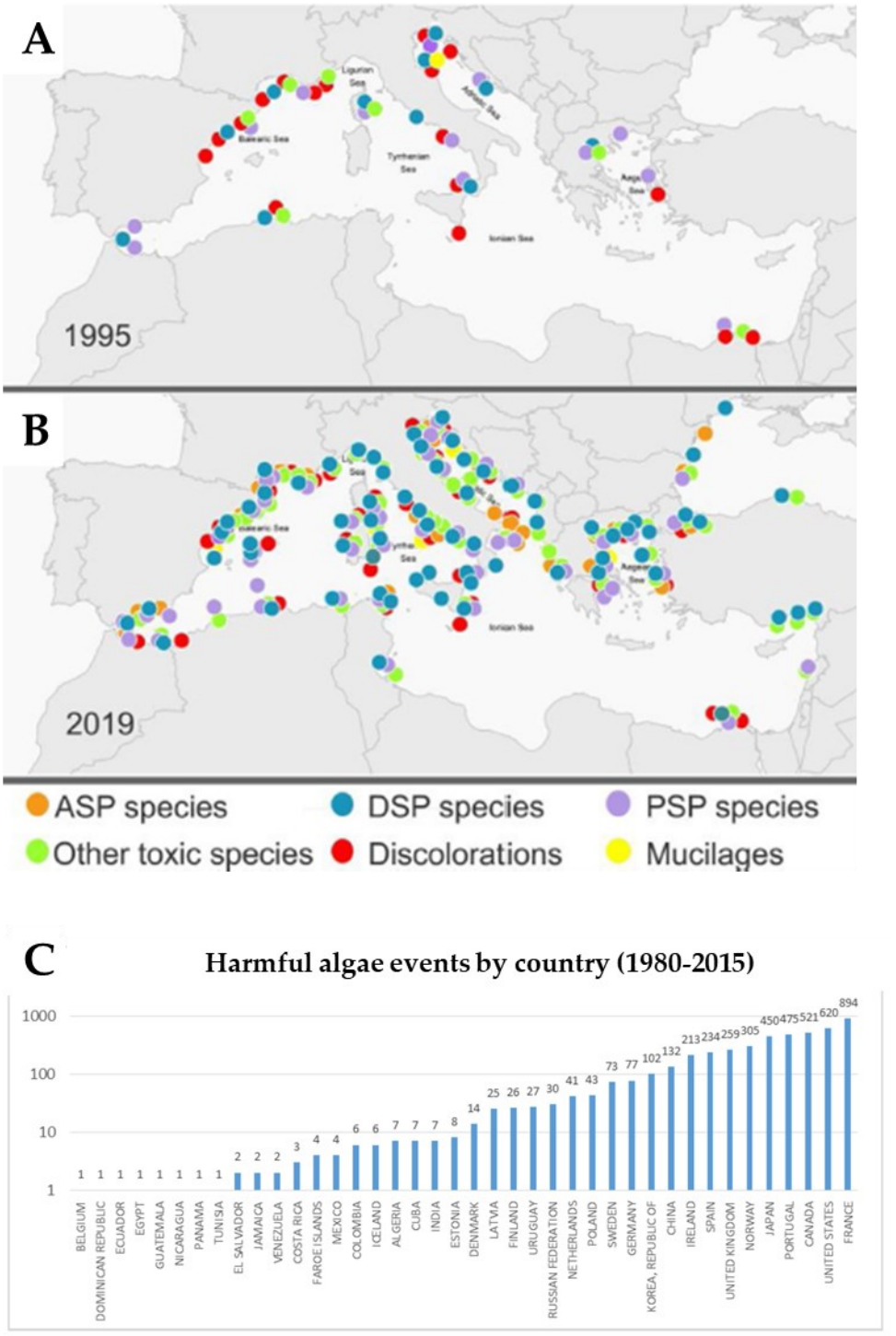

Figure 2. Distribution of potentially toxic species, mucillages and discolorations in the Mediterranean Sea A) until 1995 and B) until 2019 (excluding Ostreopsis and Ciguatera fish poisoning species)[12] and C) Total Number of Harmful Algae Events reported globally by single countries during the period 1980-2015 to the Harmful Algal Events Dataset (HAEDAT)[6] (figures modified).

1.2 Toxigenic algae and biotoxins

More than 140 potentially toxic species are listed in the IOC-UNESCO taxonomic reference list[12]; the main groups of algae that are able to produce toxins are Cyanobacteria, Dinoflagellates, Diatoms, Raphidophytes, Pelagophytes, and Haptophytes[15]. Biotoxins produced by the aforementioned algae can be classified according to different parameters: (i) eight class based on their chemical structure, according to the Workshop 'Joint FAO/ IOC/WHO[16]; (ii) two classes according to the their solubility (water- or fat-soluble marine biotoxins), the water-soluble toxins includes saxitoxins, domoic acid and analogues, tetrodotoxin, palytoxins; the fat-soluble group includes okadaic acid and analogues, yessotoxins, brevetoxins, verenotoxin, ciguatoxins, azaspiracids[17]; (iii) a classification based on the syndrome that each toxin(s) cause in humans. The main HAB-related syndromes are (fig. 3)[17]:

- Amnesic shellfish poisonings (ASP), firstly recognised in 1987, in Canada. This intoxication is caused for example by domoic acid (identified in red alga *Chondria armata* and diatom *Pseudo-nitzschia*[18]), which is associated not only with neurotoxicity but also with gastrotoxic or enterotoxic action. In the first 24-48 h after the poisoning the symptoms usually involve the gastrointestinal system. Following that, neurological symptoms arise, often characterized by amnesia.
- Diarrhoetic shellfish poisonings (DSP), a seafood intoxication characterized by a quick onset (3 h) of gastrointestinal symptoms, including vomiting and diarrhoea, that in general resolve within 2–3 days. Examples of DSP toxins are okadaic acid (OA) and its derivatives dinophysistoxins (DTXs). The main producer of these toxins are dinoflagellates belonging to the genus *Dinophysis* spp.
- Azaspiracid shellfish poisonings (AZP), induced by azaspiracid (AZAs) that are produced by the dinoflagellate *Azadinium spinosum*[19]. The ingestion of food contaminated with these toxins induces in human serious acute gastrointestinal symptoms such as nausea, diarrhoea, vomiting and stomach cramps.
- Paralytic shellfish poisonings (PSP). The toxin responsible of this poisoning is saxitoxin and its analogues that can cause in human neurological symptoms and, in severe cases, respiratory paralysis. Saxitoxin is produced by dinoflagellates (*Alexandrium* sp., *Gymnodinium catenatum*, and *Pyrodinium bahamense*) and by cyanobacteria (*Anabaena circinalis*, *Aphanizomenon*, *Cylindrospermopsis raciborskii*, *Lyngbya wollei*, and *Planktothrix* sp.)[20].

- Neurotoxic shellfish poisonings (NSP), associated with the ingestion of seafood contaminated with brevetoxins produced by the marine dinoflagellate *Karenia brevis*, and inducing, within 30 min after ingestion, a large range of symptoms, both gastrointestinal and neurological such as nausea, vomiting, diarrhoea, arrhythmias, hypotension, cramps, bronchoconstriction, seizures, paralysis[17].
- Ciguatera fish poisoning (CFP), caused by ciguatoxins (the main producer is the dinoflagellates of the genus *Gambierdiscus toxicus*) accumulated in fish. The ingestion of this toxin is associated with gastrointestinal, cardiovascular and neurological symptoms.

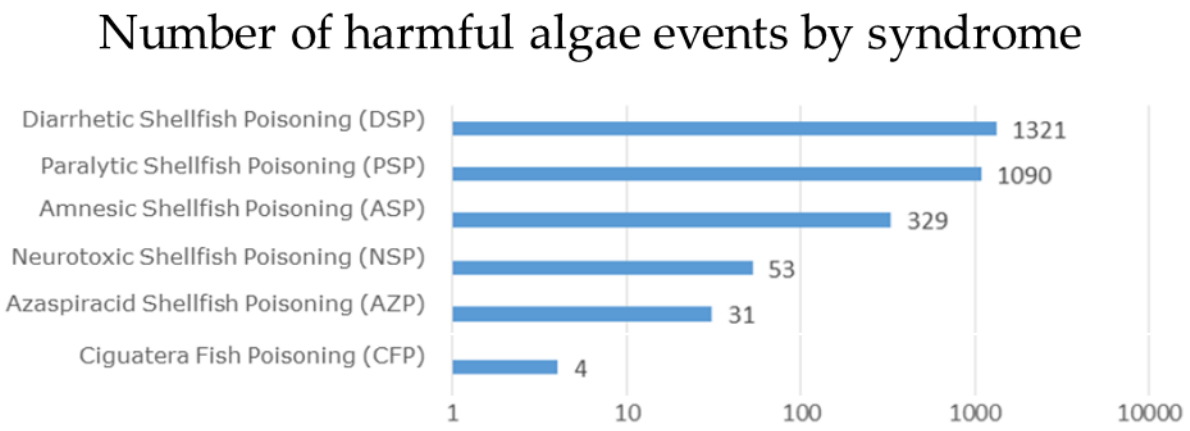

Figure 3. Total number of harmful algae events by syndrome reported globally during the period 1980-2015 to the Harmful Algal Events Dataset (HAEDAT)[6] (figure modified).

Among the numerous toxins associated with negative effects at the human and environmental levels and detected during HABs, this thesis is focused on palytoxin (PLTX), okadaic acid (OA) and two analogous of the latter, dynophysistoxins 1 and 2 (DTX1 and 2). All these toxins have been frequently detected in the Mediterranean Sea.

2 Palytoxin (PLTX)

Palytoxin (PLTX) is a marine non-protein toxin considered to be among the most toxic substances in the world; it was initially isolated from a soft coral traditionally called "Limu make or Hana" and subsequently identified as *Palythoa toxica*. PLTX and its analogues are a family of toxins called palytoxins (PLTx)[21].

2.1 Producing organisms

PLTx was identified in different marine organisms: (i) soft corals of the genus *Palythoa* (*P. toxica*[22], *P. margaritae*[23], *P. vestitus*[24], *P. caribaeorum*[25], *P. caesia*[26], *P. tubercolosa*[27], *P. heliodiscus*[28]); (ii) zoanthids corals of genus *Zoanthus* (*Z. sociatus* e and *Z. solanderi*) and *Parazoanthus*[29]; (iii) dinoflagellates of genus *Ostreopsis* (*O. siamensis*, *O. mascarensis*, *O. ovata*, producing also some PLTX analogous, such as ostreocin-D[30], mascarenotoxins-a, -b and -c[31] and ovatoxins, in particular ovatoxin-a[32], respectively); (iv) marine cyanobacteria of the genus *Trichodesmium,* in which PLTX and its analogous 42-OH-PLTX were detected [33]. The presence of PLTXs in phylogenetically so different organisms has suggested that the producer of these toxins may be a symbiotic organism, not yet identified[34,35]. The hypothesis advanced is that the producer is a bacterium; indeed in 1998, Carballeira and colleagues revealed a PLTX-like haemolytic activity in bacteria isolated from *Palythoa caribaeorum*, belonging to the genus *Pseudomonas*[36], *Brevibacterium*, *Acinetobacter* and *Bacillus cereus*[37], while Frolova *et al*. used anti-PLTX antibodies, detecting PLTX-like compounds in *Aeromonas* sp. And *Vibrio* sp.[38].

2.2 Chemical structure of PLTXs

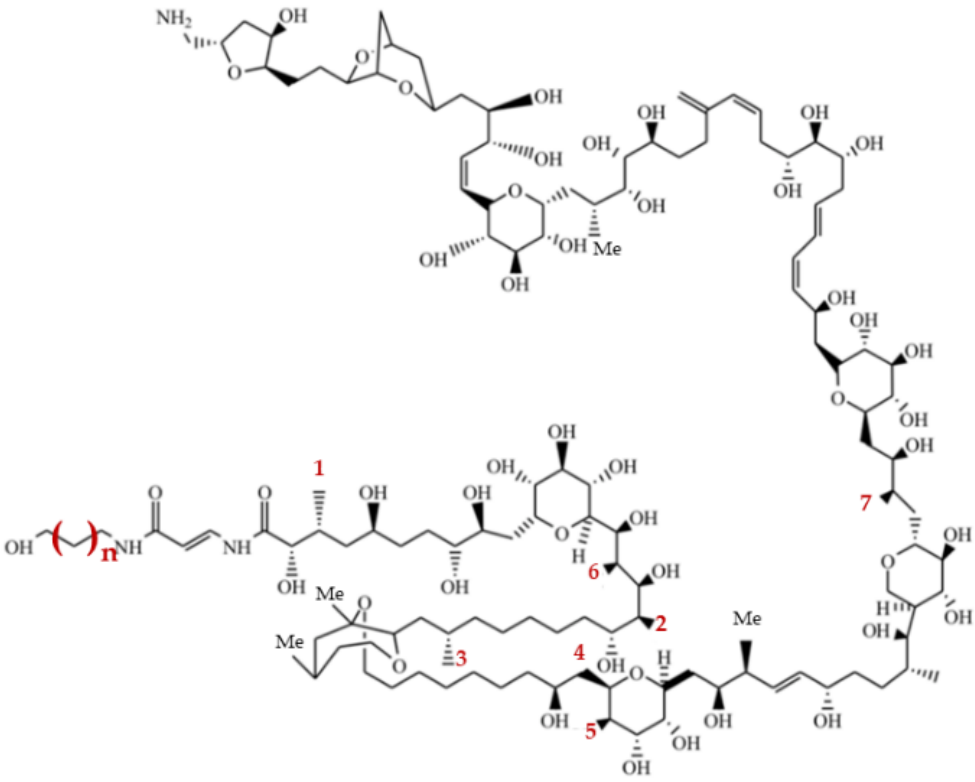

	n	R_1	R_2	R_3	R_4	R_5	R_6	R_7
PLTX	1	Me	OH	Me	H	OH	OH	OH
Homo-PLTX	2	Me	OH	Me	H	OH	OH	OH
42-OH-PLTX	1	Me	OH	Me	OH	OH	OH	OH
Ost-D	1	H	H	H	OH	H	OH	OH
OVTX-a	1	Me	OH	Me	OH	H	H	H

Figure 4. Chemical structure of PLTX[39] and some of its analogues[40] (figure modified)

After 10 years from the discovery of PLTX, which took place in 1971, two research groups elucidated the chemical structure of this toxin[41,42]. The chemical formula of PLTX is $C_{129}H_{223}N_3O_{54}$ with a molecular weight of 2680.13 Da. It is considered one of the most complex non-protein molecules existing in nature, which has both a lipophilic and a hydrophilic region. It is soluble in pyridine, in dimethyl sulfoxide (DMSO) and in water[21]. It is heat-stable, also in neutral aqueous solutions for prolonged periods; however, in acidic or alkaline conditions it can undergo rapid hydrolysis which leads to the loss of its toxicity[39,43]. The molecule of PLTX is formed by a long aliphatic chain consisting of 129 carbon atoms, 2 diene systems, 40 hydroxyl groups, an acrylamide-enamide conjugate

system, 3 double bonds, 2 hydrophobic hydrocarbon chains, a cyclic ether, bicyclic acetals and 64 chiral centres, which can lead to a large number of stereoisomers[41]. PLTX family also includes about 20 PLTX analogues such as ostreocins, ovatoxins and mascarenootoxins[44] , homopalitoxin, bisomopalitoxin, neopalitoxin and deoxy-palytoxin[34]. These analogues are different from the main molecule in terms of presence or absence of hydroxyl and/or methyl groups or by chirality (fig. 4) and they have different toxicities[45]. Under a chemical and biological point of view, the most studied PLTX analogues are[46]: (i) 42-hydroxy-palitoxin (42-OH-PLTX), found mainly in *Palythoa toxica*[47], characterized by a comparable toxicity in mice with respect to PLTX[48], while its stereoisomer (isolated from *P. tuberculosa*) is characterized by a 100-fold lower cytotoxicity on human keratinocytes *in vitro*[49]; (ii) Ostreocin-D, found in *Ostreopsis siamensis*, characterized by a lower toxicity than that of PLTX[50]; and (iii) ovatoxin-a, the structural analogue of PLTX mostly present in *Ostreopsis* cf. *ovata* in the Mediterranean Sea (fig. 5), characterized by a similar toxicity in rats after aerosol administration as compared to PLTX[51], but lower cytotoxic potential in human keratinocytes[52].

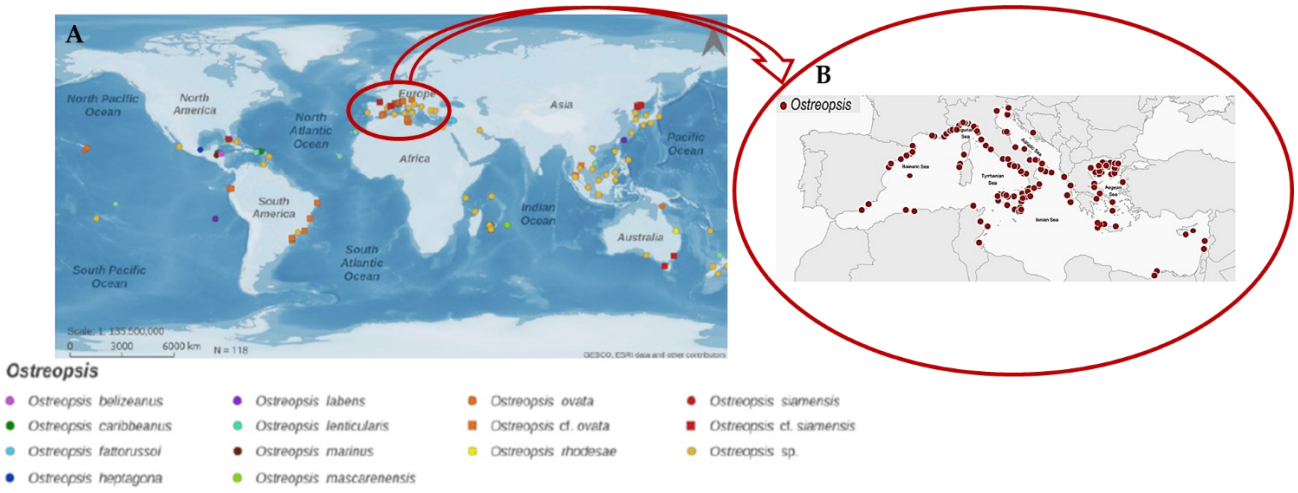

Figure 5. A) Distribution of different Ostreopsis species in the world (data represented comes from a series of data collected and published between 1995 and 2019 including those shown in Global Ecology and Oceanography of Harmful Algal Blooms (GEOHAB) in 2012 and Rhodes et al.[53] (2011)). B) Distribution of Ostreopsis spp. in the Mediterranean Sea[12] (modified figures).

2.3 Mechanism of action

The molecular target of PLTX is the Na^+/K^+ ATPase pump[54–57], expressed in all eukaryotic cells and essential for some vital functions for the cell such as regulation of volume, maintenance of pH, generation of action potential and secondary active transport, involved in the maintenance of cellular homeostasis[58,59]. Indeed, this transmembrane pump, belonging to the P-type ATPase family, is involved in the maintenance of the correct ionic gradient between the intra- and extra-cellular environment. The pump is able to transport against the concentration gradient three Na^+ ions outside the cell across two K^+ ions, through the hydrolysis of an adenosine triphosphate (ATP) molecule to obtain energy[60,61]. The Na^+/K^+ ATPase pump is composed of 3 subunits (fig. 6): the α subunit is located in the intracellular region, with catalytic activity, which displays the binding sites for Na^+ and is responsible for the cationic movement and binding of ATP; the β subunit is found in the extracellular part, it is necessary for ion translocation, able to bind ions and it is essential for the modification of the pump conformation[62] and a regulatory subunit γ. In humans, different isoforms have been identified, both intra-[63] and inter-individual, of the α and β subunits[64,65].

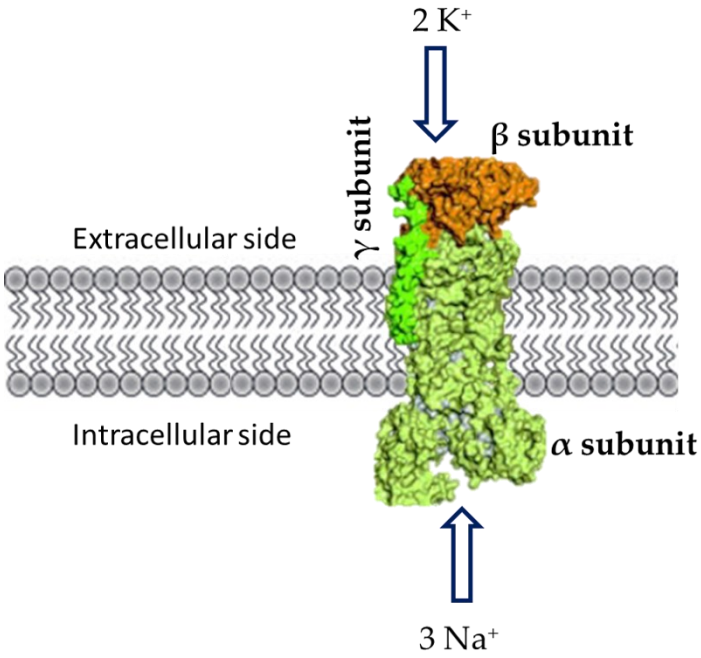

Figure 6. Na^+/K^+ ATPase pump subunits.

The pump mechanism, illustrated in figure 7, is characterized by a cyclic alternation into two conformational states: the E1 state (with higher affinity for Na^+) allows the binding of three Na^+ ions leading to the phosphorylation of the pump thanks to the hydrolysis

of a molecule of ATP; in this condition the intracellular gate closes inducing the change of the conformation into the E2 state. In this state, the binding site has a low affinity for Na^+ and a high affinity for K^+, therefore allowing the release of Na^+ to the extracellular side and the binding of two K^+ ions to the external site with greater affinity. Following the dephosphorylation of the protein, the extracellular gate closes and the release of K^+ into the intracellular space completes the pump cycle bringing it to the initial conformation E1[66]. The binding of PLTX on the extracellular portion of the ATPase pump causes a conformational change by converting the pump into a non-selective cation channel permeable to ions, in particular to monovalent cations such as Li^+, Na^+, K^+, Rb^+ [41,67,68]. PLTX is able to bind the Na^+/K^+ ATPase pump both in the E1 and E2 conformation, with greater binding affinity for the former[69]. The formation of the cation channel already occurs at very low concentrations of PLTX (approximately 1 pM, according to the experimental model), while the blocking of the pump activity occurs only at high toxin concentrations (> 100 nM)[70].

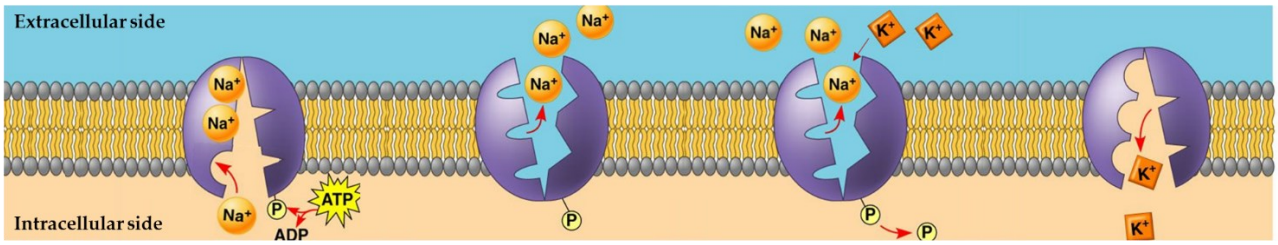

Figure 7. Schematic representation of the mechanism of function of the Na^+/K^+ ATPase pump [71] (figure modified).

As a consequence, PLTX interaction with the Na^+/K^+ ATPase pump increases the intracellular Na^+ flux, involving secondary effects such as (i) an increased Ca^{2+} influx, therefore opening K^+ or Cl^- channels, leading to a further increase of the ionic balance[72]. Moreover, the variation of Ca^{2+} concentrations leads to interferences with the correct functioning of excitable tissues such as neuronal[73,74], cardiac[48,75,76] and muscle[72] cells in addition to the activation of Ca^{2+}-dependent proteases that exert their function on actin filaments, disrupting the cytoskeleton[77] which is essential to maintain cell shape and is involved in other important activities such as intracellular transport, mobility and cell division[78]; (ii) reduction of cellular pH caused by the inverted function of the Na^+/H^+ exchanger[72] which leads to an alteration of the activity of the mitochondrial electron transport chain as a possible consequent cell necrosis[79]; (iii) a high concentration of intracellular Na^+ tends to draw water into the cell leading to cell swelling up to cell lysis[70,72].

2.4 Effects of PLTX on humans

PLTX can accumulate in marine organisms and along the food chain up to humans through the consumption of contaminated seafood. Although no legislations regulating the maximum permissible level of PLTX in fish products are currently available, the European Food Safety Authority (EFSA) has proposed a provisional maximum limit of 30 μg of PLTX-equivalent/kg of shellfish meat[80].
PLTX induces a range of symptoms in humans based on the exposure route[40]:

- oral exposure: after the ingestion of contaminated fish or crustaceans, due to PLTX accumulation through the food chain in marine organisms[78,81]. PLTX vectors are mainly crabs[82], goldspot sardines[83–85] and fish belonging to the Serranidae family[84] while the analogue OVTX-a has been found mainly in molluscs and echinoderms, such as crustaceans and sea urchins. This route of exposure is the most dangerous even if cases of food poisoning have only been reported in tropical and subtropical areas[40,84,85]. Symptoms of poisoning initially involve the gastrointestinal tract (abdominal cramps, nausea, diarrhea and vomiting) and the nervous system (convulsions, dizziness, numbness and restlessness); excitable tissues can be also involved, such as skeletal muscle, in which symptoms such as muscle cramps, myalgia and rhabdomyolysis occur and the cardiovascular system, with bradycardia and tachycardia. Clinical signs worsen when the respiratory tract is involved, with increased respiratory rate, cyanosis and dyspnoea which in some cases can lead to respiratory failure and death[48,86]. The most common complication is rhabdomyolysis[87], a syndrome characterized by damage to the skeletal muscle[88]. Other clinical symptoms manifested in PLTX intoxication are elevated serum levels of creatine phosphokinase (CPK) and changes in the electrocardiogram[89]. Death often occurs due to myocardial damage[78]. In the Philippines, some cases of human death after the consumption of PLTX-contaminated crabs have been described[82], while in Japan, Madagascar and the USA some intoxications due to the consumption of contaminated fish have been reported[89]. Additional cases have been described in Madagascar[83], Japan[84] and Taiwan[85]. In all these cases, the presence of PLTX and related compounds was found by analytical analyses in food leftovers. However, several other cases have been ascribed to the toxin only on the basis of the symptoms and the organisms responsible for the intoxication, but without confirmatory analytical analysis demonstrating the presence of the toxin[90–92].

- cutaneous exposure: by direct contact with zoanthid corals frequently used as decorative elements of home aquaria or by contact with sea water during blooms of *Ostreopsis* cf. *ovata*. Both local symptoms, such as oedema and erythema, and systemic symptoms such as paraesthesia and dysgeusia, and in the most severe cases also transient changes in cardiac functions have been reported[35,40,93]. The first case dates back to the 1960s in Hawaii, during a collection of *Palythoa toxica*[35], but other cases have been associated with the handling of corals in home aquariums[88,93,94] or to direct contact with seawater during proliferation of *Ostreopsis* cf. *ovata* as reported in 2005 along the Italian Ligurian coasts[95], between 2006 and 2009 in France[96] and in 2009 in the Gulf of Trieste (Italy)[97].

- inhalation exposure: due to the inhalation of vapours during the cleaning of aquariums containing *Palythoa* corals or by inhalation of marine aerosols during *O*. cf. *ovata*; symptoms occur mainly at the respiratory level and include rhinorrhoea, cough, dyspnoea, but also systemic symptoms such as myalgia, paraesthesia, tachycardia, hypotension and fever have been described[28,35]. The first well-documented case of intoxication was in 2010, in Virginia (USA)[28], followed by other cases correlated with the inhalation of vapours from corals contaminated by PLTX during the cleaning of both domestic or industrial aquaria[98–104]. The presence of PLTXs in corals was quantified only in two of these cases, equal to 309-613 μg of equivalent of PLTX/g of corals[28] and 7.3 mg/g of coral[99]. Since 1998, cases of intoxication after inhalation in the marine aerosol have also been recorded during *Ostreopsis* blooms, especially in the Mediterranean Sea along the coasts of Italy, Spain and France[86,105], as well as in Croatia, Tunisia and Greece[106]; moreover, in the summer of 2009, proliferations involving numerous symptomatic patients were also reported in Algeria[96].

- ocular exposure: only 3 cases of ocular irritation have been ascribed to PLTX exposure following the manipulation of zoanthid corals during aquarium cleaning. The main symptoms are keratoconjunctivitis with symptoms such as eyes pain, swelling of the eyelids, photophobia, purulent discharge, redness and blurred vision; only in one case symptoms become more severe with dyspnoea, nausea and chills[104,107]. Other cases of ocular toxicity have been observed along the coasts of Spain[108], France[96] and Italy[109] during the proliferation of *Ostreopsis* cf. *ovata*. However, in none of these cases the presence of PLTX was demonstrated by analytical analyses.

2.5 Effects of PLTX on aquatic organisms

In addition to human intoxications following exposure to PLTXs, literature data report also negative effects induced by the toxin in marine organisms. In 2003, Sansoni *et* al. report, in presence of high quantities of *Ostreopsis* cf. *ovata*, an increased mortality in bivalves, gastropods, cephalopods and echinoderms, abnormal size of the byssus in bivalves and anatomical malformations in echinoderms. In particular, loss of spines in sea urchins, and loss of arms in starfish have been observed[110,111]. Reduced sperm motility following exposure to *Ostreopsis* spp. have also been reported in sea urchins[112]. In Italy, following the anomalous presence of *O*. cf. *ovata*, massive mortality was observed in marine invertebrates and macroalgae[63], with impacts on sessile animals such as barnacles, bivalves and gastropods, or on mobile organisms such as echinoderms, small fish or cephalopods[109,113]. In tissues of the mussel *Mytilus galloprovincialis*, collected in the Adriatic Sea in the summer of 2009 during an *Ostreopsis* blooms, a slight increase in oxidative markers was found[114]. However, despite it is well known that blooms of *Ostreopsis*, in particular *O*. cf. *ovata*, can results in numerous problems for marine organisms, as summarized by several authors[114–116], a direct correlation with the presence of PLTX has not been ascertained, so far.

In addition, it should be underlined that no evidence of direct negative effects on fish, which play the role of vectors for the spread of PLTXs in the food chain, has been reported[26]. Several animals that typically feed on PLTXs producing organisms, such as some species of sponges, soft corals, molluscs, crustaceans, polychaetes, starfish and fish, have developed a high tolerance to the toxin. This phenomenon, together with the fact that these organisms have been found to accumulate high concentrations of toxins[26,83,84], represent an important observation considering the entrance of PLTX into the food web, up to humans.

In addition to the abovementioned negative effects at the environmental level, numerous laboratory studies have highlighted the toxic potential of PLTXs in different model organisms. So far, considering marine invertebrates, almost all these studies analysed the effects by exposing the target organism to *O*. cf. *ovata* cell culture, and often the type of toxins and their quantities produced in culture are not analysed. Since the quantity and composition of the toxins produced by *Ostreopsis* spp. is not always the same, this approach could potentially lead to misleading results. In general, these studies show negative effects on sea urchins, triggering interferences on sperm motility, embryogenesis and first larval stages development of these echinoderms[117–119]. In the bivalve *Mytilus galloprovincialis*, a long-term laboratory exposures (7 and 14 days) to cell cultures of *Ostreopsis* sp. Mainly revealed histological alterations in the tissues, an increase in the enzymatic activity of catalase, glutathione reductase and glutathione peroxidases and

the involvement of the immune system[120]. For this bivalve, the toxicity of PLTX alone was also analysed in terms of metabolic activity of mantle and hepato-pancreas cells, showing a half-maximal inhibitory concentration (IC_{50}) of $18.2x10^{-9}$ M and $16.2x10^{-9}$ M respectively[121]. An increase in mortality was also observed on the copepod *Tigriopus fulvus* and on the barnacle *Amphibalanus amphitrite* in the presence of *O*. cf. *ovata* cells[116], while juvenile of *Litopenaeus vannamei* exposed to *O*. cf. *ovata* extracts (estimating 0.3588 μg/mL of PLTXs), showed an increase in mortality and a variation of different parameters such as antioxidant enzymes activity, oxidative damage to lipids, carbonylation of proteins, and mRNA expression levels of immune genes[122].

Using the same approach, also the effects on the brine shrimp *Artemia* spp. was analysed: *A. salina* showed increased mortality in the presence of *O*. cf. *ovata* cultures in nauplii[116,123] and adults[124] and in presence of *O. siamensis* cells (250 cell/test, estimating 0.3 pg of PLTX-equivalent/cell) in nauplii[125]. Also *A. franciscana* nauplii were considered, and the contact with *O*. cf. *ovata* cells (estimating 44 ± 17 pg PLTX equivalent/cell) produced significant mortality[126]. Moreover, the exposure to cell lysates of *O*. cf. *ovata*[118] or *Palythoa caribaeorum*[127] induced an increase in mortality on *A. salina* nauplii. Furthermore, *Artemia* spp. nauplii were found to be more sensitive to the exposure of *O*. cf. *ovata* cells, compared to the copepod *Tigriopus fulvus*, to the patella *Amphibalanus amphitrite*[116] and to the copepod *Sarsamphiascus cf. propinquus*[126].

On vertebrate organisms, the effects of the toxin were analysed especially considering its impact on the reproduction and development[39], highlighting embryotoxic and teratogenic effects in *Xenopus laevis* embryos. In fact, Franchini and collaborators (2008) demonstrated that in frog embryos PLTX caused: (i) mortality up to 80% at $3.7x10^{-7}$ M after 5 days of exposure; (ii) embryo malformations, the most frequent changes were along the antero-posterior axis of the body and swelling of the visceral mass; (iii) growth retardation; (iv) structural changes in nerve tissue (neurons and spinal ganglia) and muscle tissue (skeletal tail musculature); (v) general reduction in size of major internal visceral organs (i.e. intestine, pancreas and liver), but no morphological changes and (vi) particularly damaged cardiac structure[128]. The following year, the same research group analysed the variation in the expression of some genes related to the neuronal and muscle development following exposure to PLTX: results showed an up-regulation of these genes which allowed a partial explanation of the previous observations[129].

3 Okadaic acid (OA) and its analogous, dynophysistoxins (DTXs)

3.1 Producing organisms

Okadaic acid (OA) is a DSP toxin, firstly isolated from two porifera: *Halichondria okadai* and *H. melanodocia*[130]. Subsequently, OA and its derivatives were also found in marine dinoflagellates of the genera *Dinophysis* (such as *D. fortii*, *D. acuminata*, *D. acuta*, *D. caudata*, *D. miles*, *D. ovum* and *D. sacculus*[131]), *Phalacroma* and *Prorocentrum* (nowadays only two species have been identified: *P. lima* and *P. rhathymum*, but no toxicity events have been related with their presence[12,132]). The production of these toxins can vary considerably both at the interspecies and intraspecies level, considering the different morphotypes[133].

3.2 Chemical structure of OA and DTXs

OA is a polyether with a molecular weight of 805.015 g/mol with the chemical formula $C_{44}H_{68}O_{13}$. Being fat-soluble, it cannot be dissolved in water, but is soluble in organic solvents such as chloroform, ethanol, methanol, acetone and ethyl acetate. The structure of OA, DTX1 and DTX2 were determined in 1981[130], 1982[134] and 1992[135], respectively. DTX3 is not synthesized by dinoflagellates, in spite of being present in bivalves[136], and is a 7-OH acylated derivative of either okadaic acid (OA) or DTX1. The ratio between acylated and non-acylated forms detected in digestive glands of DSP-exposed bivalves depends on the bivalve species. It was reported that Japanese scallops possess a higher capability to convert DTX1 to DTX3 in comparison to mussels[137]. In addition, DTX4[138] and DTX5[139], produced by the dinoflagellate *Prorocentrum* spp., have not been reported in bivalves to date. OA is a long-chain compound, characterized by a carboxyl group that folds on itself in aqueous solution to form a pseudo-ring structure with a hydrophobic tail. The structures of the analogues DTX1 and DTX2 are very similar: they are different from OA only in the number and relative spatial orientation of the methyl groups in C31 and C35 (fig. 8).

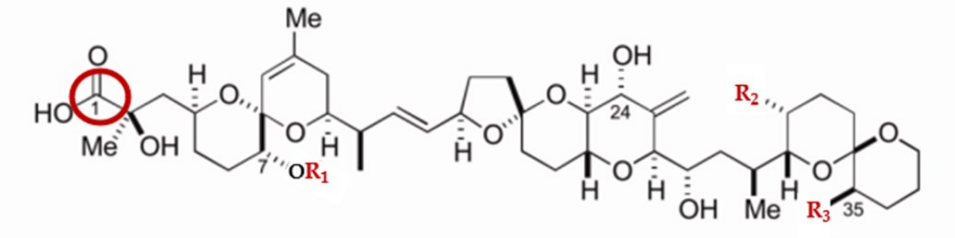

	R_1	R_2	R_3
OA	H	Me	H
DTX1	H	Me	Me
DTX2	H	H	Me
DTX3	Acyl	R_2/R_3=H/Me R_2/R_3=Me/H R_2/R_3=Me/Me	

Figure 8. Chemical structure of OA and the main analogues, the characteristic carboxylic group of OA is circled in red [140] *(figure modified).*

3.3 Mechanism of action

Given their lipophilic nature, OA and DTXs can easily cross the phospholipid bilayer of cell membranes[141]. Okadaic acid is a potent inhibitor of protein phosphatase 1 (PP1) and 2A (PP2A)[142] (with dissociation constants of 1.5×10^{-7} M and 3.0×10^{-11} M, respectively[143]), two classes of phosphatases which act on the dephosphorylation of proteins on serine and threonine residues. The other two main classes of phosphatases (PP2B and PP2C), on the other hand, undergo the effects of okadaic acid only slightly (in the case of PP2B) or not at all (in the case of PP2C). Protein phosphatases are essential for many cellular processes, such as cell division and differentiation, muscle contraction and neuronal activity[144]. The binding between OA and protein phosphatases leads to a rapid increase in phosphorylated proteins that control the secretion of sodium ion, for example, in intestinal cells, leading to the development of gastro-intestinal symptoms in humans. Indeed, OA causes diarrhoea without directly stimulating intestinal secretion, but acts indirectly, increasing the paracellular permeability of intestinal epithelial cells[145]. OA binds to a hydrophobic region located near the active site of phosphatases and, interacting with the residues within the active site, inhibits the activity of phosphatases[146]. X-ray crystal structure revealed the well-folded structure of OA in the catalytic subunit of PP2A, showing the presence of an intramolecular hydrogen bond between the carboxyl group and C24-OH[130,147]. OA analogues inhibit phosphatases to different degrees. Several studies have shown that the modification of the carboxy group in C1 considerably decreases the ability of the toxin to inhibit phosphatases[148]. Furthermore, the methylation associated

with the hydroxyl groups of the molecule (C2, C7, C24, C27) makes the toxin substantially ineffective. Recent studies have indicated that, while DTX1 shows an affinity for PP2A similar to that of OA, DTX2 shows a lower affinity[149]. Modifications of these toxins also lead to different toxic effects, for example hydrolysis of diol esters of OA or DTX4 and -5 leads to an increase of toxicity by restoring binding ability to serine/threonine protein phosphatases 1 (PP1) and 2A (PP2A)[150].

3.4 Effects of OA and DTXs on humans

OA and DTXs are associated with the Diarrhoeic Shellfish Poisoning (DSP) in humans, after ingestion of contaminated seafood[136]; indeed, OA and its analogues ca be accumulated in adipose tissues of shellfish, for example in the hepatopancreas of bivalve molluscs, after filtering seawater containing toxic phytoplankton[131]. These toxins cannot be perceived during consumption because they do not affect the taste of contaminated shellfish and, being thermostable, they are not degraded during seafood freezing or cooking[133]. DSP syndrome is characterized by several gastro-intestinal disorders, including diarrhoea (92%), nausea (80%), vomiting (79%) and abdominal pain (53%)[151]. These symptoms appear after 30 minutes up to 4 hours from ingestion and persist for about three days. DSP symptoms occur following an intake of at least 40 μg of OA equivalents[152]. This intoxication, although not lethal for humans, is an important health problem worldwide[17]. DSP toxins in mussels represent the most frequently reported cases of seafood contamination in the Mediterranean Sea. Eight toxic species of the genus *Dinophysis*, plus two of the genus *Phalacroma*, have been observed along the Mediterranean coasts[12] (fig. 9). The documented cases of the presence of OA and DTXs in the Mediterranean Sea were summarized by Zingone and colleagues [12]: high levels of OA and/or DTXs in several instances led to halt or block shellfish harvesting along the French, Spanish, Greek, Tunisian and Italian coasts. High levels of DSP toxins have been reported in the eastern Mediterranean and Tunisian waters. Nonetheless, only few cases of DSP diagnoses in humans are documented in the Adriatic and Tyrrhenian Seas. The most important accidents occurred in 2000 for a *Dinophysis* bloom in the Thermaikos Gulf (Greece, North Aegean Sea), causing important economic losses (€ 5 million) to aquaculture, and in 2010 in Piemonte by the consumption of toxic mussels from the northern Adriatic Sea. Considering the potential impact of OA and DTXs intoxications, on April 2004 the European Parliament and the Council issued the regulation (EC) N. 853/2004 on the hygiene of products of animal origin, reporting a limit of 160 μg of OA equivalent/kg of bivalve molluscs placed on the market and intended for human consumption (measured in the whole body or in parts that can be consumed separately)[153].

Figure 9. Geographic distribution of potentially toxic species in the Mediterranean Sea. Distribution of species known to produce toxins related to the Diarrhoetic Shellfish Poisoning (DSP)[12] (figure modified).

In addition to the recorded intoxication events, multiple *in vitro* and *in vivo* studies have analysed the effects of OA and DTXs, highlighting that OA could be neurotoxic (fig. 10), cytotoxic, immunotoxic, embryotoxic and act as a tumour promoter[154]. The main cytotoxic effect is the induction of apoptosis, as observed in various cells, including neuronal, hepatic and blood cells[155]. The mechanisms involved in this process include alteration in the expression of specific genes, decrease in mitochondrial membrane potential, inhibition of protein synthesis and alterations of the cytoskeleton[154]. OA has also shown the ability to induce oxidative stress in several *in vivo* and *in vitro* studies[156,157], and to alter various catabolic and anabolic pathways, including glycolysis, lipolysis and gluconeogenesis[158]. Exposure to OA causes genotoxic effects on various cells and animals. These damages include DNA lesions, oxidative DNA damage, and DNA strand breaks[154]. Furthermore, OA can alter DNA repair from damage induced by other genotoxic compounds[159]. Okadaic acid is currently not classified as a tumour promoter by IARC (International Agency for Research on Cancer). However, several studies have shown a potent activity of OA and DTX1 as tumour promoters on the skin, lungs and liver, stomach due to the inhibition of phosphatases PP1 and PP2A[160].

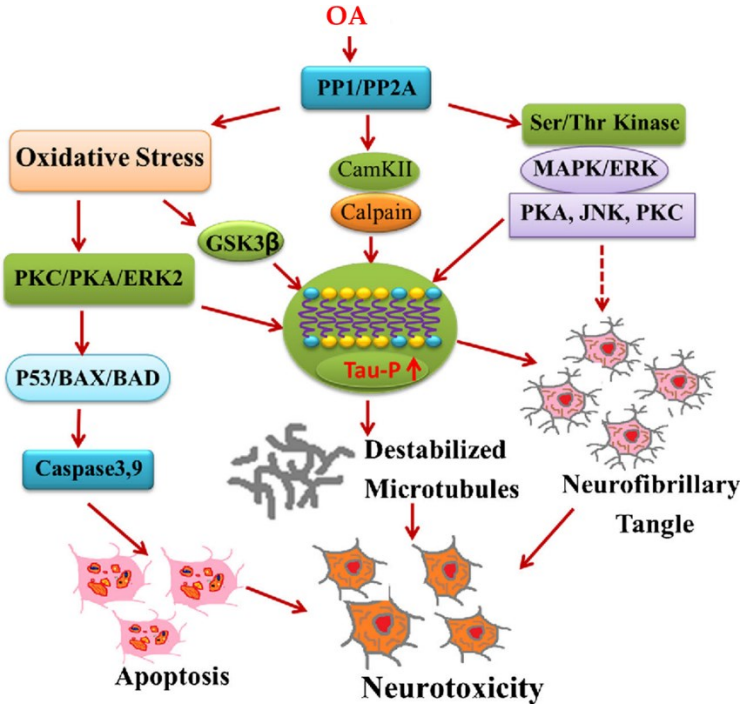

Figure 10. Mechanism of OA on kinase activity[161].

3.5 Effects of OA and DTXs on aquatic organisms

Numerous studies have analysed the effects of OA and its analogues on mammals, but currently few studies have evaluated the effects of these biotoxins on aquatic – and in particular marine – organisms. Most of the studies have been conducted on bivalve molluscs, because of their high commercial value and for their surprising resistance to these biotoxins. For example, studies have been carried out to evaluate the genotoxicity of OA on clams (*Ruditapes decussatus*), but these have shown conflicting results. Studies carried out *in vitro*, in which haemocytes were exposed to increasing concentrations of OA, showed a rapid genotoxic effect of OA on clam DNA[162]. In contrast, a study on whole organism revealed genetic material damage only in gill tissue and at low OA concentrations. The induction of micronuclei has also been identified in bivalve molluscs[163], which originate from the loss of chromosomal fragments or entire chromosomes. However, the frequency of micronuclei in some bivalve molluscs exposed to high concentrations of OA decreased, and this could indicate the activation of cell repair mechanisms[164].

Other studies used embryos of zebra- and medaka-fish as experimental tools in developmental studies in order to analyse the OA effects on embryo development. Anatomopathological analysis carried out on the surviving embryos indicate that OA treatment resulted in significant increases in liver and digestive tract areas compared to controls[165].

The section A of the present thesis will focus on the evaluation of the ecotoxicological impact of these toxins (PLTX, OA and DTXs) using the microcrustacean *Artemia franciscana* as a model organism for the marine environment. The most toxic compound was PLTX, and this toxin was chosen in the section B of this thesis, focusing on human toxicity. In particular, human embryotoxicity will be considered, since this aspect is still scarcely studied in scientific literature. For this aim, a human induced pluripotent stem cell line will be used as an *in vitro* model to study the effects on the early embryonic developmental phases.

Section A

Introduction

1 *Artemia* spp.

The genus *Artemia* (Leach 1819) includes saltwater crustacean species. It is distributed globally, with the exception of Antarctica[166]. The size range of *Artemia* is 0.4-0.5 mm in the first development stage and about 10 mm in the adults. The first observation of *Artemia*, dates back to 982 in Lake Urmia by an Iranian geographer[167]. Linnaeus initially called these crustaceans "Cáncer" in 1758; later on in 1819, Leach renamed them *Artemia* [168]. The genus *Artemia* belongs to the Family Artemiidae, Order Anostraca, Class Crustacea and Phylum Arthropoda. *Artemia* is characterized also by "sibling species" and superspecies distinguished by reproductive isolation that make the genus complex[166]. Indeed, the systematics and phylogenetics of *Artemia* species still remain an open question for the taxonomists[169,170]. Nevertheless, numerous species of the genus *Artemia* have been identified, including *A. salina*, *A. urmiana*, *A. sinica* , *A. tibetiana*, *A. parthenogenetica*, *A. franciscana* and *A. persimilis*[166]. These organisms have developed adaptation properties for extreme environment colonization, such as salt marshes[171]. Indeed, *Artemia* is present in natural and/or man-made hypersaline lakes, temporary desert ponds, coastal lagoons, saltern ponds, pools and saltmarshes[166] due to its particular energetic properties. In aquaculture[172], breeding and aquarium[173], it is used as a food source for different organisms, such as foraminifers, coelenterates, flatworms, polychaetes, cnidarians, squids, insects, chaetognaths, fish (especially tropical fish[174]), and other crustaceans[175] (around 2000 tons of cysts are marketed worldwide each year); Moreover, in its natural habitat, *Artemia* spp. is an essential food source for birds[176]. *Artemia franciscana*, is a sexually reproducing species originally found in North America (San Francisco Bay) and in the Caribbean. This species has become exotic in most of the rest of the globe due to its intensive use in aquaculture as a food source on farms[177,178]. *A. franciscana* has also be found in Asia, Australia and South America[179], and is currently the most widespread *Artemia* species in the world and the most studied species of this genus.

1.1 Life cycle

The genus *Artemia* includes species characterized by both sexual (*A. franciscana*, *A. persimilis*, *A. salina*, *A. urmiana*, *A. sinica*, *A. tibetiana*) or parthenogenetic reproduction (*A. parthenogenica*)[166]. In parthenogenetic species, the development of the egg occurs without fertilization, and the resulting diploid individuals are genetically identical. In the case of species with sexual reproduction, female can reproduce both in an ovoviparous and oviparous way. In the first case, the embryonic development takes place in the ovisack until the release of the larva[166]. In the second case, the embryo interrupt its vital functions at the gastrula stage, it is subsequently released into the environment as a cyst in a cryptobiosis state[180]. This state can be maintained for several years, especially in case of low temperatures and oxygen[171]. *Artemia* prefers ovoviparity although in adverse environmental conditions (e.g. lack of food, thermal and salinity stress) oviparity is choosen[181]. The cysts will hatch under favourable conditions and nauplii will emerge. Nauplii are the first developmental stages of *Artemia* spp., its life cycle continues with 15 larval stages[174], becoming adults after about 20 days and it can reproduce after 40 days. The mean lifetime of an *Artemia* organism is around 3-4 months, extendable to 5 months in case of favourable environmental conditions[166] (fig. 11).

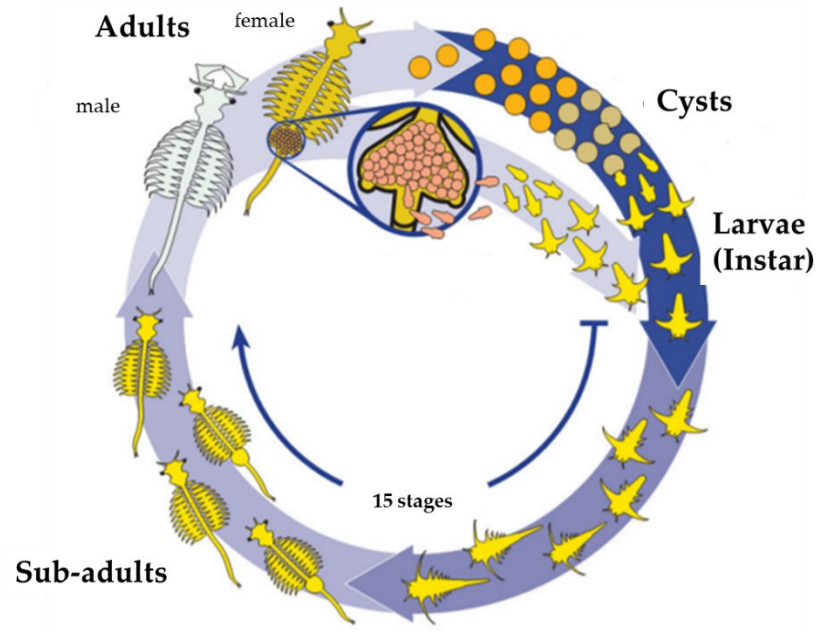

Figure 11. Summary of the life cycle of Artemia spp. [182].

1.2 *Artemia* spp. morphology

Although there are several species of *Artemia*, the general morphology has been conserved at the genus level for over 200 million years. At the larval stages, the cuticle covering the body of nauplii varies between 0.3 – 1.0 μm in thickness[166]. At the first stage, the larva called "Instar I" is 0.4-0.5 mm long and has a brown-orange colour. It also has a red eye in the head area and three pairs of appendages: the first antennae, also called antennule, have a sensory function; the second antennae have a function of locomotion and filtration; the mandibles, that have the function of absorbing the nourishment. At this stage, nauplii do not yet possess the digestive tract, they are unable to take in the nutrients from the external environment but survive thanking to the reserves of yolk released by the cyst or embryo[183,184] . After more than 8-36 hours after hatching, depending on the environmental temperature, the transition to the second stage (Instar II) occurs[185]. The larva, free to move, and with a functioning digestive tract, is able to obtain the food (e.g. bacteria, microalgae or debris) not larger than 50.0 μm[183]. Through several moults (15 in total), larvae grow and differentiate. Lobular structures appear in the trunk area that will shape the thoracopods, while compound eyes are formed in the anterior part. The most important functional and morphological changes occur around the tenth moult, such as the loss of locomotion function of the antennae and sexual maturity of the adult stage. Thereafter, individuals pass to the sub-adult stage, characterized by a length of about 0.6-0.7 mm[186]. At the adult stage, after around 20 days after cysts hatching, *Artemia* spp. is characterized by a segmented body, with appendages and divided into the head, thorax and abdomen. The average length of an adult is about 10 mm (i.e. male: 8-10 mm; female 8-13 mm)[166]. The head is the most specialized region of the body. Here, there are 6 segments: 1 proximal and 5 metameric, containing the compound eyes, the labrum, the primary and secondary antennae, the mandibles and finally the primary and secondary maxillae[166]. When sexual maturation is reached, notable dimorphism is observed. Indeed, male and female antennae take on different shapes and functions: in males they become useful prehensile claws while in females they are transformed into sensory appendages[186]. The thorax is made up of 11 segments, each one equipped with a couple of appendages with swimming, respiratory, nutrition and osmoregulation functions[166]. In the abdominal area, adults has 8 segments without appendages, except the last one which possesses the furca[166]. The adult body is covered with a fine and flexible chitin exoskeleton to which the muscles are internally attached. The thickness of the exoskeleton varies in the body regions up to 7.0 μm in the male gonads and 1.0-1.5 μm in the thoracic appendages[171]. The change of the exoskeleton is a periodic phenomenon and in female it occurs before each ovulation. In male, however, no correlation has yet been found between the moult and the reproductive period[166].

1.3 Ecology and distribution

Artemia is a euryhaline organism, typical of hypersaline environments, found in tropical, subtropical and temperate climatic zones, along coasts and inland areas. Its distribution (fig. 12) is discontinuous, not all high salinity biotopes are populated by this crustacean. It cannot migrate from one habitat to another due to the presence of numerous predators[183]. The wind and the avifauna are the most important vectors for the dispersion of *Artemia* cysts. In fact, lack of migratory birds may be the reason for the absence of the organism in certain regions[183]. The habitats of *Artemia* spp. have simple trophic structure and low diversity. In these environments, the sources of nutrient are bacteria, protozoa and algae that are the basis of its diet[171]. The physico-chemical parameters that most influence the distribution of these crustaceans are temperature, salinity and dissolved oxygen[171]. *Artemia* spp. can tolerate very high salinities (> 70 g/L)[174], and this physiological adaptation allows it to effectively defend itself from predators, which are unable to survive in the same environmental conditions. These organisms have different adaptations giving them high resistance: an efficient osmoregulatory system, the ability to produce quiescent cysts, and respiratory pigments that allow them to resist in environments characterized by low oxygen levels and high salinity[174]. In addition, also the temperature is an environmental parameter that influences the distribution of *Artemia* spp.. In the tundra and in habitats where the recorded temperatures are extremely low, no *Artemia* spp. have been found. Low temperatures preclude the development of *Artemia* spp. and decrease the ability of cysts to hatch[187]. It has been reported that *A. franciscana* does not survive for prolonged periods at temperatures below 5 °C, except in the form of cysts[188]. The maximum temperatures that the populations of this crustacean can withstand are around 35 °C, values frequently reached in tropical areas[166].

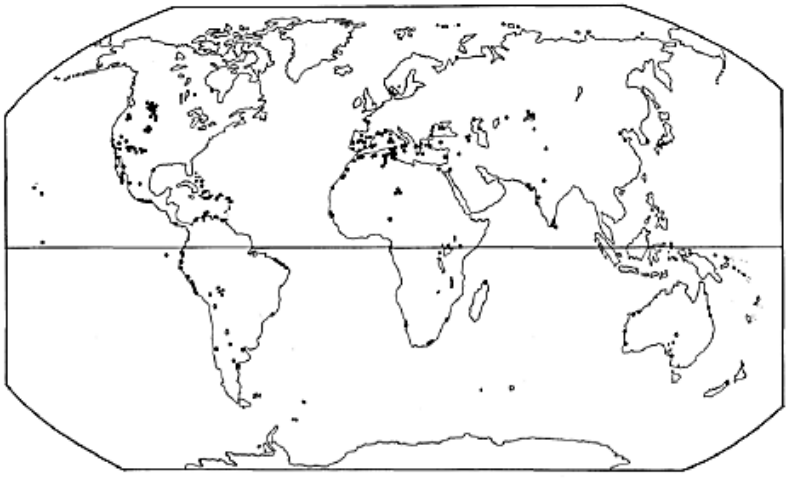

Figure 12. Distribution of Artemia species in the wold[187]

In recent decades, several studies have been carried out on the biogeography of *Artemia* spp. but the global distribution of this taxa is not well defined. Being strongly influenced by the abiotic conditions of the environment in which it is located, its distribution should be updated periodically, as variations in temperature or other physico-chemical parameters, in view of climate changes, could lead to the disappearance or appearance of suitable habitats[187].

1.4 *Artemia* spp. as a model organism

Artemia spp. is an organism widely used as a model organism for ecotoxicology studies[173] but also for pharmacological[189], epigenetics[190] and evolutionary biology studies[191]. Regarding the former, *Artemia* spp. is commonly used for aquatic ecotoxicological studies, in particular for the marine environment[192] and for bioaccumulation studies along the food web[193]. The use of *Artemia* spp. is particularly advantageous due to many characteristics, such as high adaptability to environmental conditions, short life cycle, high fecundity, bisexual/parthenogenetic reproduction strategies, small body size, wide geographic distribution and adaptability to varied nutrient resources as it is a non-selective filter feeder. Researchers found the use of *Artemia* spp. advantageous also because this organism is suitable to laboratory conditions, resistance to manipulation, its laboratory culture and maintenance are relatively simple, there is good knowledge of its ecology and physiology and aseptic techniques are not required. Therefore, *Artemia*-based tests guarantee reliability, rapidity, simplicity, feasibility and convenience in terms of low cost, reduction of test volumes, amount of produced waste, and space needed[194]. *Artemia franciscana* is largely used in ecotoxicology studies for toxicity testing as model of marine zooplankton species [192,194–196], both in short- and long-term toxicity tests[197].

So far, *Artemia* has been employed to evaluate the effects of a wide range of substances, such as: drugs and antibiotics[198,199], toxins[200], nanomaterials[201], insecticides[202] and many chemical compounds such as arsenic[203]. The acute toxicity tests are the most frequently performed, evaluating the effects by means of cysts hatching, nauplii or adults mortality, growth and movement. Some long-term exposure test protocols have been developed in recent years, but they have not been standardized, yet[204,205].

Aim

The term Harmful Algal Bloom (HAB) was introduced by the scientific community to define the proliferation and occasional dominance of particular species of toxic or harmful algae. HABs occur worldwide in marine, estuarine, and freshwater environments and can have significant impacts on aquatic ecosystems and on human health. At the environmental level, HABs can cause negative impacts via three primary routes: oxygen depletion and damage or clog of fish gills caused by algae and toxins production[2].

In this section of the thesis, the ecotoxicological impact of four toxins detected during HABs, also in the Mediterranean Sea, will be analysed: PLTX, OA and its two analogous, DTX1 and DTX2. PLTX is a marine non-protein toxin considered to be among the most toxic substances in the world[21]. Following blooms of PLTX-producing microalgae (*Ostreopsis* spp.), toxic effects on marine organisms (such as bivalves, cephalopods and echinoderms) were recorded, suggesting a negative ecotoxicological impact, also confirmed by laboratory studies. However, the majority of these studies exposed the analysed organism directly to PLTX-producing microalgae without reporting PLTX concentrations actually produced by the algal cells. OA and its analogues are another class of algal toxins frequently detected also in the Mediterranean area, produced by dinoflagellates of the genus *Dinophysis* and *Prorocentum*[136]. Also in this case, few studies report the effects of these toxins at the environmental level, suggesting a potential ecotoxicological impact on the marine environment.

For this reason, the potential ecotoxicological impact of PLTX, OA, DTX-1 and DTX-2 will be evaluated on *Artemia franciscana,* a globally distributed saltwater microcrustaceans, considered a model organism for ecotoxicological studies, especially of the marine environment[192,194–196].

The experimental design is represented in figure 13. Briefly, the toxicity of PLTX ($1.0x10^{-10}$-$1.0x10^{-8}$ M), OA, DTX1 and DTX2 ($1.0x10^{-10}$-$1.0x10^{-7}$ M) will be evaluated by means of cysts hatching and mortality of *Artemia* organisms at two development stages: nauplii Instar I and adults. The results obtained will allow the selection of the most sensitive stage and exposure conditions (toxins concentrations and exposure times) to investigate the relevant mechanisms of toxicity. The mechanism of toxicity will be analysed in terms of oxidative stress induction, evaluated by means of ROS production and enzymatic activity of three main antioxidant enzymes (glutathione S-transferase, GST; superoxide dismutase, SOD; catalase, CAT). Toxic effects will be evaluated also by means of altered *Artemia* movement at the stereomicroscope and, in case of a reduced movement induced by the treatment, the role of cholinesterase activity will be evaluated.

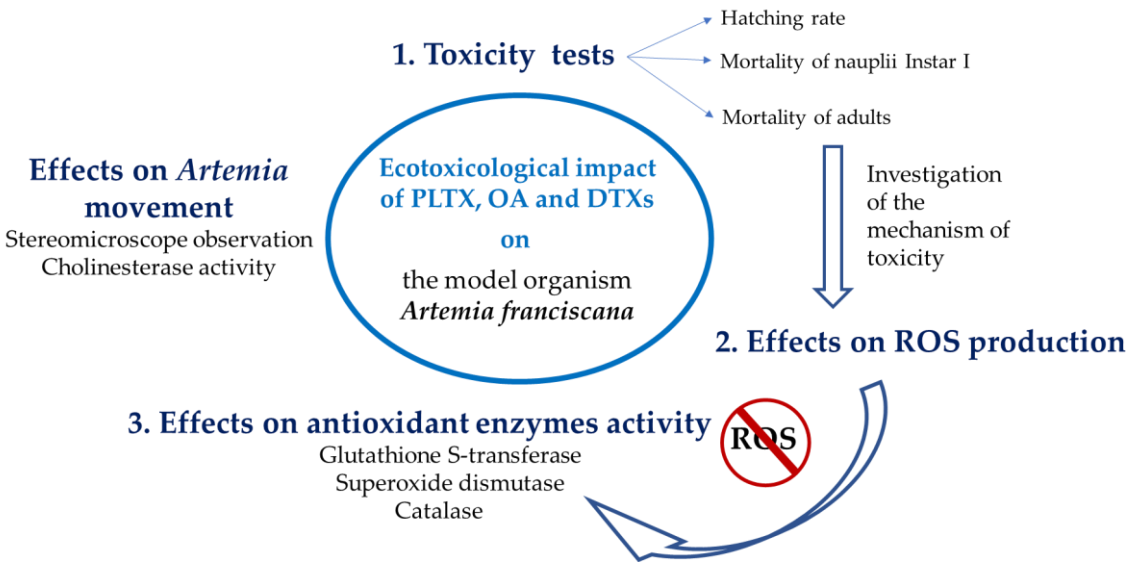

Figure 13. Schematic representation of the experimental design of section A of this thesis.

Materials and methods

1 Toxins

The toxins analysed in the present study are palytoxin (PLTX), okadaic acid (OA) and its analogous dinophysistoxin (DTX)-1 and -2. PLTX was purchased from Wako Pure Chemicals Industries Ltd. (Osaka, Japan), isolated from *Palythoa tuberculosa* (purity > 90%) and was diluted in ethanol (EtOH) 1:1 in distilled water. OA, DTX1 and DTX2 dissolved in methanol (MeOH) 100% were kindly provided by Dr. Jane Kilcoyne (Marine Institute, Rinville, Ireland).

2 *Artemia franciscana*

Since inter-species sensitivity variations have been shown among *Artemia* species (*i.e. A. franciscana* and *A. salina*), to avoid taxonomic inaccuracies, genetic identification of the organism employed in this study was carried out in collaboration with the group of Prof. Pallavicini (University of Trieste). PCR sequencing of the COI gene region confirmed the identity of *Artemia franciscana* by BLASTn comparison with *A. franciscana* isolates (GenBank IDs: DQ119645 and MK393317), which resulted in 99.0% sequence identity, as previously reported[201]. The sequence shared with that of *Artemia salina* ranged only between 84.8 and 84.2%, allowing the exclusion of the species *A. salina*.

3 Hatching and breeding of *Artemia franciscana*

Dehydrated cysts of *A. franciscana* and products for the hatching and breeding of this crustacean were purchased from Hobby (Gelsdorf, Germany). To obtain Instar I stage larvae, approximately 300 mg cysts were hatched in a specific *Artemia* hatchery dish in 750 mL artificial seawater (for each litre of deionized H_2O, 36 g of Optimum Sea basic salt; Wave, Italy) in the constant presence of artificial light at 25 °C for 24 h. Subsequently, larvae were separated from unhatched cysts, transferred into fresh artificial seawater and (i) used for the mortality test or (ii) transferred into a beaker and bred in artificial seawater for 21 days to obtain *A. franciscana* adults. During the first 10 days after hatching, *Artemia* were fed three times a week with liquid (Liquizell, Hobby, Gelsdorf, Germany), and subsequently, solid food (Mikrozell, Hobby, Gelsdorf, Germany), specific for *Artemia* culturing. The organisms were maintained at 25 °C under a 16:8 h light/dark cycle.

4 Toxicity tests

The toxins concentrations range was $1.0x10^{-10}$-$1.0x10^{-8}$ M for PLTX and $1.0x10^{-10}$-$1.0x10^{-7}$ M for OA and DTXs with a dilution factor of 10, maintaining constant the % of the solvent used to dissolve the toxins. This concentration ranges include the environmental relevant concentration detected or predicted in seawater or marine organisms for PLTX/PLTX-like toxins[206–210] or OA and analogues[211–218] based on literature data (<$1.0x10^{-8}$ M, ≤$1.0x10^{-9}$ M, ≤$1.0x10^{-11}$ M, ≤$1.0x10^{-12}$ M, respectively). For each test, the negative control was obtained exposing the organisms to the same % of the solvent used to dissolve the toxins: EtOH 0.5% for PLTX and MeOH 0.1% for OA and DTXs.
These solvents concentrations did not affect viability of *Artemia* up to the longest time of exposure considered (72 h), as resulted from preliminary experiments (for the details see Appendix A and B).

4.1 Hatching test

Hatching test was performed according to Migliore *et al*.[199]. Briefly, in a 96-well plate 10 cysts/well were transferred in a total volume of 200 μL of seawater and treated with the toxins. The amount of nauplii was counted every 24 h up to 96 h under the stereomicroscope (3x of magnification, Kyowa, Tokyo, Japan) and hatching was calculated as number of free-hatched nauplii/number of treated cysts. Results are represented as % with respect to the negative control (CTRL) after 96 h of treatment.

4.2 Mortality test on nauplii Instar I

After cysts hatching in the hatchery dish, nauplii Instar I were transferred in 96-well plate (5 nauplii/well in a total volume of 200 μL in seawater) and treated with the toxins. During the mortality test, nauplii did not receive the feed. According to Zulkifli *et al*.[219] animals that did not present any movement for 10 seconds, observed under the stereomicroscope (Kyowa, Tokyo, Japan at 3× magnification) were considered dead. The amount of dead nauplii was counted after 24, 48 and 72 h (given its high toxicity, for PLTX also 8 and 12 h of exposure were considered). Mortality induced by the toxins was expressed as % with respect to the total number of treated nauplii in each sample.

4.3 Mortality test on adults

After 21 days of breeding, 10 organisms/well were transferred in a 24-well plate and treated with the toxins in a total volume of 1.5 mL in seawater. Adults were fed with solid food 24 h before the test and 24 h after the start of the test. Similar to the mortality test on nauplii, adults were considered dead in case of absence of movement for 10 seconds observed under the stereomicroscope (Kyowa, Tokyo, Japan at 1× magnification) and the results were reported as % of mortality with respect to the total number of treated organisms in each sample.

5 Sample preparation for ROS production measurement and antioxidant enzymes activity assays

To analyse the induction of oxidative stress and the antioxidant enzymes activity after 12 h exposure to PLTX ($1.0x10^{-10}$-$1.0x10^{-8}$ M), or 24 and 72 h exposure to OA and DTXs ($1.0x10^{-9}$-$1.0x10^{-7}$ M), samples were prepared as previously reported[220] with few modifications to adapt the protocols to *Artemia* adults organism. Briefly, 50 adults were transferred in a 6-well plate, treated with the toxins or vehicle (EtOH 0.5% for PLTX and MeOH 0.1% for OA and DTXs) in a total volume of 4.5 mL. After exposure, organisms were washed 3 times in phosphate buffer (PB) 50.0 mM, pH 7 (composed by sodium phosphate dibasic and sodium phosphate monohydrate; Sigma-Aldrich, Milan, Italy) added with 5.0 mM ethylenediaminetetraacetic acid (Sigma-Aldrich, Milan, Italy). The organisms of each group were transferred in eppendorf with 400 µL of 50.0 mM PB pH 7, homogenized for 15 seconds using an immersion sonicator (Ultrasonic processor UP50H; Hielscher, Teltow, Germany); after centrifugation of 25 min at 15 000g at 4 °C, the supernatant was collected and preserved at -80 °C.

6 Reactive oxygen species (ROS) production

ROS production after 12 h of exposure to PLTX or 24 h and 72 h exposure to OA or DTXs was measured using the fluorogenic probe 2',7'-dichlorofluorescin diacetate (DCFDA; Sigma-Aldrich, Milan, Italy) on *Artemia* as preciously reported[201,220]. DCFDA is a non-fluorescent, lipophilic and non-ionic compound capable of diffusing and crossing cell membrane into cytoplasm where it is deacetylated by intracellular esterases, producing 2′,7′–dichlorofluorescin (DCFH), a non-fluorescent and membrane impermeable compound. Different ROS such as H_2O_2[221], peroxyl and hydroxyl radicals[222] are able to oxidase DCFH in a fluorescent compound (fig. 14) [223].

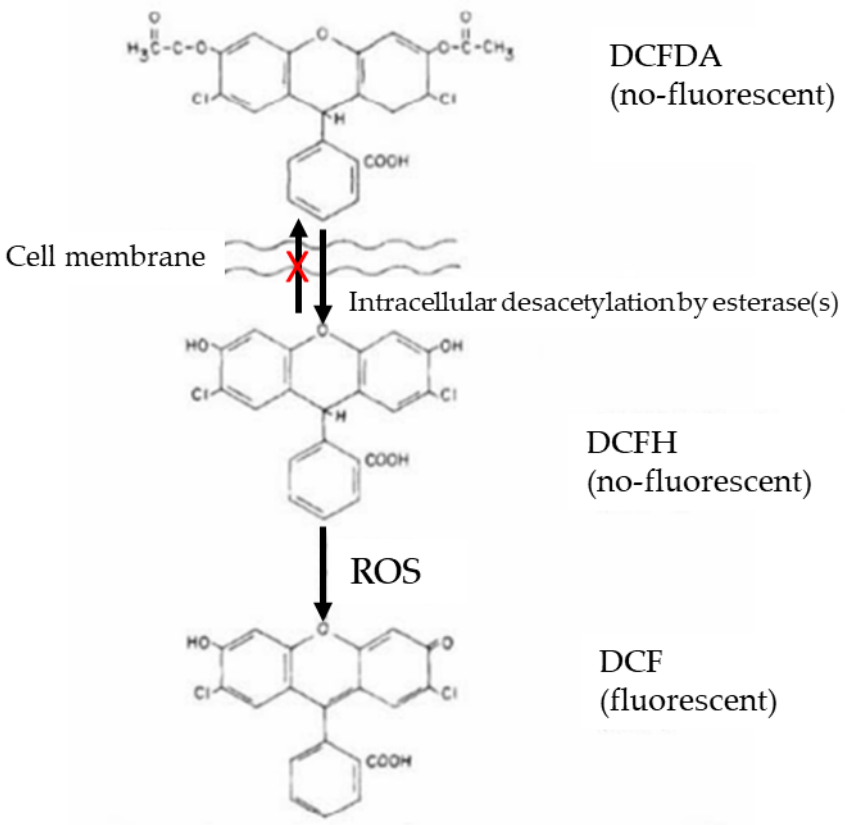

Figure 14. Mechanism of DCFDA probe for the quantification of ROS production[223] *(figure modified).*

In each well of a 96-well plate, 175 µL of phosphate buffered saline (PBS) were added to 5 µL of samples and 20 µL of 4.0×10^{-7} M DCFDA (Sigma-Aldrich, Milan, Italy). Two blanks were included: the first was created by adding 175 µL of PBS to 5 µL of PB 50.0 mM pH 7 (instead of the sample) and 20 µL of 4.0×10^{-7} M DCFDA; the second blank consisted in 195 µL of PBS and 5 µL of samples (none of these blanks produced a significant increase in fluorescence). All the samples were tested in triplicate. The plate was incubated for 30 min at 37 °C in the dark and the fluorescence was read at 485 nm and 520 nm (excitation and emission wavelengths, respectively) using a microplate reader (FLUOstar Omega, BMG LABTECH, Offenburg, Germany). Results were reported as mean Relative Fluorescence Unit (RFU) measured at the microplate reader and normalized on mg of proteins of each sample.

7 Antioxidant enzymes activity assay

Antioxidant enzymes activity was evaluated after 12 h of exposure to PLTX, or 24 h and 72 h exposure to OA or DTXs, considering three main enzymes: glutathione S-transferase (GST), superoxide dismutase (SOD) and catalase (CAT). The activity of these enzymes was measured in sample prepared as reported in the chapter 5 of Materials and methods.

7.1 Glutathione S-transferase activity

Glutathione S-transferase is a family of phase II detoxification enzymes, that conjugates reduced glutathione (GSH) to a wide variety of electrophilic compounds[224].
The activity of GST can be measured using chromogenic substrates such as 1-chloro-2,4-dinitrobenzene (CDNB) which, after the conjugation with GSH by GST, turns a yellow colour upon reaction with glutathione (GSH) with an absorbance pick at 340 nm[225] (fig. 15).

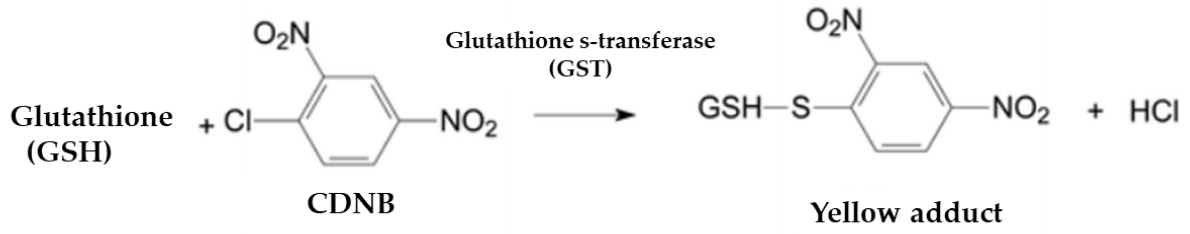

Figure 15. Mechanism of GST activity quantification assay based on the chromogenic substrate CDNB[225] (figure modified).

GST activity assay was based on the methods described by Habig et al.[226] and previously reported[227] and adapted to *Artemia* adults. Briefly, the reaction mix was prepared using 1.3 mM reduced L-glutathione (Sigma-Aldrich, Milan, Italy), 1.3 mM 1-chloro-2,4-dinitrobenzene (CDNB; Sigma-Aldrich, Milan, Italy) in PB (100.0 mM, pH 6.5). In a 96-well plate, 75 µL of the reaction mix was added to 25 µL of each sample and the absorbance was read immediately at 304 nm every 30 sec for 3 min using a microplate reader (FLUOstar Omega, BMG LABTECH, Offenburg, Germany). The blank was prepared in the same way, without the probe (CDNB), being replaced with the buffer.

7.2 Superoxide dismutase activity

Superoxide dismutases are metalloenzymes that convert superoxide radicals to H_2O_2 and O_2. Three different types of SODs are found in nature, which are characterized based on their folding and metal cofactors as follows: Fe- or Mn-dependent, Cu/Zn-dependent, or Ni-dependent[228]. According to Zhao et al.[229], the activity of superoxide dismutase (SOD) was quantified by measuring the enzyme ability to inhibit the photochemical reduction of nitro blue tetrazolium (NBT) (fig. 16).

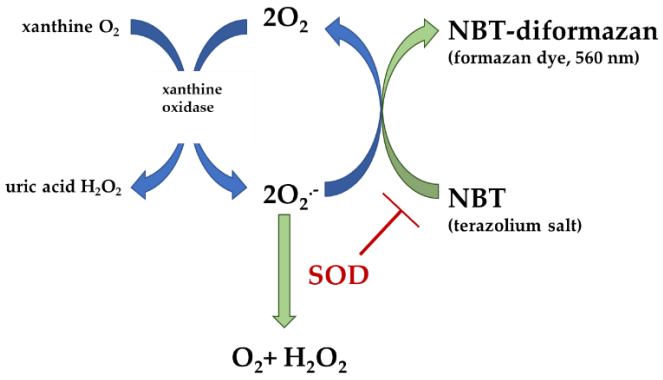

Figure 16. Scheme of SOD activity measurement based on the inhibition of photochemical reduction of NBT[230] (picture modified).

The assay was performed using 96-well plates, adding to each well 25 µL of sample and 75 µL of reaction mixture. The reaction mixture was composed by 50.0 mM phosphate buffer pH 7.8 (composed by Na_2HPO_4 and NaH_2PO-$4H_2O$; Sigma-Aldrich, Milan, Italy), containing 140.0 mM L-methionine (Sigma-Aldrich, Milan, Italy), 0.7 mM NBT (Sigma-Aldrich, Milan, Italy), 0.02 mM Riboflavin (Sigma-Aldrich, Milan, Italy) and 0.1 mM Na_2EDTA (Sigma-Aldrich, Milan, Italy). Blank was created replacing 25 µL of each sample with the same volume of phosphate buffer. The 96-well plate was incubated at room temperature for 30 minutes under a 900-lumen lamp to allow the photochemical reaction, then the absorbance was read at 560 nm using a microplate reader (FLUOstar Omega; BMG Labtech; Ortenberg, Germany).

7.3 Catalase activity

Catalase is an enzyme belonging to the oxidoreductase class involved in detoxification of the cell from ROS. It uses the hydrogen peroxide (H_2O_2) to create water and oxygen, through the following reaction[231]: $2H_2O_2 \rightarrow 2H_2O + O_2$.

H_2O_2 has a UV absorption peak at 240 nm, and the decrease in absorbance at this wavelength corresponds to the amount of hydrogen peroxide eliminated and is therefore a parameter for measuring the activity of this antioxidant enzyme.

CAT activity in *A. franciscana* adults exposed to PLTX for 12 h was quantified as previously described by Zhao *et al.*[229] on earthworms, adapting the assay for *Artemia*. Briefly, 4 µL of sample was inserted in duplicate together with 46 µL of PB (50.0 mM, pH 7.0) inside 96-well UV-transparent plates. Afterwards, 50 µL of a 20.0 mM H_2O_2 solution was added (Sigma-Aldrich, Milan, Italy) to obtain a final concentration in the well of 10.0 mM. Blank was made for each sample, replacing 50 µL of hydrogen peroxide with an equal volume of PB. Then, the plate was read at a wavelength of 240 nm every 30 seconds for 3 minutes, using a microplate reader (FLUOstar Omega; BMG Labtech; Ortenberg, Germany).

7.4 Cholinesterase activity

Cholinesterases (ChE) are a family of enzymes related to neuronal activity, and, in particular, acetylcholinesterase catalyses the hydrolysis of acetylcholine to acetic acid and thiocholine. This one reacts with 2,2-dinitro-5,5-dithiobenzoic acid (DTNB) and forms a yellow compound that absorbs at a wavelength of 405 nm. The increase of the absorbance in the unit of time is proportional to the activity of cholinesterase in the sample[232] (fig. 17).

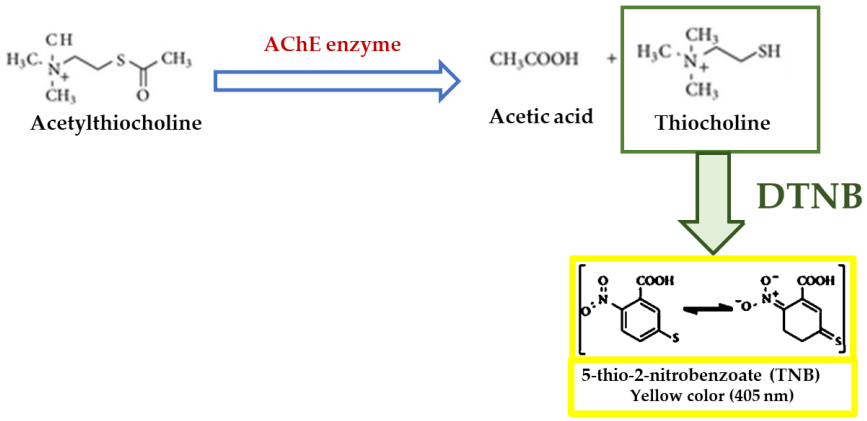

Figure 17. Schematic picture of ChE activity measurement based on DTNB reagent[233] *(picture modified).*

ChE activity was measured following the procedure reported by Jemec *et* al.[234]. In each well of a 96-well plate, 50 µL of *A. franciscana* samples were diluted with 50 µL of a reaction mixture consisting of 100.0 mM potassium phosphate buffer pH 7.4, containing 2.0 mM acetylthiocholine iodide (Sigma-Aldrich, Milan, Italy) and 1.0 mM 2,2-dinitro-5,5-dithiobenzoic acid (DTNB; Sigma-Aldrich, Milan, Italy). The reaction mixture of blank was prepared replacing DTNB with the buffer. The absorbance

of the sample was measured at 405 nm, every minute for 3 min, with a microplate reader (FLUOstar Omega; BMG Labtech, Ortenberg, Germany).

7.5 Enzyme's activity calculation

The enzymes (GST, CAT and ChE) activities were expressed as Enzyme Units (EU), calculated by the following formula:

$$EU = \frac{\frac{\Delta Absorbance}{min}}{\varepsilon * l} * \frac{V\ total}{V\ supernatant}$$

where ε was 9 600 M^{-1} x cm^{-1} for GST, 43.6 M^{-1} x cm^{-1} for CAT, and 13 600 M^{-1} x cm^{-1} for ChE activity assays. The enzymes activity was normalized on mg of proteins (EU/mg proteins) of each samples and the relevant measure units were nmol/min for GST and ChE and μmol/min for CAT.
Instead, one EU of SOD was defined as the amount of enzyme needed to inhibit the photochemical reduction of NBT by 50%, and SOD activity was reported as EU/mg of proteins.

8 Protein content

Protein content in each *A. franciscana* sample prepared to determine the enzymes activity and ROS production were quantified using a NanoDrop 2000 (ThermoFisher Scientific, Milan, Italy) at 280 nm.

9 Statistical analysis

All the results are expressed as mean ± standard errors of the mean (SE) of at least three independent experiments. The concentration inducing 50% of lethality in treated organisms (LC_{50}) was calculated by variable slope (four-parameter) non-linear regression at a statistical confidence interval of 95%, using the GraphPad Prism software version 6.
Depending on the biological assays, data were analysed by one- or two-way analysis of variance (ANOVA) and Bonferroni's post-test, or by the Student's t-test, using GraphPad Prism software version 6. Significant differences were considered for $p < 0.05$.

Results

1 Effects of PLTX on *Artemia* cysts hatching and mortality

The toxic effect of PLTX on different life cycle stages of *Artemia* were evaluated by means of cysts hatching after 96 h of exposure to PLTX ($1.0x10^{-10}$, $1.0x10^{-9}$ and $1.0x10^{-8}$ M) and mortality induced in nauplii Instar I and adults after 8, 12, 24, 48 and 72 h exposure. The negative control (CTRL) represents *Artemia* exposed to EtOH 0.5% (fig. 18).

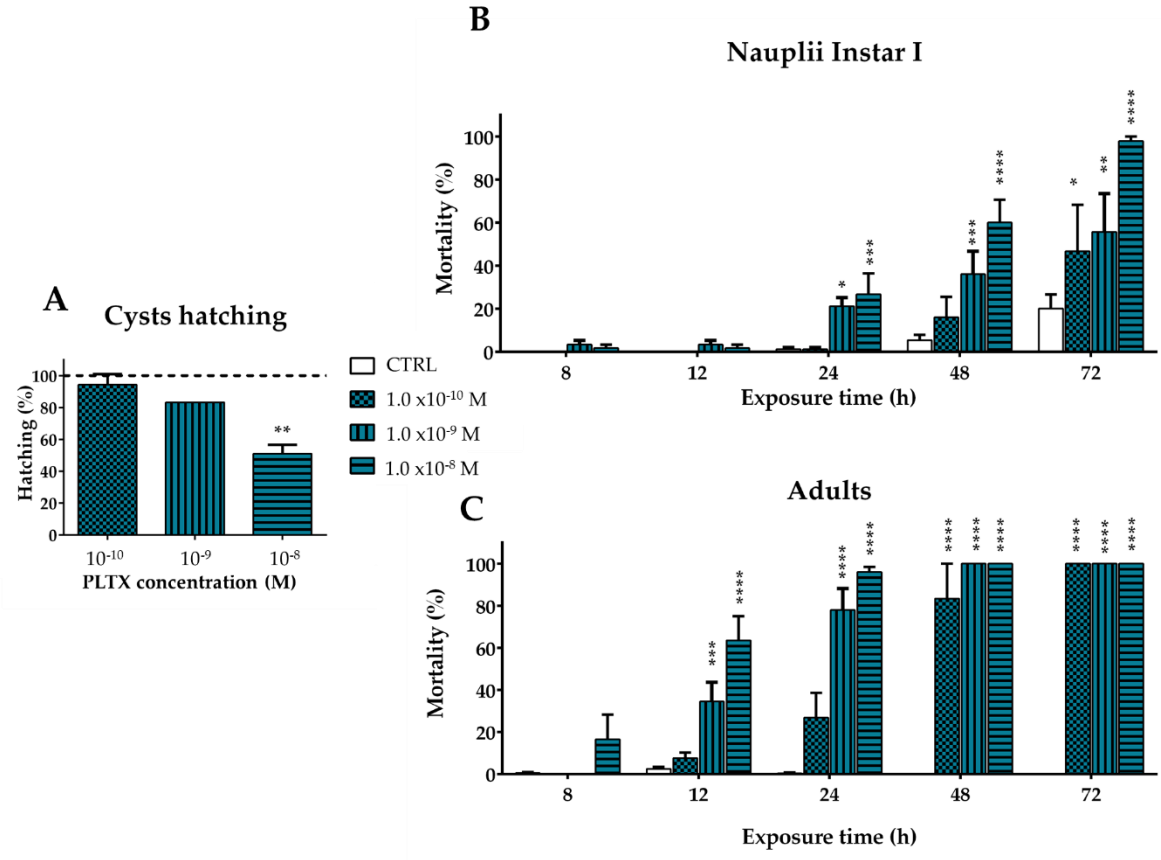

*Figure 18. Effects of PLTX on Artemia franciscana evaluating: A) cysts hatching after 96 h exposure to PLTX ($1.0x10^{-10}$-$1.0x10^{-8}$ M); B) mortality of nauplii Instar I; C) mortality of adults exposed to PLTX ($1.0x10^{-10}$-$1.0x10^{-8}$ M) up to 72 h, evaluated by stereomicroscope. Data are presented as: A) % of free-hatched nauplii with respect to the total number of cysts exposed to the toxin and the dashed line represents the hatching of cysts not exposed to the toxin (CTRL); B) and C) % of dead organisms with respect to the total number of treated animals. Data are expressed as mean ± SE of three experiments. Statistical differences: *, $p < 0.05$; **, $p < 0.01$; ***, $p < 0.001$; ****, $p < 0.0001$ (A) one-way ANOVA and Bonferroni post-test; B) and C) two-way ANOVA and Bonferroni post-test.*

The effect of PLTX ($1.0x10^{-10}$, $1.0x10^{-9}$ and $1.0x10^{-8}$ M) on *A. franciscana* cysts hatching was evaluated after 96 h exposure to the toxin. As compared to cysts not exposed to PLTX (negative control; CTRL), the toxin induced a significant decrease of cysts hatching (49.0%; $p < 0.01$) only at the highest concentration ($1.0x10^{-8}$ M) (fig. 18 A).

Subsequently, PLTX ($1.0x10^{-10}$, $1.0x10^{-9}$ and $1.0x10^{-8}$ M) was evaluated for its ability to induce mortality of *A. franciscana* nauplii Instar I (24 h after hatching) and adults (21 days after hatching) after 8 h exposure to the toxin and up to 72 h. PLTX induced a significant mortality of nauplii starting from 24 h exposure to the concentrations of $1.0x10^{-9}$ M (21.1%; $p < 0.05$) and $1.0x10^{-8}$ M (26.7%; $p < 0.001$). The lowest concentration ($1.0x10^{-10}$ M) induced a significant mortality only after 72 h exposure (46.7%, $p < 0.05$), when the highest toxin concentration ($1.0x10^{-7}$ M) provoked 100.0% mortality of nauplii (fig. 18 B). At this exposure time, the toxin concentration reducing nauplii viability by 50% (LC_{50}) was $0.2x10^{-9}$ M [95% Confidence Intervals (C.I.) = $0.2x10^{-10}$–$2.7x10^{-9}$ M]. In adults, PLTX induced a significant mortality already after 12 h exposure to the concentrations of $1.0x10^{-9}$ M (34.5% $p < 0.001$) and $1.0x10^{-8}$ M (63.5%; $p < 0.0001$), with a LC_{50} of $2.3\ x10^{-9}$ M (C.I. 95%=$1.2\text{-}4.7x10^{-9}$ M). After 24 h exposure, the LC_{50} was $0.3x10^{-9}$ M (C.I. 95%= $0.1\text{-}0.6x10^{-9}$ M). The lowest toxin concentration ($1.0x10^{-10}$ M) induced a significant mortality already after 48 h exposure (83.0 %; $p < 0.0001$), whereas 100% mortality was induced by 72 h exposure to each PLTX concentration (fig. 18 C). These results indicate that adults are more sensitive than nauplii Instar I to the toxic effects of PLTX, with a significant effect on their viability already after 12 h exposure. Thus, the subsequent studies have been carried out on adults exposed to PLTX for 12 h.

2 Effects of PLTX on ROS production and antioxidant enzymes activity

To evaluate the possible mechanism of toxicity induced on *Artemia* adults after 12 h exposure to PLTX ($1.0x10^{-10}$, $1.0x10^{-9}$, $1.0x10^{-8}$), ROS production and the activity of 3 main antioxidant enzymes (GST, SOD and CAT) were considered (fig. 19).

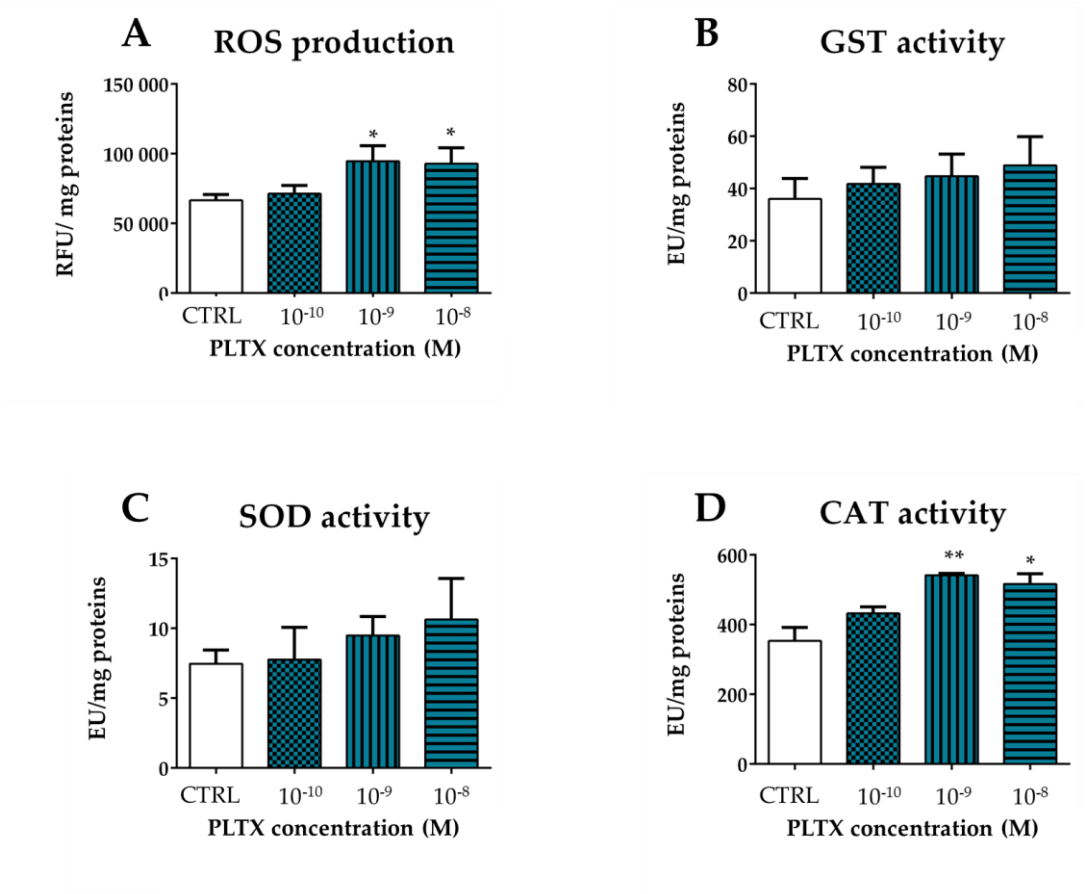

*Figure 19. A) ROS production in A. franciscana adults after 12 h exposure to PLTX evaluated by the DCFDA assay. Data are presented as Relative Fluorescent Units normalized on mg proteins in each sample and are expressed as mean ± SE of four experiments. Statistical differences: *, $p < 0.05$ (Student's t-test). Activity of glutathione S-transferase (GST; B), superoxide dismutase (SOD; C) catalase (CAT; D), in A. franciscana adults after 12 h exposure to PLTX. Data are presented as Enzymatic Unit (EU) normalized on mg of proteins in each sample and are expressed as mean ± SE of at least three experiments. Statistical differences: *, $p < 0.05$; **, $p < 0.01$ (Student's t-test).*

As compared to negative control, the toxin induced a significant increase of ROS production at the concentrations of $1.0x10^{-9}$ and $1.0x10^{-8}$ M (42.0% and 39.0%, respectively; $p < 0.05$) (fig. 19 A). Regarding the activity of the antioxidant enzymes analysed, the most significant effect was recorded for CAT, which activity was significantly increased after exposure to PLTX at the concentrations of $1.0x10^{-9}$ and $1.0x10^{-8}$ M (53.4 % and 46.3 %, respectively; $p < 0.01$ and $p < 0.05$) (fig. 19 D). *A. franciscana* exposure to PLTX induced also a slightly, but not significant, increase of GST and SOD activities (fig. 19 B and C).

3 Effects of PLTX on mobility

Stereomicroscopy observations revealed that exposure of *A. franciscana* adults to PLTX reduced crustacean motility in a concentration-dependent manner. At the highest concentration ($1.0x10^{-8}$ M), *A. franciscana* motility was almost completely hampered (data not shown). To verify whether this effect could be related to an altered cholinergic transmission, the activity of cholinesterase (ChE), an enzyme involved in the regulation of *Artemia* spp. movements, was evaluated in adults exposed to the toxin for 12 h. The results obtained show that the enzyme activity in *A. franciscana* adults was not significantly influenced by their exposure to PLTX (fig. 20).

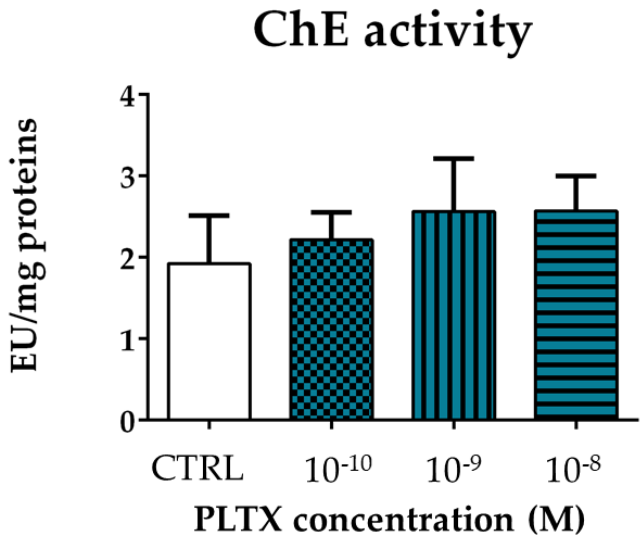

Figure 20. Cholinesterase activity in A. franciscana adults exposed to PLTX for 12 h. Data are presented as Enzymatic Unit (EU) normalized on mg of proteins and expressed as mean ± SE of three experiments.

4 Effects of OA on *Artemia* cysts hatching and mortality

The toxic effects of OA on different life cycle stages of *Artemia* were evaluated by means of cysts hatching after 96 h of exposure to OA ($1.0x10^{-10}$-$1.0x10^{-7}$ M) and mortality induced in nauplii Instar I and adults after 24, 48 and 72 h. The negative control (CTRL) is represented by *Artemia* exposed to MeOH 0.1% (fig. 21).

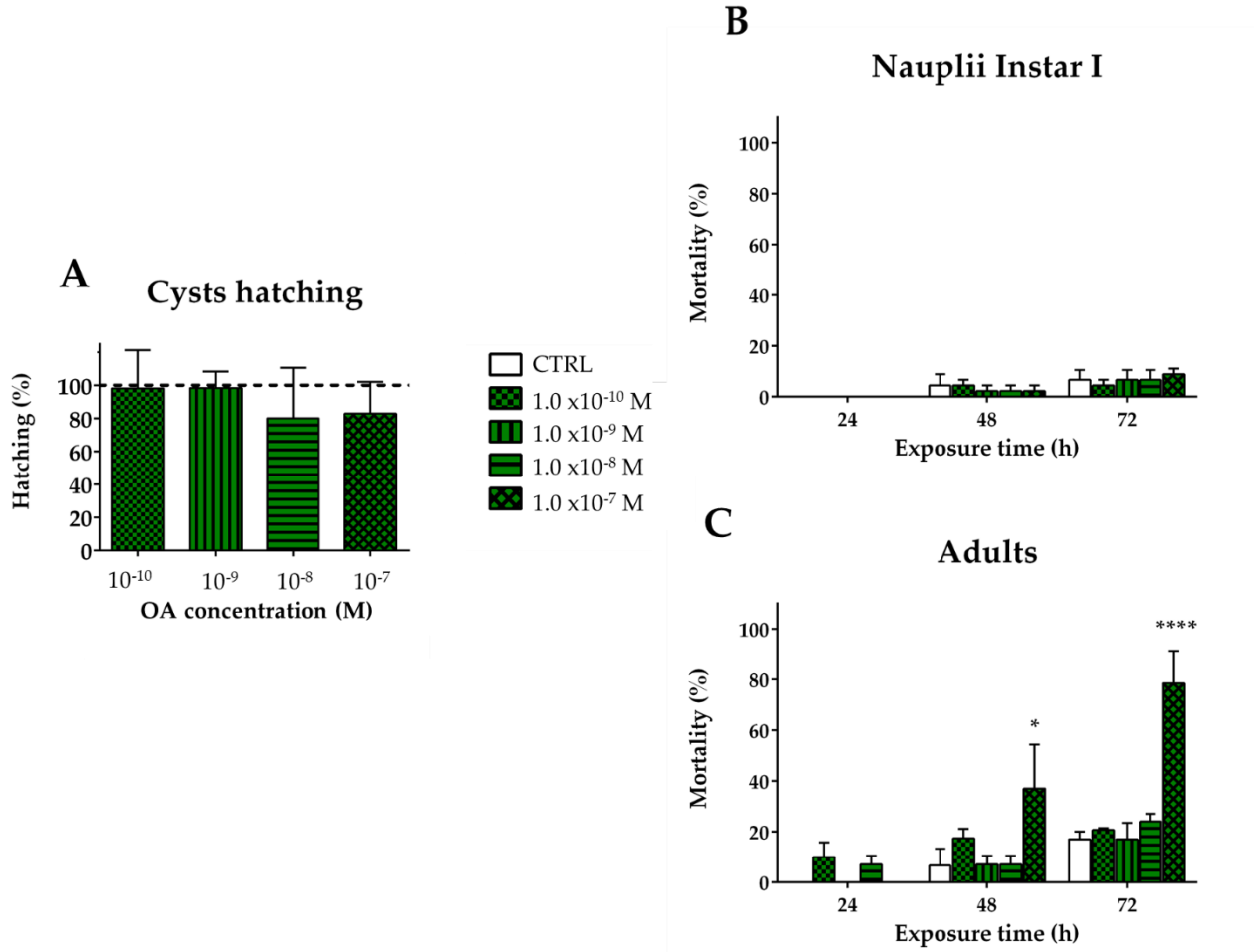

*Figure 21. Effects of OA on Artemia franciscana evaluating A) cysts hatching after 96 h exposure to OA ($1.0x10^{-10}$-$1.0x10^{-7}$ M); B) mortality of nauplii Instar I; C) mortality of adults exposed to OA ($1.0x10^{-10}$-$1.0x10^{-7}$ M) up to 72 h, evaluated by stereomicroscope. Data are presented as: A) % of free-hatched nauplii with respect to the total number of cysts exposed to the toxin and the dashed line represents the hatching of cysts not exposed to the toxin (CTRL); B) and C) % of dead organisms with respect to the total number of treated animals. Data are expressed as mean ± SE of three experiments. Statistical differences: *, $p < 0.05$; ****, $p < 0.0001$. A) one-way ANOVA and Bonferroni post-test, B) and C) two-way ANOVA and Bonferroni post-test).*

Following a 96-h exposure, no significant reduction of cysts hatching compared to the negative control was noticed (fig. 21 A).

In nauplii (Instar I) exposed for 24, 48 and 72 h to OA, none of the concentrations tested significantly increased mortality as compared to the negative control (fig. 21 B). Conversely, in adult organisms (fig. 21 C), mortality significantly increases after exposures of 48 and 72 h at the highest tested concentration ($1.0x10^{-7}$ M), inducing mortalities of 37.0% ($p < 0.05$) and 78.5% ($p < 0.0001$), respectively. The LC_{50} at 72 h exposure was $48.5x10^{-9}$ M (C.I. 95% = $25.9\text{-}91.0x10^{-9}$ M).

On the whole, as shown for PLTX, also for OA the most sensitive developmental stage was the adult one, that was chosen for the subsequent analysis.

5 Effects of OA on ROS production and antioxidant enzymes activity

Artemia adults exposed for a short time to the toxin (24 h, fig. 22) and for a longer time (72 h, fig. 23) were selected to analyse the possible mechanism of toxicity in terms of ROS production and activity of antioxidant enzymes (GST, SOD and CAT). The lowest concentration ($1.0x10^{-10}$ M) was excluded because it did not give any toxic effect at any time and at any stage of *Artemia* life cycle considered.

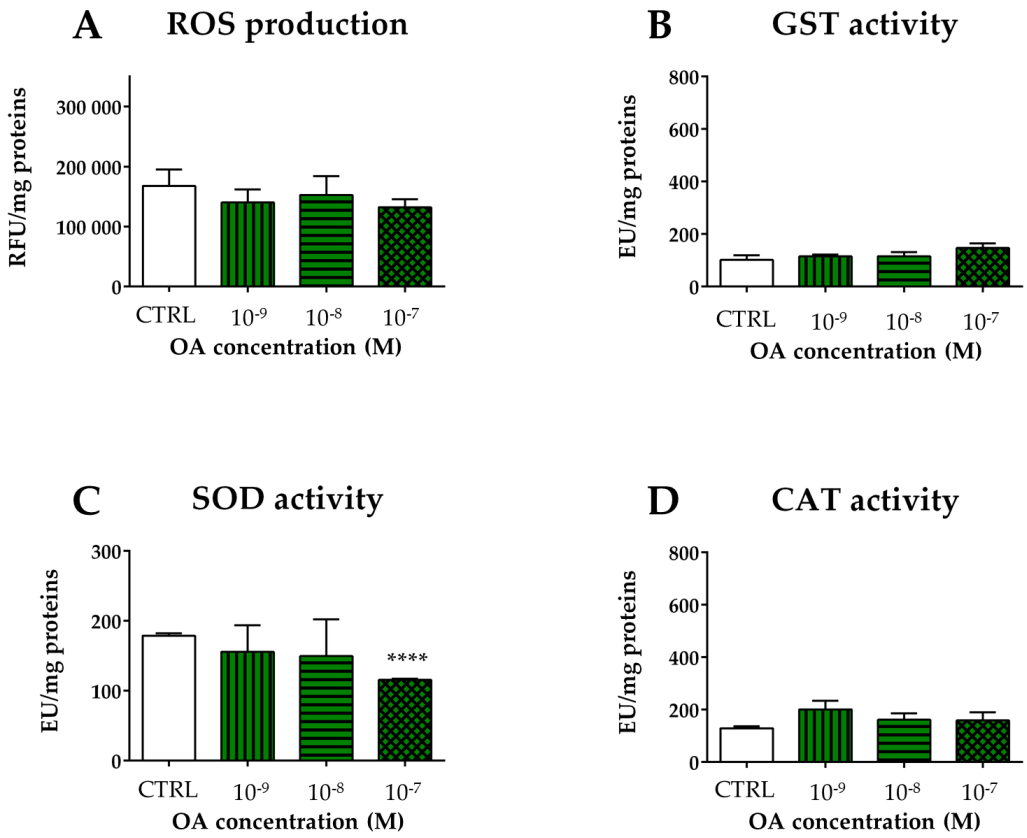

*Figure 22. A) ROS production in A. franciscana adults after **24 h** exposure to OA evaluated by the DCFDA assay. Data are presented as Relative Fluorescent Units normalized on mg proteins in each sample and are expressed as mean ± SE of three experiments. Activity of glutathione S-transferase (GST; B), superoxide dismutase (SOD; C) catalase (CAT; D), in A. franciscana adults after **24 h** exposure to OA. Data are presented as Enzymatic Unit (EU) normalized on mg of proteins in each sample and are expressed as mean ± SE of three experiments. Statistical differences: ****, $p < 0.0001$ (Student's t-test).*

Figure 22 shows the results obtained after 24 h exposure of *A. franciscana* adults to OA. The toxin did not induce a significant increase of ROS production (fig. 22 A) and did not alter the activities of GST and CAT (fig. 22 B and D), in contrast of SOD (fig. 22 C) which activity was decreased by 35.4% ($p < 0.0001$) with respect to the negative control (CTRL) at the highest concentration of toxin ($1.0x10^{-7}$ M).

Analysis of ROS and enzymatic activities of GST, SOD and CAT was carried out also after 72 h exposure to the same OA concentrations. An increase of ROS was recorded only at $1.0x10^{-8}$ M concentration, although this increase was not significant compared to the negative control (fig. 23 A). However, the same concentration of OA significantly increased the activity of GST (235.8%; $p < 0.01$) as compared to the negative control (fig. 23 B). On the contrary, the activities of SOD and CAT were not influenced by 72 h exposure to OA (fig. 23 C and D).

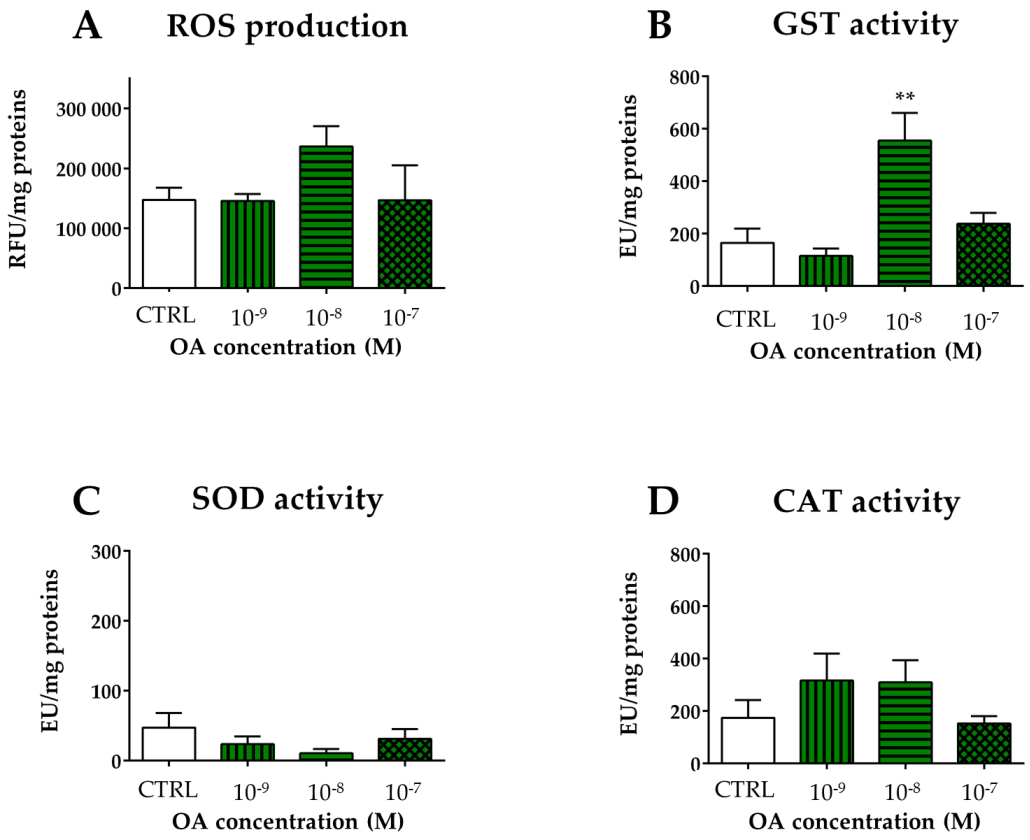

*Figure 23. A) ROS production in A. franciscana adults after **72 h** exposure to OA evaluated by the DCFDA assay. Data are presented as Relative Fluorescent Units normalized on mg proteins in each sample and are expressed as mean ± SE of three experiments. Activity of glutathione S-transferase (GST; B), superoxide dismutase (SOD; C) catalase (CAT; D), in A. franciscana adults after **72 h** exposure to OA. Data are presented as Enzymatic Unit (EU) normalized on mg of proteins in each sample and are expressed as mean ± SE of three experiments. Statistical differences: **, p < 0.01 (Student's t-test).*

6 Effects of DTX1 on *Artemia* cysts hatching and mortality

The same conditions tested for OA were also carried out for the first of the two analogues of this toxin, dinophysistoxin 1 (DTX1) (fig. 24).

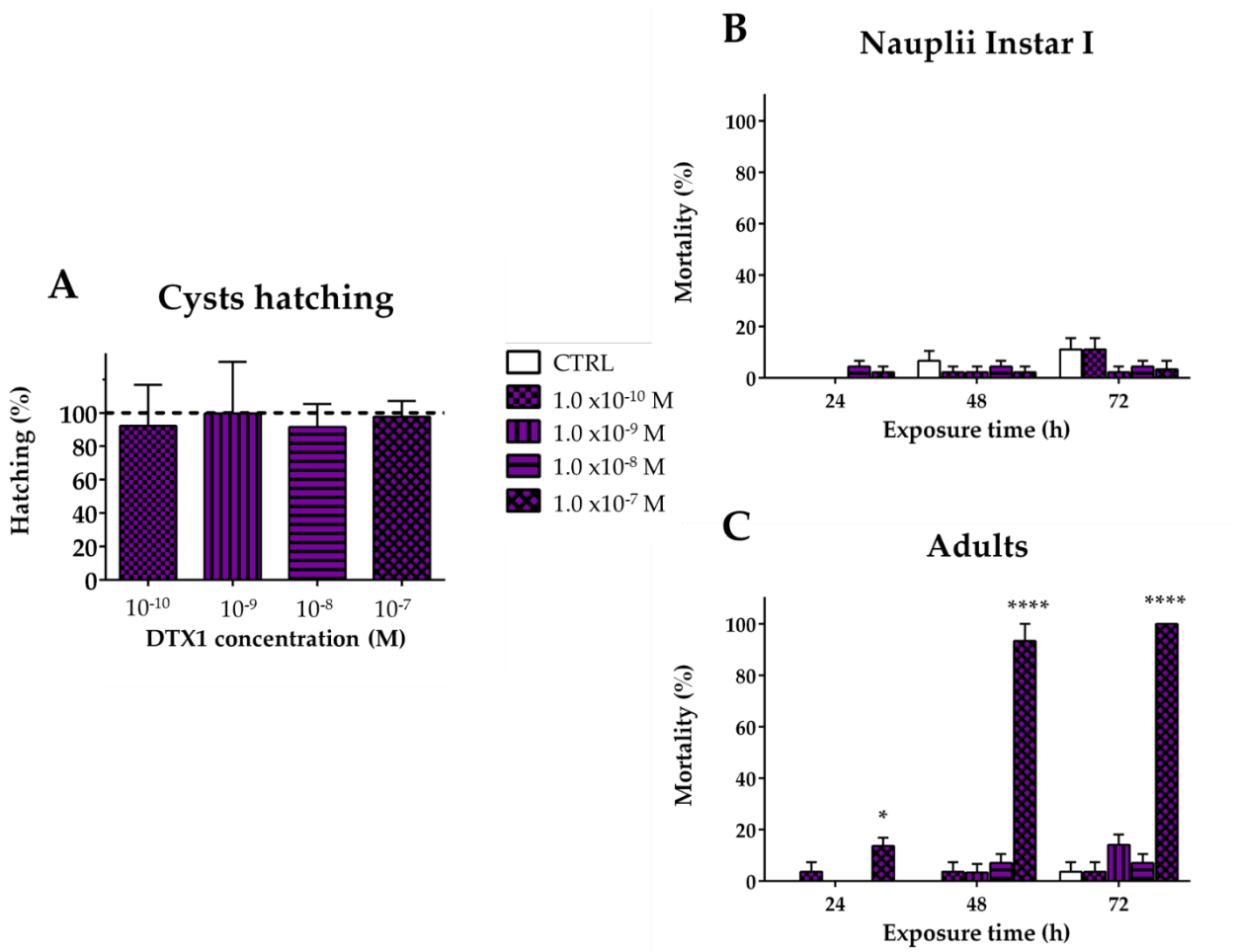

*Figure 24. Effects of DTX1 on Artemia franciscana evaluating: A) cysts hatching after 96 h exposure to DTX1 ($1.0x10^{-10}$-$1.0x10^{-7}$ M); B) mortality of nauplii Instar I; C) mortality of adults exposed to DTX1 ($1.0x10^{-10}$-$1.0x10^{-7}$ M) up to 72 h, evaluated by stereomicroscope. Data are presented as: A) % of free hatched nauplii with respect to the total number of cysts exposed to the toxin and the dash line represents the hatching of cysts not exposed to the toxin (CTRL); B) and C) % of dead organisms with respect to the total number of treated animals. Data are expressed as mean ± SE of three experiments. Statistical differences: *, $p < 0.05$; ****, $p < 0.0001$. A) one-way ANOVA and Bonferroni post-test, B) and C) two-way ANOVA and Bonferroni post-test).*

After 96 h, DTX1 did not alter the hatching rate of the cysts as compared to the control, at any of the concentrations tested (fig. 24 A). Also, no mortality was observed in nauplii (Instar I), following exposure of 24, 48 and 72 h (fig. 24 B). Conversely, in adult organisms (fig. 24 C), mortality was significantly increased after exposures of 24, 48 and 72 h at the

highest concentration tested ($1.0x10^{-7}$ M). This concentration induced a significant mortality compared to the control already after 24 h of exposure (13.7%; $p < 0.05$), which increased to 93.3% ($p < 0.0001$) and 100.0% ($p < 0.0001$) after 48 and 72 h, respectively. The LC_{50} at 72 h of exposure to DTX1 was $17.3x10^{-9}$ M (C.I. 95%= 1.7–$171.1x10^{-9}$ M). Also in this case, comparing the results obtained at the different developmental stages, the adult one appeared to be more sensitive than the first larval stage. For this reason, subsequent tests (ROS analyses and enzymatic activity assays) were carried out taking into consideration only the adult stage.

7 Effects of DTX1 on ROS production and antioxidant enzymes activity

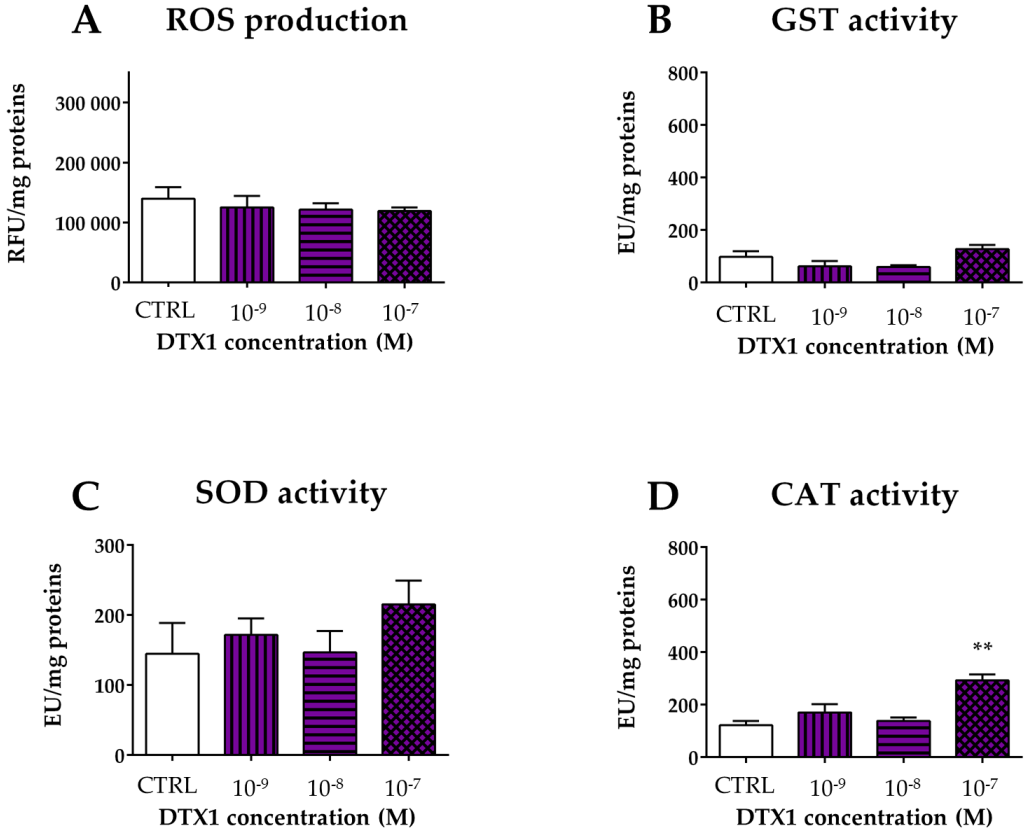

*Figure 25. A) ROS production in A. franciscana adults after **24 h** exposure to DTX1 evaluated by the DCFDA assay. Data are presented as Relative Fluorescent Units normalized on mg proteins in each sample and are expressed as mean ± SE of three experiments. Activity of glutathione S-transferase (GST; B), superoxide dismutase (SOD; C) catalase (CAT; D), in A. franciscana adults after **24 h** exposure to DTX1. Data are presented as Enzymatic Unit (EU) normalized on mg of proteins in each sample and are expressed as mean ± SE of three experiments. Statistical differences: **, p < 0.01 (Student's t-test).*

The percentage of ROS and the activity of the antioxidant enzymes GST and SOD, following 24 hours of exposure to DTX1, were not altered at any of the concentrations considered (fig. 25 A, B and C). On the contrary, analysing the activity of CAT, a significant ($p < 0.01$) increase was observed at the highest concentration of $1.0x10^{-7}$ M (fig. 25 D). This increase of CAT, equal to 141.6% compared to the negative control at 24 h, reached 211.1% ($p < 0.05$) after 72 h of exposure to the toxin (fig. 26 D). At this exposure time, an increase in SOD activity was also observed (fig. 26 C), both at the concentrations of $1.0x10^{-8}$ M (457.5% compared to CTRL; $p < 0.01$) and $1.0x10^{-7}$ M (487.9% compared to CTRL; $p < 0.0001$), while the activity of GST (fig. 26 B) and the production of ROS (fig. 26 A) remained unchanged.

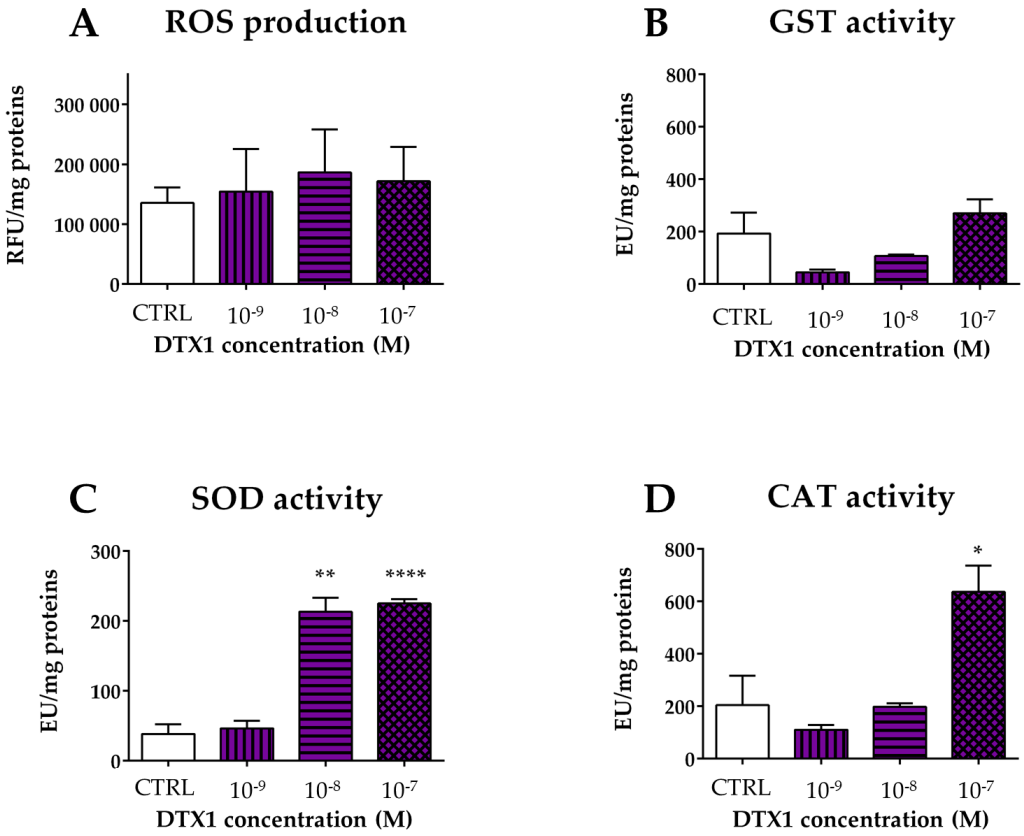

*Figure 26. A) ROS production in A. franciscana adults after **72 h** exposure to DTX1 evaluated by the DCFDA assay. Data are presented as Relative Fluorescent Units normalized on mg proteins in each sample and are expressed as mean ± SE of three experiments. Activity of glutathione S-transferase (GST; B), superoxide dismutase (SOD; C) catalase (CAT; D), in A. franciscana adults after **72 h** exposure to DTX1. Data are presented as Enzymatic Unit (EU) normalized on mg of proteins in each sample and are expressed as mean ± SE of three experiments. Statistical differences: *, p < 0.05; **, p < 0.01; ****, p < 0.0001 (Student's t-test).*

8 Effects of DTX2 on *Artemia* cysts hatching and mortality

The effects of the second analogue of OA, dinophysistoxin 2 (DTX2, $1.0x10^{-10}$-$1.0x10^{-7}$ M) were analysed similarly to the other toxins (fig. 27).

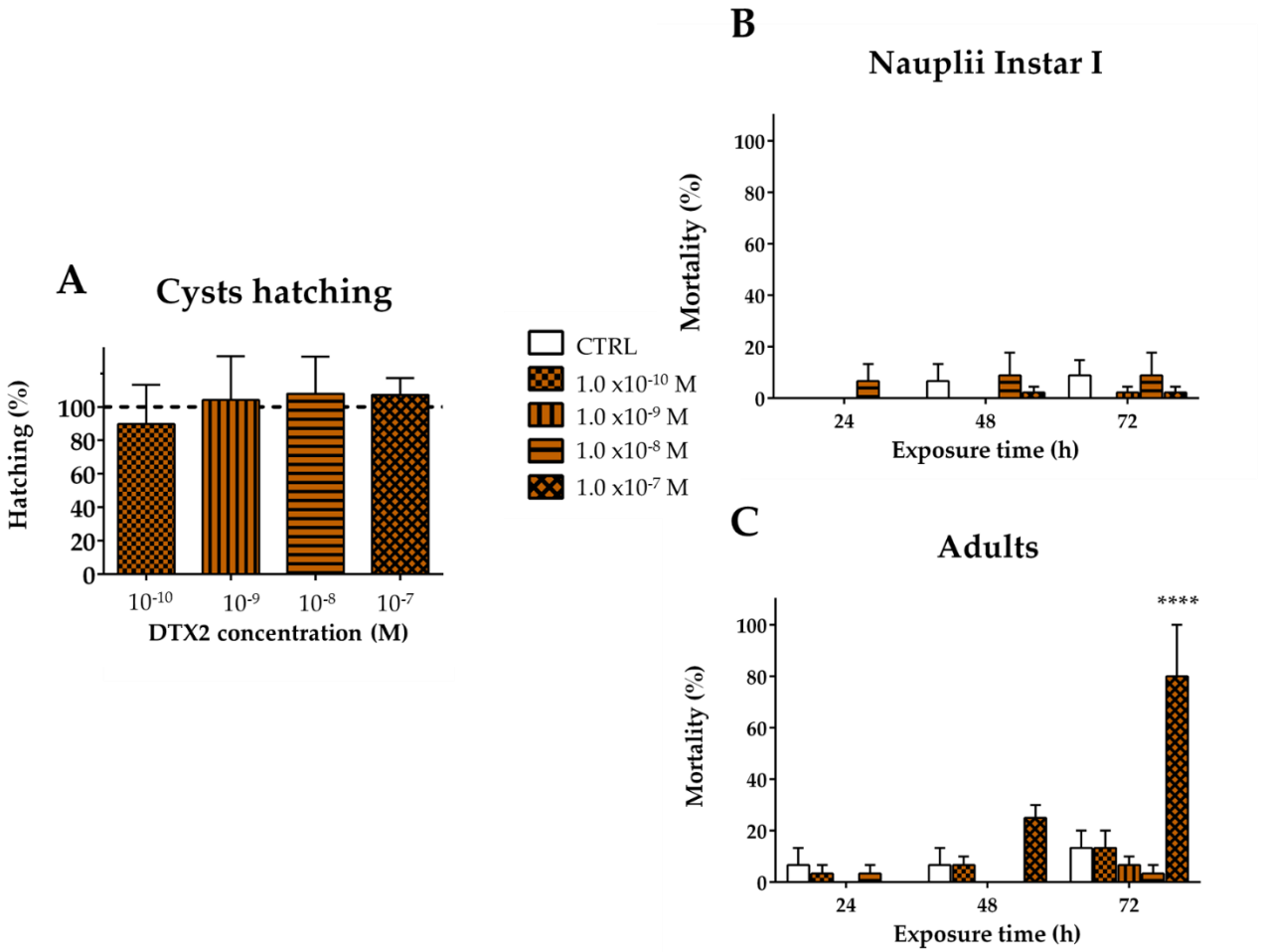

*Figure 27. Effects of DTX2 on Artemia franciscana evaluating: A) cysts hatching after 96 h exposure to DTX2 ($1.0x10^{-10}$-$1.0x10^{-7}$ M), B) mortality of nauplii Instar I; C) mortality of adults exposed to DTX2 ($1.0x10^{-10}$-$1.0x10^{-7}$ M) up to 72 h, evaluated by stereomicroscope. Data are presented as: A) % of free-hatched nauplii with respect to the total number of cysts exposed to the toxin and the dashed line represents the hatching of cysts not exposed to the toxin (CTRL); B) and C) % of dead organisms with respect to the total number of treated animals. Data are expressed as mean ± SE of three experiments. Statistical differences: ****, $p < 0.0001$. A) one-way ANOVA and Bonferroni post-test, B) and C) two-way ANOVA and Bonferroni post-test).*

As found for OA and DTX1, after 96 h, DTX2 did not alter the hatching rate of cysts with respect to the control at any of the concentrations tested (fig. 27 A).

In nauplii (Instar I), following exposures of 24, 48 and 72 h, no mortality was significantly induced by the toxin as compared to the negative control (fig. 27 B). On the contrary, in adult organisms (fig. 27 C), mortality was significantly increased, but only after exposures of 72 h and at the highest concentration tested (1.0×10^{-7} M), inducing a mortality of 80.0% ($p < 0.0001$) with a LC_{50} of 49.7×10^{-9} M (C.I. 95%= $35.9–68.6 \times 10^{-9}$ M). On the basis of these results, also in this case *A. fransciscana* adults were more sensitive than the first larval stage.

9 Effects of DTX2 on ROS production and antioxidant enzymes activity

The most sensitive stage was exposed to DTX2 for a short time (24 h, fig. 28) and a long time (72 h, fig. 29) to the toxin and the possible mechanism of toxicity was analysed in terms of ROS production and activity of antioxidant enzymes (GST, SOD and CAT).

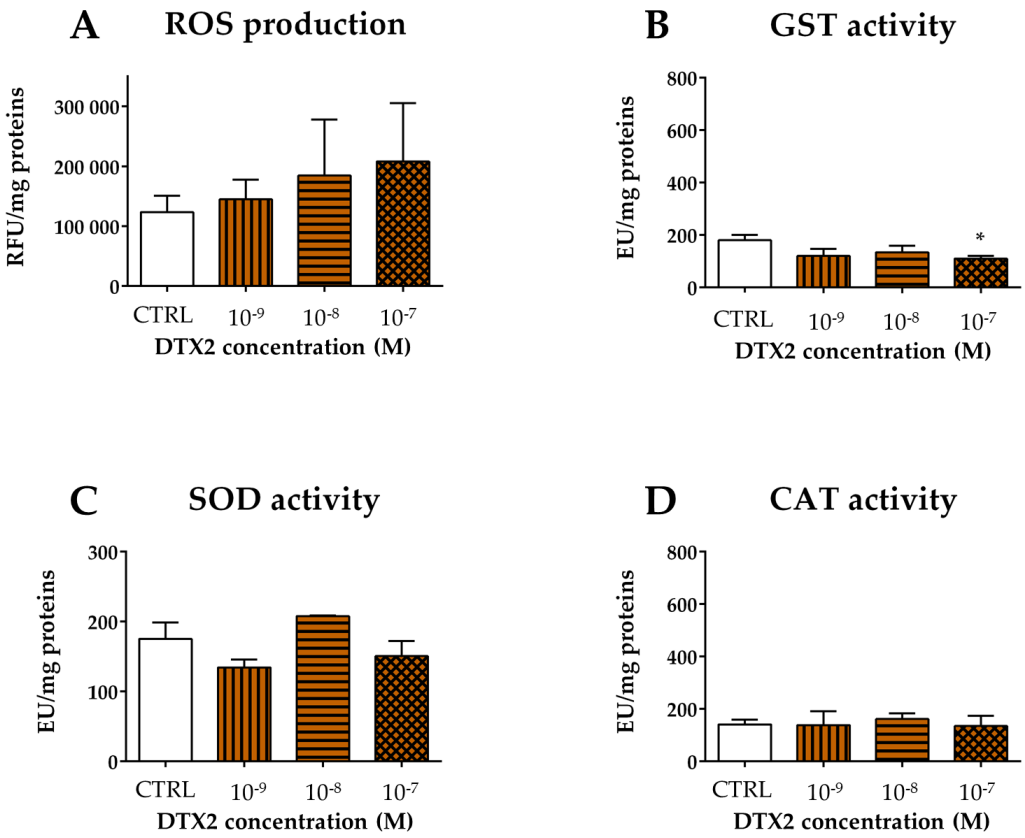

*Figure 28. A) ROS production in A. franciscana adults after **24 h** exposure to DTX2 evaluated by the DCFDA assay. Data are presented as Relative Fluorescent Units normalized on mg proteins in each sample and are expressed as mean ± SE of three experiments. Activity of glutathione S-transferase (GST; B), superoxide dismutase (SOD; C) catalase (CAT; D), in A. franciscana adults after **24 h** exposure to DTX2. Data are presented as Enzymatic Unit (EU) normalized on mg of proteins in each sample and are expressed as mean ± SE of three experiments. Statistical differences: *, $p < 0.05$ (Student's t-test).*

After 24 h of exposure, DTX2 induced a concentration-dependent ROS production, although not significant (fig. 28 A). The enzymatic activity of GST (fig. 28 B) slightly, but significantly, decreased ($p < 0.05$) in comparison to the negative control, at the highest concentration (1.0×10^{-7} M). Conversely, no alterations were detected considering the enzymatic activities of SOD and CAT (fig. 28 C and D) after 24 h of exposure. However, after 72 h of exposure, at the highest concentration (1.0×10^{-7} M), DTX2 significantly increased ROS production (fig. 29 A) as compared to the negative control (80.4%; $p < 0.05$). Similarly, the activities of GST and SOD (fig. 29 B and C) were also significantly increased at this concentration (254.2% and 320.1% respectively; $p < 0.05$). On the contrary, DTX-2 had no effect on the enzymatic activity of CAT (fig. 29 D).

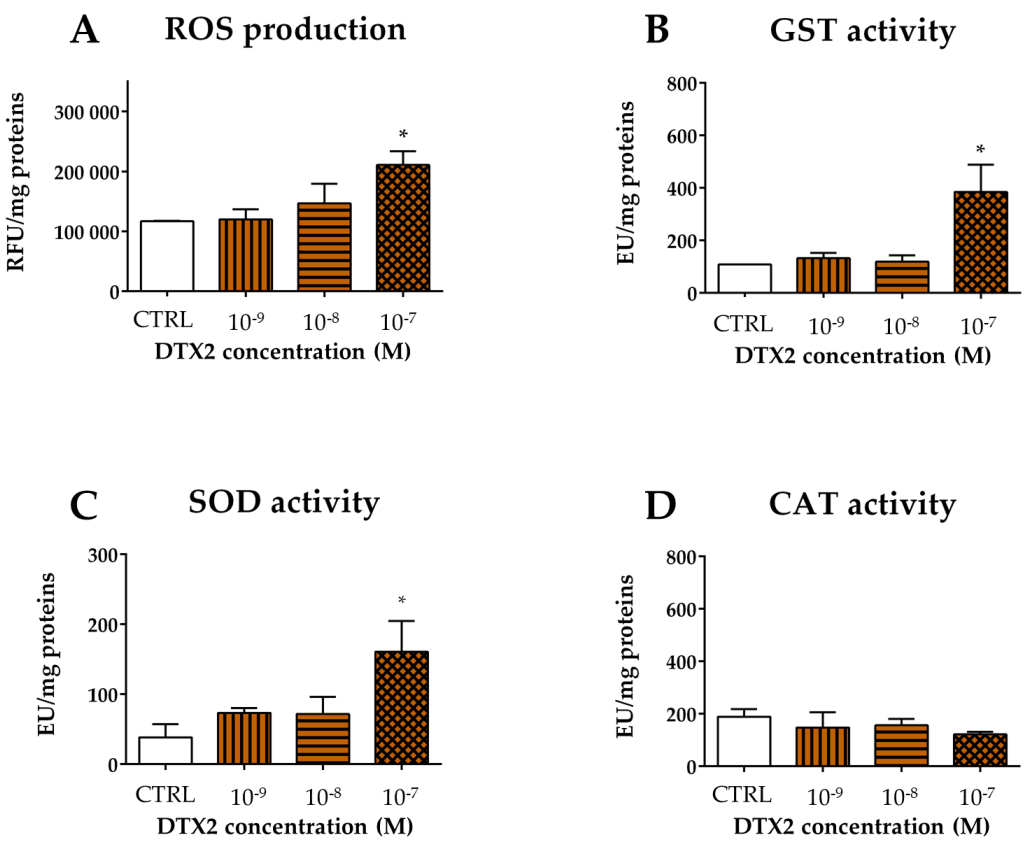

*Figure 29. A) ROS production in <u>A. franciscana</u> adults after **72 h** exposure to DTX2 evaluated by the DCFDA assay. Data are presented as Relative Fluorescent Units normalized on mg proteins in each sample and are expressed as mean ± SE of three experiments. Activity of glutathione S-transferase (GST; B), superoxide dismutase (SOD; C) catalase (CAT; D), in <u>A. franciscana</u> adults after **72 h** exposure to DTX2. Data are presented as Enzymatic Unit (EU) normalized on mg of proteins in each sample and are expressed as mean ± SE of three experiments. Statistical differences: *, $p < 0.05$ (Student's t-test).*

Discussion and conclusion

The expansion of algal toxin producers due to climate changes and anthropogenic actions[121,235–238] is leading to a growing interest towards the possible environmental impact of these toxins. As regards PLTX, OA and DTXs, negative effects on marine organisms have already been recorded following blooms of the relevant producing microalgae[110,111,163]. However, the relevant ecotoxicological impact of the produced toxins still need to be clarified. For this reason, this study was carried out to investigate the effects of PLTX, OA and DTXs on the microcrustacean *Artemia franciscana*. *Artemia* species are considered as representative organisms of marine zooplankton and, therefore, they are widely used as models for ecotoxicological studies[117,118,124,125]. This organism can be used for acute or chronic toxicity studies on different stages of its life cycle (cysts, nauplii at different stages of development and adults) and, having a good knowledge of its biology, it is possible to analyse different physiological parameters, biomarkers of oxidative stress and toxicity, movement and reproductive toxicity analyses are also possible[197]. In this study, the toxic effects induced by PLTX, OA and DTXs were considered on cysts (evaluating the toxin effect on cysts hatching through a rapid, simple and sensitive assay[197]), nauplii stage I and adults (evaluating the mortality induced by the toxin).

Considering the effects induced by PLTX, the hatching analysis revealed that it is the only toxin, among those considered in this study, able to significantly affect cysts hatching, with a reduction of < 50% at the highest concentration tested ($1.0x10^{-8}$ M). This result suggests that PLTX can reduce the number of individuals of *Artemia* population by reducing the release of nauplii from cysts.
Considering the mortality test, this is the first study assessing the toxic effects of purified PLTX (purity > 90%) on *Artemia* adults, suggesting that the organisms at this developmental stage are more sensitive to the toxin than larvae. In adults, the PLTX LC_{50} after 24 h exposure was $0.3x10^{-9}$ M (C.I. 95%= $0.1\text{-}0.6x10^{-9}$ M), but the mortality was significantly increased already after 12 h exposure. This effect appears higher than that recorded by Pezzolesi *et* al.[123] in *Artemia* sp. nauplii (not specified species and nauplii stage) exposed to PLTX for 24 h with a median lethal concentration (LC_{50}) of 4.606 ng/mL (corresponding to around $1.7x10^{-9}$ M PLTX). This different lethal effect is in line with the observation that adults are more sensitive than nauplii, as demonstrated by our study. In addition, the variable inter-species sensitivity is considered in different reviews as one of possible factors influencing the response of *Artemia* crustaceans to numerous substances[194,197]. Pavaux *et* al.[126] recorded about 80% mortality of *A. franciscana* metanauplii

(stages II-III) after 24 h exposure to *O.* cf. *ovata* (4 cells/mL; PLTX equivalents content: 44 ± 17 pg/cell by UHPLC-UV-HRMS). However, it is difficult to compare the results of our study with those obtained by Pavaux and colleagues since the type and the amount of the individual toxins in *Ostreopsis* culture have not been specified. Furthermore, it is known that the major toxin produced by cultures of *O*. cf. *ovata* is ovatoxin-a, PLTX being produced only in traces[123].

In general, comparing the toxin-induced mortality on nauplii and adults of *A. franciscana*, the most sensitive developmental stage was the adult one. This greater sensitivity of adults compared to Instar I nauplii could be due to the different physiology of these organisms; indeed the Instar I nauplii have a digestive tract that is not fully developed and functioning[166], which could limit the absorption of the toxin, with consequent reduction of the toxic effect. Hence, the possible mechanism of toxicity was analysed in more detail at this developmental stage after 12 h exposure to PLTX. In particular, the possible induction of oxidative stress (in terms of ROS production) and activity of three antioxidant enzymes (GST, SOD and CAT) was analysed. Indeed, GST belongs to the phase II detoxification enzymes, and conjugates reduced glutathione (GSH) to a wide variety of electrophilic compounds[224]. It has been identified at significant levels also in *Artemia* where it can bind a wide range of substrates[239], including xenobiotics and ROS. However, the first line of defence toward increased ROS levels in aquatic invertebrates is represented by SOD and CAT antioxidant enzymes[240,241].

Considering ROS, PLTX increased their production at the same concentrations inducing mortality after 12 h of exposure, in association with a significant increase of CAT activity. Induction of oxidative stress by PLTX was already observed in both marine animal cells[120,120,122] and human cells[79,242,243]. Considering that ROS overproduction can damage proteins, lipids and DNA[244] and is implicated in many cell processes, including apoptosis[245] , it cannot be excluded that PLTX-induced oxidative stress may be a possible mechanism of toxicity also in *Artemia*. In addition, our results suggest also a particular role for hydrogen peroxide, in view of the specific increase of CAT activity, that has been reported to be involved in the removal of this ROS[231]. However, despite PLTX is able to induce ROS production and oxidative stress, the low effect on antioxidant enzymes activity, especially GST, suggests that the detoxification systems are not sufficiently activated to protect the crustacean from PLTX toxicity.

Furthermore, stereomicroscopy observations of *A. franciscana* exposed to PLTX showed a concentration-dependent decrease of adults motility, as previously noted in *A. salina* adults exposed to *O*. cf *ovata* cells[124]. Hypothesizing a PLTX effect on the cholinergic transmission system, the activity of cholinesterase has been evaluated in adults exposed to PLTX, considering the role of the enzyme in maintaining normal neuromuscular function. In fact, an increased level of acetylcholine in synapses, consequent to cholinesterase

enzymes inhibition by xenobiotics, can impair the neuromuscular functions[246]. However, cholinesterase activity was not influenced by PLTX in *A. franciscana* adults, ruling out a role for this enzyme. Therefore, it cannot be excluded that the reduced movement could be ascribed to an altered ion homeostasis involving the physiological control of fluid dynamics, as already hypothesized for PLTX analogues produced by *O*. cf *ovata* in *A. salina* adults[124] and for other toxins produced by the dinoflagellate *Prorocentrum lima* in *A. salina* nauplii[247].

Regarding DSP toxins (OA, DTX1 and DTX2), the hatching analysis did not reveal any significant alteration of cysts hatching, in contrast with what observed for PLTX.
The mortality test showed that OA, DTX1 and DTX2 did not induced a significant mortality on nauplii Instar I. On the contrary, these toxins induced a mortality on *A. franciscana* adults.
Regarding OA, its effects on *Artemia* mortality were previously analysed by Gong et al.[248] . The authors showed similar sensitivities between stage I nauplii and adults of *Artemia* spp. exposed to different concentrations of OA with, respectively, an LC_{50} of approximately 170.0 μg/L (C.I. 95%= 143.4-201.7 μg/L) for nauplii Instar I and 186.4 μg/L (C.I. 95%= 156.1-222.6 μg/L) for the adult stage after 24 h of exposure, which correspond to approximately $2.2x10^{-7}$ M and $2.3x10^{-7}$ M of OA, respectively. However, analysing the effects at the lowest concentrations tested by Gong et al. (which correspond to approximately $3.0x10^{-8}$ M, $6.2x10^{-8}$ M and $1.24x10^{-7}$ M), and which are therefore comparable to those used in this thesis ($1.0x10^{-10}$-$1.0x10^{-7}$ M), mortality always remained below 20% after 24 h of exposure for both adults and Instar I nauplii, as also found in the present study.
Regarding DTXs, a first study was carried out by Koukaras and colleagues in 2014[249] exposing nauplii (24 h from hatching) and adults for 24 h to phytoplankton samples taken from Thermaikos Gulf in 2002 during algal blooms containing also *Dinophysis* cf. *acuminata* (55–65% of the total phytoplankton biomass). The authors did not record an increase in mortality of nauplii, while in adults, 50% of mortality was found. However, not all the types of microalgae collected by the authors were reported, as well as the presence of algal toxins and their concentrations. In a recent study, an LD_{50} of 0.0819 μg/mL (i.e., about $1.0x10^{-7}$ M) was found for DTX1 on *A. salina* nauplii (stage not specified)[250], in contrast with the results of this thesis not reporting mortality in nauplii. The difference could be due to different stages of development of *Artemia* nauplii (not specified by the authors) as well as to the different species of *Artemia*[194,197].
Also in the case of DSP toxins, the most sensitive developmental stage of *A. franciscana* was represented by adults, on which all the subsequent analysis were carried out. In particular, OA and DTX1 did not induce oxidative stress in adults of *Artemia franciscana* either after

24 h and 72 h of exposure. However, they altered the activities of the antioxidant enzymes analysed in this study. Specifically, after 72 h of exposure, a significant increase of GST was observed for OA, suggesting an activation of the detoxification system which could explain the non-significant increase of ROS production observed for this toxin. Considering DTX1, 24 and 72 h exposure increased CAT activity, an enzyme specific for the removal of hydrogen peroxide[231], as mentioned above. In addition, also SOD activity was significantly increased after 72 h exposure, an enzyme that converts superoxide radicals to H_2O_2 and O_2[228], suggesting that also superoxide anion could be involved. The combination of both SOD and CAT activation may imply an efficient detoxification from superoxide radicals and, subsequently, from the resulting hydrogen peroxide, and could in part explain the absence of ROS production detected after 72 h exposure to DTX1.
Among DSP toxins, the only able to significantly increase ROS production was DTX2. A significant increase was observed after 72 h exposure to the highest concentration which was also associated with a high mortality. At the same concentration ($1.0x10^{-7}$ M) and exposure time (72 h) a significant increase of GST and SOD activities was also observed suggesting that the detoxification system was activated even if it was not sufficient to protect the organism.
On the whole, basing on our data, the rank of toxic potential of DSP toxins is DTX1 > OA = DTX2. The fact that DTX1 is more potent with respect to OA and DTX2 has already been reported in the literature[251]. According to Huhn *et* al.[252], the difference in toxicity found between the three toxins could be due to the affinity of the latter for protein-phosphatase 2A (PP2A), fundamental enzyme for many cellular processes, including cellular division and differentiation and neuronal activity. DTX1 and DTX2 have methyl groups on C35, respectively in equatorial and axial position, as opposed to OA, which does not have a methyl group in the same position. In DTX1, the favourable positioning of the methyl group compared to the aromatic bonds of His191 in PP2A explains its greater affinity towards that toxin. Conversely, the placement of the methyl group in DTX2 creates an unfavourable interaction and reduces the binding energy, decreasing its affinity for PP2A.

In conclusion, these results suggest a potential ecotoxicological impact of these four toxins due to a possible reduction of *Artemia* population. Being *Artemia* spp. a model organism of the marine zooplankton, which is at the basis of the marine food web, a reduction of its population at the environmental level could have repercussions on organisms at higher trophic level. However, it is important to underline that for all the toxins considered, the toxic effects on *Artemia* were recorded at concentrations higher than those detected at the environmental level. In fact, OA concentrations was detected in the marine environment ranging from $1.0x10^{-9}$ M (in seawater in Spain) to $1.9x10^{-12}$ M (in seawater in China) and

$0.38x10^{-12}$ M (in marine phytoplankton in China)[214,215]; while the concentrations of DTX1 was detected in seawater ranging from $1.0x10^{-11}$ M (in China, in the waters of the Bohai Sea) to $4.0x10^{-13}$ M (in China, in the waters of Daya Bay)[214,253]. And finally, the concentrations of DTX2 detected in the marine environment vary from 3.0 to $8.0x10^{-13}$ M in the Bohai Sea (China)[254], and between $1.2x10^{-12}$ M and $1.9x10^{-12}$ M in the Yellow Sea and Bohai Sea (China)[216]. For PLTX, concentrations < $1.0x10^{-8}$ M were measured in *O.* cf *ovata* cultures[206]. However, it must be kept in mind that incidence and frequency of HABs and the expansion of the producers of these toxins are constantly increasing. Furthermore, population of microalgae during HABs could be heterogeneous and/or produce different types of toxins, leading to cumulative effects on the exposed marine organisms. For this reason, further studies are necessary to better understand the negative effects of HABs on marine organisms, specifically analysing the toxic effects induced by combined exposure to different toxins that are often detected in the environment during algal blooms.

Section B

Introduction

1 Human stem cells

Stem cells are non-specialized cells characterized by self-renewal and differentiation properties towards different somatic cell types. On the basis of this capability, they can be classified into totipotent, pluripotent or multipotent stem cells: (i) totipotent cells are able to differentiate into any type of cells of an organism, including extraembryonic cells; (ii) pluripotent stem cells (PSC) can differentiate into the 3 primary germinative layers (endoderm, mesoderm and ectoderm) which are then able to give rise to the different organs and tissues of the organism; (iii) multipotent cells, on the other hand, are able to differentiate into a limited number of somatic cells belonging to the same embryonic layer and represent the majority of adult somatic cells. PSCs possess the ability to carry out a certain number of replicative cycles maintaining the same differentiation stage, a characteristic that makes them a good model for different types of studies, both pharmacological (for example in the field of regenerative and personalized medicine) and toxicological ones. The first stem cells to be used for such studies were derived from embryonic stem cells (ESC), isolated from the internal cell mass (ICM) of the mammalian embryo blastocyst. However, cell extraction led to embryonic destruction leading to ethical [255] and clinical problems, the latter characterized by the appearance of teratomas and the risk of rejection after transplantation[256]. In 2006, the research group of Takahashi and Yamanaka, introducing 4 genes encoding transcription factors in murine fibroblasts, discovered the possibility of inducing their conversion into pluripotent stem cells. This discovery gave rise to the so-called induced Pluripotent Stem Cell (iPSC), pluripotent stem cells artificially generated starting from somatic cells. The transcription factors in question are: POU class 5 homeobox 1 (*POU5F1*, also called *OCT4*), box-SRY 2 (*SOX2*), Kruppel-like factor 4 (*KLF4*) and proto-oncogene MYC (*C-MYC*)[257]. During the following years, also other genes have been added such as Nanog homeobox (*NANOG*) and *Lin-28* (fig. 30). In particular, *NANOG* and *OCT3/4*, control the self-renewal of pluripotent stem cells, and constitute a pair of transcriptional factors essential for pluripotency. The expression of most pluripotency-associated genes, including fibroblast growth factor 4 (*FGF4*), undifferentiated embryonic transcription factor 1 (*UTF1*), F-box protein 15 (*FBXO15*), the determining factor left-right 1 (*LEFTY1*) and *NANOG*, are regulated in association with *OCT3/4* and *SOX2* in undifferentiated cells but not in differentiated cells. Furthermore, *SOX2* plays a crucial role in the control of *OCT3/4* expression[258] while *C-MYC* is a

proto-oncogene associated with the development of various types of tumours, with the function of recruiting proteins that modify chromatin, leading to widespread transcriptional activation. KLF4 acts as an oncoprotein and is capable of activating *SOX2*[259]. Although the precise mechanisms have not been fully elucidated, the coordination of these factors leads to the reprogramming of somatic cells into pluripotent ones. Initially, in order to reprogram somatic cells into iPSC, mainly integrative methods, such as retroviruses and lentiviruses, were used. However, this type of methods led to the development of insertional mutations with a consequent risk of tumorigenicity. To avoid these drawbacks, other non-integrative methods have been developed, including reprogramming using adenoviruses, vector plasmids and Sendai viruses[260]. The introduction of iPSC has allowed the overcoming of ethical problems related to ESC but not of the risk of carcinogenicity, due to the fact that the expression of oncogenes can increase when cells are reprogrammed[261]. This is also due to the use of viral vectors such as retroviruses and lentiviruses for reprogramming which can lead to chromosomal instability and carcinogenesis through insertional mutagenesis. However, in recent years, new safer and non-integrative reprogramming methods have been developed, achieving better efficiency and decreasing the aforementioned problems. Other limits on the use of iPSC concern epigenetic memory and clonal variability. These, in fact, can present an epigenetic memory of the mother somatic cell which can influence the propensity to differentiate into the original lineage. This peculiarity of iPSC, not characteristic of ESC, can predispose them to differentiate more readily into their parental cells than others. However, this aspect could be useful in cell replacement therapy[262]. The other problem concerns the intra-variability differences of the clones of the same patient[262], as well as the inter-variability differences due to the intrinsic variations in different individuals[255], considered more relevant than intra-individual differences[263]. However, the data regarding clonal intra-variability are conflicting and therefore other studies are needed to elucidate the genetic and epigenetic characteristics of the different clones.

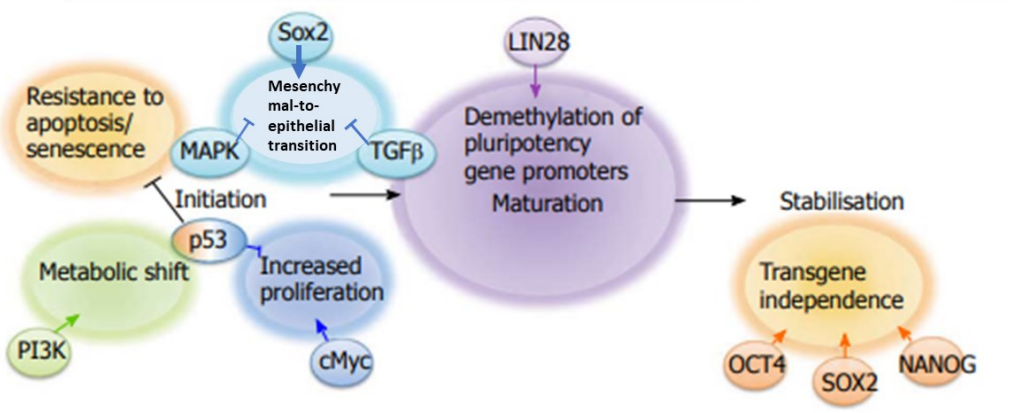

Figure 30. The key stages in human induced pluripotent stem cell reprogramming and the signalling pathways that regulate them[264].

Many characteristics of iPSC are shared with ESC, including the expression of stem cell markers, the formation of tumours containing cell types from all the three embryonic layers, and the ability to contribute to the formation of many tissues. ESC and iPSC appear to have similar defence mechanisms against reactive oxygen species that damage DNA, with comparable capabilities for maintaining genomic integrity[265]. However, comparative genomic analysis revealed differences between the two cell types. For example, hundreds of genes are differentially expressed in ESC and iPSC[266], and subtle but detectable epigenetic differences, such as DNA methylation, have been reported[267]. Currently, it is unclear whether these differences are shared between cell lines reprogrammed using different protocols[266]. Furthermore, it should be noted that the functional implications of the observed differences are currently unknown and such differences may eventually prove to be functionally irrelevant. Therefore, other studies are needed to better understand the efficacy and safety of these cells[268].

2 Potential uses of iPSC

Reprogramming of somatic cells to iPSC can be carried out on cells that are easily retrieved by humans' tissues, such as skin fibroblasts or peripheral blood mononuclear cells (PBMC) collected from blood. This feature makes them an innovative model for patient-specific studies. In particular, patients' fibroblasts or PBMC can be reprogrammed to a state of pluripotency while maintaining the genetic characteristics of both the patient and the disease. Therefore, iPSC could become excellent models not only in personalized medicine and for developing and screening drug candidates, but also for cell replacement therapy in regenerative medicine.

Here are some potential uses of iPSC[269] (fig. 31):

- Transplants: organ rejection is the main complication in these cases. Hence, organ and tissue transplantation involve the use of immunosuppressants, with significant side effects, that not always are able to avoid rejection. The use of differentiated organs or tissues starting from iPSC obtained by reprogramming the patient's somatic cells could circumvent these problems, minimizing the chances of rejection by making the use of immunosuppressants no longer necessary.

- Cell therapy and disease models: another key advantage of using iPSC compared to the current transplant approach is the ability to repair pathogenic mutations by homologous recombination in iPSC, differentiate them in the tissue of interest and transplant them into the patient. Promising experiments performed in mice suggest the feasibility of this approach. For example, murine cells affected by anemia were reprogrammed to iPSC and, after having repaired the associated genetic anomaly by homologous recombination, cells were differentiated to blood progenitors and implanted in anemic mice, where they produced healthy red blood cells[269]. Thus, this approach could be applied to any disease associated with particular genetic mutations and which can be treated with cell transplantation. A second example is represented by iPSC derived from a patient with amyotrophic lateral sclerosis (ALS) that have been differentiated into motor neurons, the cells affected in this disease, in order to transplant them into patients to replace damaged motor neurons[270]. Recently, also Parkinson-associated phenotypes and functional cardiomyocytes that exhibit characteristic cardiac action potentials have been studied using iPSC[271].

- Pharmacological studies and personalization of therapy: one of the objectives of patient-based iPSC approaches is to use these personalized disease models to identify new effective drugs and study any adverse effects. Many studies related to the identification of new therapies and adverse drug effects using patient-specific iPSC are currently available[272]. Furthermore, in the pharmacological field, patient-specific iPSC were used as a basis for drug development, particularly during the drug screening process. For each drug that reaches the market, an average of 5 000 to 10 000 compounds are subjected to preclinical tests with very high costs. To reduce these costs, more precise predictive toxicity models would be useful. Also for this application, iPSC are an excellent model for drug screening, being able to recapitulate *in vitro* specific phenotypes of the disease. In addition, the use of iPSC also allows for the study of adverse drug effects related to single nucleotide polymorphisms that may affect an individual ability to effectively metabolize drugs and toxins. Adverse effects induced by drugs are the main cause leading to the discontinuation of a therapy, in particular nephrotoxicity, cardiotoxicity and

hepatotoxicity are some of the main causes of failure during preclinical tests of candidate drugs. Variable outcomes are also due to individual different response to potential therapeutic agents, that is one of the main problems in developing effective drugs for a given pathology[273].

- Toxicological studies: although one of the main objectives of stem cell research concerns regenerative medicine and clinical applications, this technology can also be applied in the toxicological field[274]. *In vitro* human stem cell systems are important for predictive toxicology, for understanding toxicity mechanisms and for obtaining detailed dose-response data directly from human models[274]. In addition, they represent a practical and economical alternative to traditional approaches, replacing the use of animals or immortalized human cells and allowing to determine in advance the toxicity and adverse effects of compounds in the pharmaceutical industry. ESC and iPSC are also a good model for embryotoxicity studies, thanks to their ability to self-renew and to their pluripotency. To predict the toxicity of a substance on the embryo, an *in vitro* toxicity test on embryonic stem cells (EST: Embryonic Stem cell Test) has been developed, in which the ability to inhibit survival and/or differentiation is determined[275]. Indeed, this cell model, representing the early stages of foetal development, are a useful tool for clarifying the mechanisms by which toxic molecules influence cell differentiation. Current test systems for embryotoxicity prediction are mainly based on animals or *in vitro*–cultured animal-derived cells and do not or not sufficiently mirror the situation in humans. In fact, although they are a good model, the application of an *in vivo* test is very expensive, time-consuming and involves lots of ethical concerns relating to the use of animals for experimental purposes[276]. Moreover, to avoid the false classification of substances due to inter-species differences, human-relevant toxicity tests are needed. iPSC are considered an *in vitro* model of 8–14 day-old fertilized ova[277], the differentiation period of 1 week is equivalent to the early phase of the absolute hypersensitivity period, and for this reason these cells are a promising model for the early phase of human embryonic development. Indeed, technical and ethical limitations create a challenge to study early human development, especially following the first 3 weeks of development after fertilization, when the fundamental aspects of the body plan are established through the process called gastrulation. Our current knowledge is derived from: (i) the anatomical and histological studies on Carnegie Collection of human embryos, which were carried out more than half a century ago. Due to the 14-day rule on human embryo research, there have been no experimental studies beyond the fourteenth day of human development; (ii) mutagenesis studies on animal models, mostly in mouse, are often extrapolated to human embryos to understand the transcriptional regulation of human development.

However, due to the existence of significant differences in their morphological and molecular features as well as the time scale of their development, it is obvious that complete knowledge of human development can be achieved only by studying the human embryo[278]. In literature, several toxicological studies using stem cells to determine the toxicity of xenobiotics and their ability to influence embryonic differentiation are currently available. One such study was conducted by Serio et al. in 2020 where the effects of ethanol on ESC differentiation were studied, demonstrating morphological changes, as well as a loss of pluripotency in treated cells[279]. Furthermore, iPSC have been used to study the effect of thalidomide on cell differentiation during foetal development as an *in vitro* model to study the mechanism of teratogenicity of this drug[280]. Moreover, other studies used stem cells as an *in vitro* embryotoxicity model to understand the effects of different substances, such as persistent pollutants routinely found in human blood (polyfluoroalkyl substances, including perfluorooctanesulfonic acid; and perfluorooctanoic acid)[281], all-*trans* retinoic acid, 13-*cis* retinoic acid, valproic acid[282]. In addition, stem cells are a good model for study pathogenesis of congenital virus infections such as coxsackievirus B3, measles virus, Rubella virus[283], Zika virus and human cytomegalovirus[284].

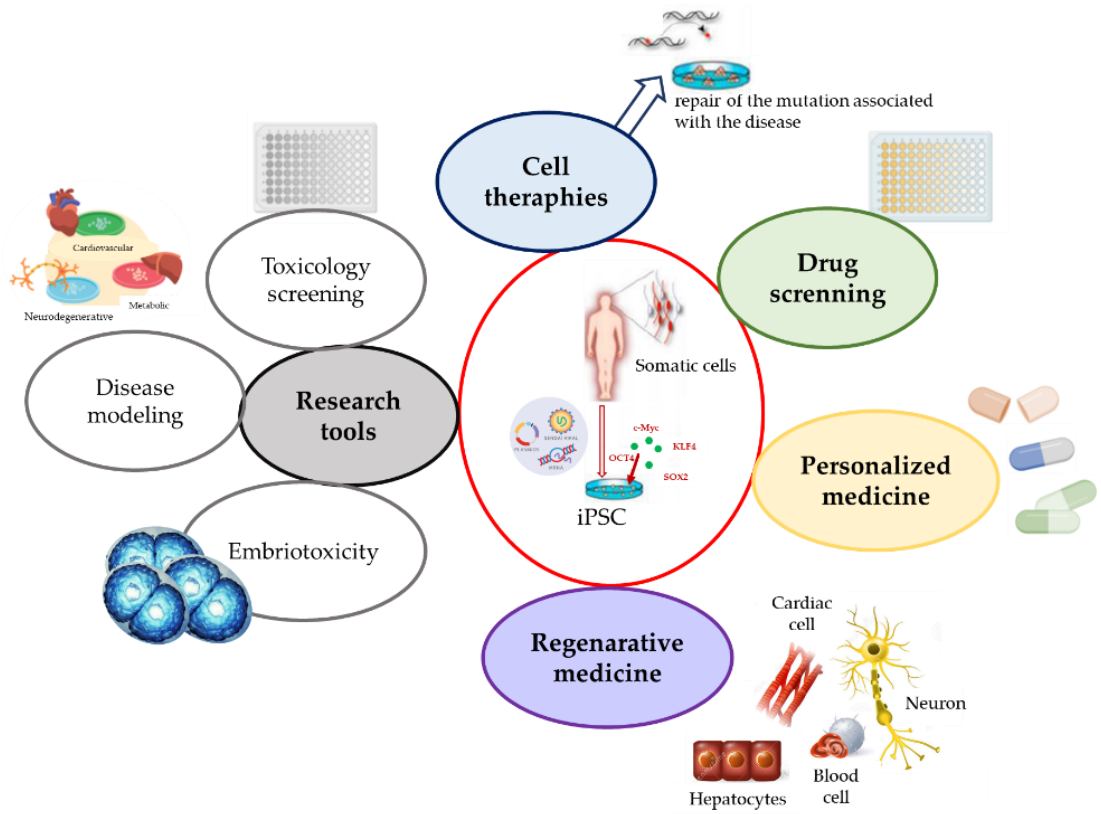

Figure 31. Summary of same potential uses of iPSC.

Aim

PLTX induces a number of symptoms in humans that depend on the route of exposure to this toxin[40], the most dangerous is certainly the oral one, leading also to few cases of deaths in tropical areas after the ingestion of seafood contaminated with this toxin. While the symptoms induced by oral, inhalation, skin and ocular exposure are well known, little is known about the potential embryotoxicity of PLTX, even though a couple of studies suggested a potential negative effect of the toxin on *Xenopus laevis* embryos[128,129]. In the section B of the present thesis, the potential embryotoxicity of PLTX will be evaluated using a human induced pluripotent stem cell (iPSC) line as an *in vitro* model for the early embryonic development stage[282–286]. These cells are characterized by self-renewal, the ability to differentiate *in vitro* into all cell types that derive from the three embryonic germ layers and the ability to form teratomas if implanted *in vivo*. The experimental design will be divided into three steps, each one representing a different stage of development (fig. 32). In the first step, the cytotoxic effect of PLTX and its impact on stemness of undifferentiated stem cells will be evaluated on iPSC as a model of blastocyst, the development step that goes from day 5 to 13 after fertilization, in which the formation of the internal mass takes place[287,288]. This aspect will be evaluated in terms of gene expression profile of a panel of 13 genes (markers of stemness and differentiation into the three embryonic layers: endoderm, mesoderm and ectoderm) and relative protein expression. The second step will analyse the effect of PLTX on the correct differentiation of iPSC into the three germ layers, a phase representative of the stage starting from day 14 after fertilization, when the embryonic stage is called gastrula in which the formation of endoderm, mesoderm and ectoderm takes place. Also in this case, gene and protein expression profile of stem cell markers and of markers of the three embryonic germ layers will be analysed. Finally, the cytotoxic effect of PLTX on the three differentiated germ layers will be analysed in the third and last step to evaluate any selective toxicity of the toxin towards one of these layers, to analyse if the toxin can potentially compromise the correct development of the derived cell types and organs.

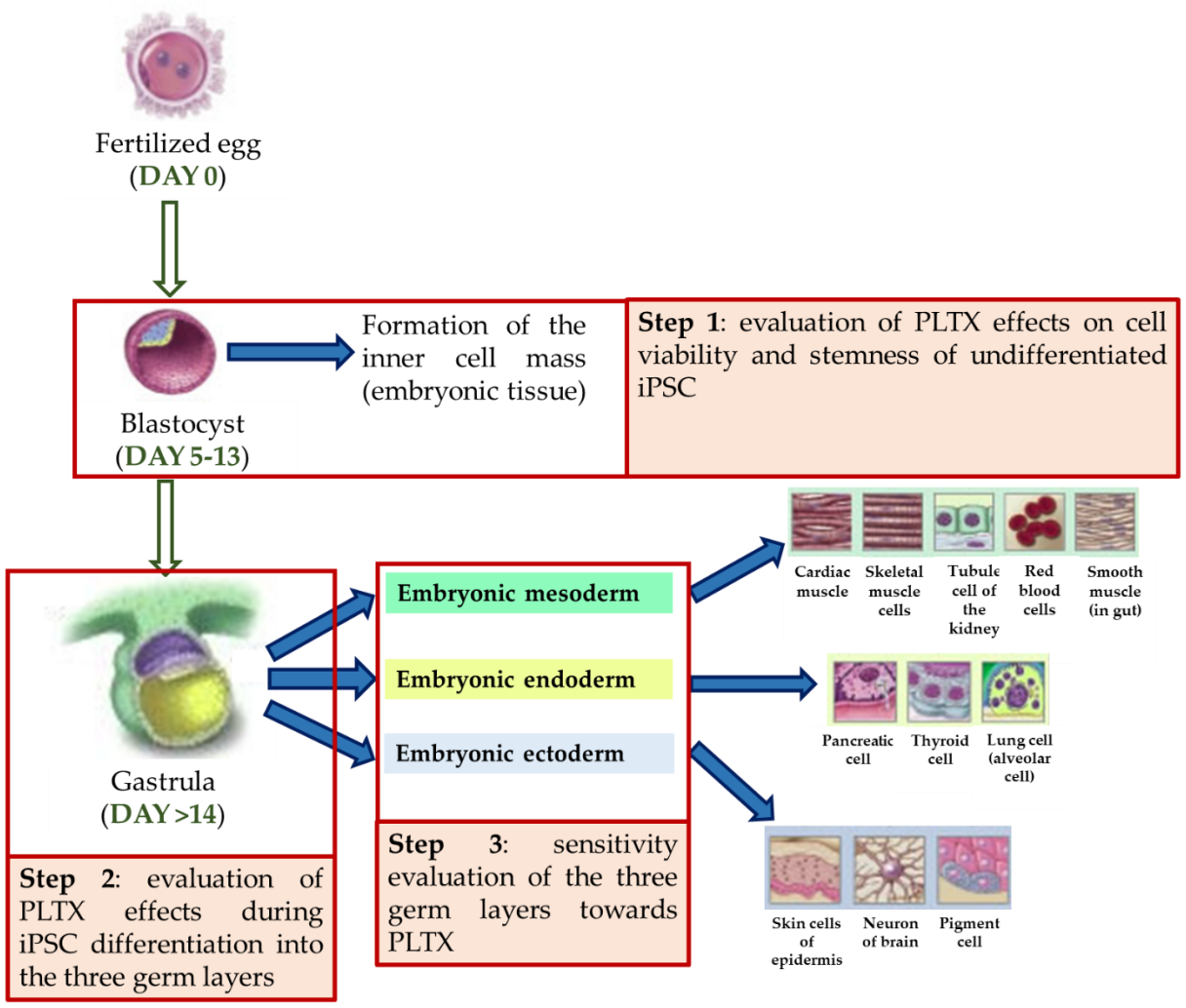

Figure 32. Schematic representation of the experimental design of section B of this thesis, based on the early embryonic development stages that occurs in humans.

Materials and methods

1 Cell culture

1.1 Induced pluripotent stem cell (iPSC)

The study was carried out on the induced pluripotent stem cell line 253G1, obtained by reprograming adult human dermal fibroblasts through viral transduction of OCT3/4, SOX2, KLF4, and C-MYC, kindly provided by Prof. Katsunori Sasaki and Fengming Yue (Shinshu University, Matsumoto, Japan). iPSC was cultured in adhesion clusters in 6-well cell culture plates under feeder-free conditions at 37 °C and 5% CO_2 in basal medium Stem Macs iPS Brew XF added with 2% supplements Stem Macs iPS Brew XF 50 X (Miltenyi Biotec, Bergisch Gladbach, Germany). To allow a better cell adhesion, the plate was pre-incubated for 2 hours with a 1:100 Geltrex® solution (LDEV-Free Reduced Growth Factor Basement Membrane Matrix; ThermoFisher Scientific, Milan, Italy) in Dulbecco's Modified Eagle Medium/Nutrient Mixture F-12 1X (DMEM/F12; Sigma-Aldrich, Milan, Italy), which was then removed at the time of cell seeding. Cell passage was carried out twice a week, when the culture is about 70-80% confluent, avoiding the complete disintegration of the formed clusters. During the passage, culture medium was removed, washed with 1 mL of Dulbecco's Phosphate Buffered Saline (PBS; Sigma-Aldrich, Milan, Italy) and the plate was incubated at 37 °C in 5% CO_2 for 3 minutes with 1 mL of a Versene solution (0.48 mM EDTA in PBS; ThermoFisher Scientific, Milan, Italy). The solution was then removed, and the cells were detached with gentle circular motions using 1 mL of culture medium. The required amount of cells for subculture was transferred to a new well resulting in a 2 mL final volume of culture medium. At the end of the step, 2 μL of ROCK inhibitor 10 mM (Y-27632; Miltenyi Biotec, Bergisch Gladbach, Germany) were added to facilitate cell adhesion, eliminated after 24 hours by medium changing.

In the case of cell seeding for *in vitro* assays, in order to allow cell counting, iPSC was passed into single cells. Specifically, after washing with PBS, cells were incubated with Versene for 6 min, using 1 mL of medium, they were detached from the well, transferred into a 15 mL falcon and centrifuged for 5 minutes at 400g. Subsequently, the supernatant was removed, the pellet was resuspended in 1 mL of culture medium and cell count was carried out in a Bürker chamber. For the count, 90 μL of a Trypan-Blue solution in PBS (1:1) were added to 10 μL of cells suspension.

The number of cells was calculated using the following formula:

$$\frac{\text{n° cells}}{\text{mL}} = \frac{\text{total cells counted}}{\text{number of chamber considered}} \text{ x } 10^5$$

The number of seeded cells and the volume of TC used for each test will be specified below. They derive from preliminary tests, taking into account the number of cells needed to obtain reliable results while preventing cells confluence, as required for the iPSC line culture maintenance protocol.

1.2 HaCaT cell line

The HaCaT cell line, a spontaneously immortalized human keratinocytes, having morphological and functional characteristics similar to those of human skin keratinocytes[289], were bought from Cell Line Service (DKFZ, Eppelheim, Germany). These cells grow in adhesion with a replication time of 24 hours in a complete culture medium consisting of: high glucose Dulbecco's Modified Eagle's Medium (DMEM; Sigma-Aldrich, Milan, Italy) added with 10% of foetal bovine serum (FBS; Euroclone, Milan, Italy), 1% L-glutamine 200 mM (Euroclone, Milan, Italy), 1% penicillin 10 000 IU/mL and streptomycin 10 000 IU/mL (Euroclone, Milan, Italy).
Cell passage was performed once a week after reaching cell confluence and after 4 days the medium was changed. During cell passage, cell medium was eliminated, cells were pre-washed with 0.05% ethylediaminetetraacetic acid (EDTA; Sigma-Aldrich, Milan, Italy) in PBS and pre-treated with additional 2 mL for 20 minutes at 37 °C in 5% CO_2. Cells were subsequently detached by adding 1 mL of 0.05% EDTA and 1 mL of 0.1% trypsin (Sigma-Aldrich, Milan, Italy) in PBS for 2 minutes. After inactivating trypsin by adding 7 mL of culture medium, cells were counted in Bürker's chamber, as reported above. The suspension was then centrifuged for 5 minutes at 400g at room temperature and the pellet was resuspended in 9 mL of culture medium. Finally, cells were seeded in 25 cm^2 flasks (500 000 cells in 7 mL of culture medium) and kept in an incubator at 37 °C in 5% CO_2. In case of cell seeding for *in vitro* assays, 5 000 and 15 000 cells/well were seeded in 96-well plates, respectively, in 200 µL, according to previously development of the protocols.

2 MTT reduction assay

The 3-(4,5Dimethylthiazol-2-yl)-2,5-diphenyltetrazolium bromide (MTT) reduction assay is a colorimetric assay that allows to measure cell viability. MTT, which is yellow in solution, is reduced by the mitochondrial succinate dehydrogenase enzyme into purple formazan salts, which are retained as a precipitate in the cytoplasm. The quantity of salts produced is proportional to the number of viable cells[290]. The viability assay used was modified from the protocol reported by Mosmann[291]. The test was performed, for all the cell lines used, in a 96-well plate by seeding 5 000 cells/well in 100 μL of culture medium for iPSC and 200 μL of culture medium for HaCaT cells. Cells were exposed to the toxin after 24 h from seeding for iPSC and after 96 h for HaCaT cells. To evaluate cytotoxicity induced by PLTX ($1.0x10^{-14}$-$1.0x10^{-7}$ M), different exposure times (from 4 up to 96 h) were considered. In particular, for the two longest exposure times (72 and 96 h), also the relevant recovery conditions were analysed in parallel, by exposing the cells for 24 h to PLTX, followed by two washes in PBS and additional 48 or 72 h exposure to toxin-free cell medium (100 μL/well).

After each exposure time, cell medium was removed and replaced with 100 μL of fresh medium added in a 10:1 ratio with 5 mg/mL MTT (Sigma-Aldrich, Milan, Italy) solution in PBS, and the cells were incubated for additional 4 h. At the end of the incubation time, culture medium was removed, and the formed formazan salts were solubilized using 100 μL/well of dimethyl sulfoxide (DMSO; Sigma-Aldrich, Milan, Italy). The absorbance was read through a spectrophotometer (FLUOstar Omega, BMG LABTECH, Offenburg, Germany) at the double wavelength of 540 and 630 nm.

The results obtained were expressed as percentage of cell viability as compared to control cells not exposed to the toxin (corresponding to 100% viability) and are the mean ± standard error (SE) of the mean.

3 Binding assay

PLTX binding to whole cells was evaluated by a cell-based ELISA developed at the University of Trieste[292,293]. Briefly, cells were exposed to PLTX, and its binding with the extracellular portion of the cell membrane Na^+/K^+ ATPase pump was detected through the use of an anti-PLTX monoclonal antibody and a secondary anti-mouse antibody conjugated with the Horse-Radish Peroxidase (HRP). Cell binding was thereafter measured by a colorimetric reaction in which the intensity of the colour was directly proportional to the number of immune complexes formed.

Cells were seeded in 96-well plates, at 5 000 cells/well for iPSC and 15 000 cells/well for HaCaT cells for 4 days at 37 ° C in 5% CO_2. For iPSC, a medium change was also performed the day after seeding to eliminate the ROCK inhibitor. Subsequently, cells were treated with PLTX ($5.1x10^{-13}$–$1.0x10^{-8}$ M) and incubated for 10 minutes at 37 °C in 5% CO_2. Culture medium was removed and cells washed twice with 200 µL of PBS to remove unbound toxin. Subsequently, cells were fixed with 4% paraformaldehyde (Sigma-Aldrich, Milan, Italy) solution (50 µL/well) for 30 minutes at room temperature. After fixing, cells were washed twice with PBS and blocked with 100 µL of a TBB solution (50.0 mM Tris-HCl, 150.0 mM NaCl, 2.0% BSA and 0.2% Tween 20, pH 7.5) added with 10.0% horse serum (Gibco, Milan, Italy) for 30 minutes at room temperature. Cell were then washed twice with PBS and 100 µL/well of primary anti-PLTX monoclonal antibody (1.5 mg/mL α-PLTX-mAB 73D3, produced and purified from a hybridoma cell culture and kindly provided by Dr. Mark Poli; U.S. Army Medical Research Institute of Infectious Diseases, Ft. Detrick, MD, USA) diluted 1:3 000 in TBB were added for 1 hour at 50 °C under stirring. After 3 washes with PBS added with 0.1% Tween 20 followed by 3 washes with PBS, 100 µL/well of 1: 6 000 diluted Horse-Radish Peroxidase (HRP) conjugated anti-mouse secondary antibody (Jackson ImmunoResearch, Newmarket, UK) in TBB buffer was added for 1 h at 50 °C under stirring. After washing with PBS added with 0.1% Tween 20 followed by 3 washes with PBS, 60 µL/well of a solution of 3,3',5,5-tetramethylbenzidine (TMB; Sigma-Aldrich, Milan, Italy) was added for 18 minutes in the dark for the colorimetric reaction to take place. This reaction was stopped by adding 30 µL/well of 1.0 M H_2SO_4 (Sigma-Aldrich, Milan, Italy) and finally the absorbance was read using a spectrophotometer (FLUOstar Omega, BMG LABTECH, Offenburg, Germany) at 450 nm.

The value of the control cells not exposed to the toxin was subtracted from the average of the absorbance values and the result obtained was then related to the µg of proteins present in each well (measured on the protein lysate, see chapter 4 of Materials and methods). The dissociation constant (Kd) was calculated by non-linear regression analysis of the hyperbola using the GraphPad Prism software, while the maximum bond (Bmax) was evaluated as the maximum optical density (OD) value normalized on µg of proteins of each sample; the calibration curve was estimated by linear regression analysis using GraphPad Prism software.

4 Protein lysates

Protein lysates were obtained by adding to each cell pellet 100 μL of Lysis buffer (consisting of: 10.0 mM TrisHCl, 100.0 mM EDTA, 100.0 mM NaCl, 0.1% SDS in distilled water, pH 7.4) added with 1.0% of protease inhibitor cocktail (Sigma-Aldrich, Milan, Italy). Each lysate was then transferred into a 1.5 mL eppendorf, sonicated for 20 seconds on ice with an immersion sonicator (ultrasonic processor UP50H; Hielscher, Teltow, Germany) and centrifuged for 5 minutes at 10 000g at 4 °C. The supernatants were finally transferred to a second eppendorf and the protein concentration was quantified using a nanodrop instrument (NanoDrop 2000; ThermoFisher Scientific, Milan, Italy).

5 Gene expression analysis

Gene expression analysis was carried out to evaluate: (i) isoforms of the molecular target of PLTX (Na^+/K^+ ATPase) expressed in undifferentiated iPSC maintained under standard culture conditions and not exposed to PLTX; (ii) stemness and differentiation marker genes in undifferentiated iPSC samples exposed to PLTX for 24, 72 and 96 h (both under continuous exposure and recovery conditions) to analyse the impact of the toxin on stemness; (iii) stemness and differentiation marker genes in iPSC samples exposed to PLTX and simultaneously differentiated into the 3 germ layers, to analyse the impact of the toxin on the correct iPSC differentiation; (iv) stemness and differentiation marker genes in iPSC selectively differentiated into the 3 germ layers using a commercial kit (see chapter 7 of Materials and methods) used as positive controls of differentiation; (v) isoforms of the molecular target of PLTX (Na^+/K^+ ATPase) expressed in iPSC differentiated into the 3 germ layers. Table 1 shows the culture characteristics used in iPSC samples prepared for RNA extraction in these different cases.

Table 1. Experimental conditions used for gene expression analysis in iPSC. The number of cells seeded was selected basing on previous protocol set-up to avoid iPSC complete confluence (ii) or according to the instruction of the differentiation kit (iii, iv and v)

	Number of cells seeded in a 6-well plate	**Volume of TC**	**Treatment**	**Genes analyzed**
(i)	Cluster passage	2 mL	No treatment	Na^+/K^+ ATPase isoforms
(ii)	150 000 cells/well	2 mL	24 and 72 h of exposure to PLTX (continuous and recovery condition)	Genes marker of stemness and differentiation into the three germ layers
(ii)	75 000 cells/well	2 mL	96 h of exposure to PLTX (continuous and recovery condition)	Genes marker of stemness and differentiation into the three germ layers
(iii)	endoderm: 600 000 cells/well; mesoderm: 380 000 cells/well; ectoderm: 500 000 cells/well	According to the instruction of the differentiation kit (see chapter 7 of Materials and methods)	Treatment with PLTX 24 h after the seeding, with a total time in culture of 6 days	Genes marker of stemness and differentiation into the three germ layers
(iv)	endoderm: 600 000 cells/well; mesoderm: 380 000 cells/well; ectoderm: 500 000 cells/well	According to the instruction of the differentiation kit (see chapter 7 of Materials and methods)	No treatment (samples used as a positive controls of differentiation), with a total time in culture of 6 days	Genes marker of stemness and differentiation into the three germ layers
(v)	endoderm: 600 000 cells/well; mesoderm: 380 000 cells/well; ectoderm: 500 000 cells/well	According to the instruction of the differentiation kit (see chapter 7 of Materials and methods)	No treatment, with a total time in culture of 6 days	Na^+/K^+ ATPase pump isoforms in the three germ layers

5.1 RNA extraction

In order to evaluate gene expression profiles in iPSC, the TRIzol RNA extraction method was used. TRIzol (ThermoFisher Scientific, Milan, Italy) is a monophasic solution of phenol and guanidine isothiocyanate that lyses cells and dissolves cellular components, while preserving the integrity of RNA[294].

The protocol consists in the elimination of the culture medium, a wash with PBS, addition of 500 μL of TRIzol for each well and incubation for 5 min at room temperature before starting the extraction. Chloroform (100 μL; Sigma-Aldrich, Milan, Italy) was then added onto each 500 μL of TRIzol, mixed by inversion for 1 min, and incubated for 3 min at room temperature. After 15 min centrifugation at 12 000g and 4 °C, a clear supernatant containing RNA, a white interphase containing DNA and a pink organic phenol-chloroform phase containing proteins were formed. Only the upper phase containing RNA was collected, added with 250 μL of isopropanol (Sigma-Aldrich, Milan, Italy) for 10 min at room temperature followed by a 10 min centrifugation at 12 000g and 4 °C. The pellet was subsequently resuspended in 500 μL of ethanol (Sigma-Aldrich, Milan, Italy) at 75% and centrifuged for 5 min at 7 500g and 4 °C. The pellet was then left to dry for 10 min at room temperature, resuspended in 20 μL of H_2O Rnase/Dnase-free (ThermoFisher Scientific, Milan, Italy) and left for 15 min at 60 °C. Once the RNA extraction is finished, the quantification of the extraction and the determination of purity was performed using a NanoDrop UV spectrophotometer (NanoDrop 2000; ThermoFisher Scientific, Milan, Italy). For each sample 3 readings of at least 2 drops (1 μL/drop) were made, subsequently calculating the average of the values obtained.

Nucleic acids have an absorbance maximum at 260 nm. The ratio of the absorbances at 260 and 280 nm is used as a measure of purity in both DNA and RNA extracts. At 260/280 the ratio of about 1.8 is generally accepted as "pure" for DNA; a ratio of about 2.0 is generally accepted as "pure" for RNA[295]. Similarly, the measurement of absorbance at 230 nm is accepted as an index of contamination from solvents, used for extraction. The 260/230 absorbance ratio, commonly in the range 2.0-2.2, is often higher than the 260/280 absorbance ratio for "pure" nucleic acid[296]. The analysis carried out in this thesis were done only on RNA samples characterized by acceptable 260/280 and 260/230 ratios.

5.2 Reverse transcription PCR (RT-PCR)

RT-PCR (Reverse Transcription Polymerase Chain Reaction) allows the complementary strand of DNA (cDNA) to be obtained from RNA thanks to the reverse transcriptase enzyme in the presence of triphosphate deoxynucleotides (dNTPs), a buffer solution, Mg^{2+} ions and primer sequences[297]. For this purpose, the High-Capacity RNA-to-cDNA™ Kit (ThermoFisher Scientific, Milan, Italy) containing Enzyme mix 20X and 2X RT Buffer mix was used. To carry out the reaction, 10 µL of buffer, 1 µL of enzyme were added to 1 000 ng of RNA and a final volume of 20 µL was made with H_2O Rnase/Dnase-free. The samples were loaded into the thermal cycler (One-Personal; EuroClone, Milan, Italy) by setting the following program: 37 °C for 60 min; 95 °C for 5 min; 4 °C ∞.

5.3 Real time-PCR (q-PCR)

Real-time PCR or quantitative PCR (q-PCR) is a variant of the standard PCR technique. The application of this method allows to exponentially and selectively amplify a DNA sequence and to quantify it simultaneously. The amplification of the DNA sequence of interest is obtained through the repetition, for 30-40 cycles, of a 3-step process carried out by a thermal cycler. It requires the use of two short sequences (primers), which are designed to complement the sequences flanking the segment of DNA to be amplified (template), and the action of a polymerase capable of synthesizing DNA. The amplification of the DNA segment is carried out by a thermal cycler through the repetition of several cycles of a three-phase process[298]. The products thus obtained, called amplicons, are duplicated at each cycle, leading to an exponential increase of the specific DNA fragment by 2^n, where n represents the number of amplification cycles completed. The quantification of the PCR product is measured at each run: for example, by using fluorescent markers incorporated in the PCR product, an increase in the fluorescence signal is obtained directly proportional to the number of amplicons generated in the exponential phase of the reaction. In this thesis, the SYBR Green (Sigma-Aldrich, Milan, Italy) intercalator was used, a non-specific fluorophore of the double strand of DNA. To quantitatively determine the expression levels of the analysed genes, a relative quantification was performed based on an internal control, the housekeeping beta-actin (*ACTB*) gene.

Each PCR reaction was set up in triplicate in 96-well plates with a final volume of 10 µL per well containing:

- 2.00 µL of cDNA (diluted 1:10 in Dnase/RNAse-free water for the stem and differentiation genes and diluted 1:50 for the Na^+/K^+ ATPase isoform genes);
- 2.10 µL of H_2O Dnase/RNAse-free;
- 0.45 µL of forward primer;
- 0.45 µL of reverse primer;
- 5.00 µL of SYBR Green.

Finally, the plate was loaded into the thermal cycler (RealTime PCR Detection System, BIO-RAD, California, USA) setting the specific program for the analysis.

For the analysis of the isoforms of the subunit α (*ATP1A1*, *ATP1A2*, *ATP1A3*, *ATP1A4*) and β (*ATP1B1*, *ATP1B3*) of the Na^+/K^+ ATPase pump (characteristics of the primers listed in Appendix C) the program was:

95°C for 3 min

95°C for 10 sec
60°C for 30 sec } Repeated 45 times

For the analysis of the *ATP1B2* isoform of the Na^+/K^+ ATPase pump, the program was:

95 °C for 3 min

95°C for 10 sec
63°C for 15 sec } Repeated 45 times
72°C for 30 sec

To evaluate the expression levels of stem cell markers, a PCR analysis was performed by analysing the following genes: *OCT4* (factor that controls and maintains pluripotency), *SOX*2 (gene that has an important role in the control of *OCT4* expression), *KLF4* (oncoprotein capable of activating *SOX2*), *NANOG* and *C-MYC* (proto-oncogenes associated with different forms of tumour)[260]. To evaluate the ability of PLTX to induce differentiation of iPSC, q-PCR analysis of the main marker genes of the specific three germ layers was performed. In particular, *FOXA2*, *SOX17* and *AFP* were used as endoderm

marker, *ACTA2*, *BRACHYURY* and *CXCR4* as marker of the mesoderm, *PAX6* and *SOX1* as marker of the ectoderm.

For the analysis of stem cell markers and differentiation genes, the protocol was (characteristics of the primers listed in Appendix D):

95°C for 3 min

95°C for 10 sec
60°C for 30 sec } Repeated 45 times

At the end of each protocol, the step for the quantification of the melting temperature has been added, which involves gradually raising the temperature by 0.5 °C up to 95.0 °C and the fluorescence is measured as a function of the temperature. Visual analysis of these melting curves is a quick and easy method to verify the lack of dimer primer formation. Indeed, since dimer primer products are typically shorter than the targeted product, they melt at a lower temperature and, if present, a second peak appears on the graph that is lower than that of the product of interest[298].
Data of the gene expression analysis (q-PCR) were analysed with the $2^{-\Delta Ct}$ method, where ΔCt represents the difference between the Ct of the gene of interest and the Ct of the housekeeping gene (*ACTB*) in the different samples analysed. Using the Rstudio program a heat map was created basing on the $2^{-\Delta Ct}$ results and a clustering analysis was carried out which allowed to group in clusters the similar gene expression patterns in the different samples. In particular, the degree of similarity of the different groups is evidenced by the length of the arms of the clusters. In this graphical representation, the samples were shown in the rows, while each column represents an analysed gene. The different colours were representative of the gene expression value ($2^{-\Delta Ct}$) of each gene in the different samples.

6 Protein expression level (western blot assay)

Western blot analysis was used to detect the presence of OCT4 (stem cell marker), SOX17 (endoderm), BRACHYURY (mesoderm) and PAX6 (ectoderm) proteins using Actin (ACT) as the reference protein. The iPSC samples analysed were the same used for gene expression analysis shown in table 1, with the exception of cells exposed to PLTX under recovery conditions which were not analysed. Protein lysates of each sample were

prepared according to the protocol reported in chapter 4 of Materials and methods. To each protein lysate sample (containing 30.0 μg of protein), 4.0 μL of loading sample buffer 4X (ThermoFisher Scientific, Milan, Italy) and 1.6 μL of reducing sample agent 10X (ThermoFisher Scientific, Milan, Italy) were added and made up to a final volume of 16.0 μL with the lysis buffer. Samples were placed in a bath at 70 °C for 10 min, before being loaded into NUPAGE 10% Bis-Tris Gels (ThermoFisher Scientific, Milan, Italy) along with 3.5 μL/well of marker (PageRuler™ Plus Prestained Protein Ladder, 10 to 250 kDa; ThermoFisher Scientific, Milan, Italy). The gel was put in specific supports into the electrophoretic chamber (Mini Gel Tank; ThermoFisher Scientific, Milan, Italy) and immersed in running buffer 20X (ThermoFisher Scientific, Milan, Italy) diluted at 1X in distilled water. The gel was run for 1.5 hour by setting the current (Electrophoresis Power Supply EPS301; GE Healthcare Bio-Sciences AB, Uppsala, Sweden) at 200 V and 160 mA. For the transfer step, nitrocellulose membranes (Power Blotter Pre-cut Membranes and Filters; ThermoFisher Scientific, Milan, Italy) were used; the transfer buffer (ThermoFisher Scientific, Milan, Italy) was diluted 1:5 in T-TBS (9.0 g/L of NaCl; 12.1g /L of Trizma Base, 1 mL/L Tween20, pH 7.5). Transfer was carried out in the Power Blot Station instrument (ThermoFisher Scientific, Milan, Italy), set at 1.3 A, 25 V, 10 min, at the end of this phase the correct transfer was checked using the Ponceau red solution (Sigma-Aldrich, Milan, Italy) which was then eliminated with distilled water. Membranes were then blocked with 5% milk in T-TBS for 1 h at 4 °C under stirring and subsequently primary antibodies were added and left to stir at 4 °C overnight. Primary antibodies were bought form Abcam (Cambridge, UK) except for the anti-actin that was bought from Millipore (Sigma-Aldrich, Milan, Italy). The following antibody dilutions in 5% milk were used:

- Anti-Actin Rabbit mAB (clone EP184E) = 1:20 000, with a band at 42 kDa
- Anti-OCT4 Mouse mAb (clone GT486) = 1:3 000 with a band at 47 kDa
- Anti-PAX6 Rabbit pAb= 1:1 000 with a band at 47 kDa
- Anti-SOX17 Rabbit mAb (clone EPR20684) = 1:1 000 with a band at 55 kDa
- Anti-BRACHYURY Rabbit mAb (clone EPR18113) = 1:1 000 with a band at 50 kDa

After incubation with primary antibodies, 3 washes of 5 min at 4 °C were carried out under stirring with T-TBS and the secondary antibody was added for 1 h at 4 °C under stirring. The secondary antibodies, donkey anti-rabbit HRP-conjugated (Sigma-Aldrich, Mulan, Italy) and the goat anti-mouse HRP-conjugated (Abcam, Cambridge, UK), were diluted 1:50 000 and 1:5 000 in 5% milk, respectively. After carrying out 3 washes of 5 min at 4 °C under agitation with T-TBS, the membranes were incubated for 5 min with the SuperSignal™ West Atto Ultimate Sensitivity Substrate (ThermoFisher Scientific, Milan, Italy) and developed using the ChemiDoc instrument (ChemiDoc MP Imaging System;

BIO-RAD, California, USA), by setting auto-exposure. The bands were then quantified with the Image-Lab program by BIO-RAD (California, USA). The quantification of the protein bands was expressed as a percentage of protein level with respect to the reference protein (ACT= 100% of protein expression).

7 Differentiation kit

To differentiate iPSC into the 3 germ layers, the StemMACS Trilineage Differentiation kit (Miltenyi Biotec, Bergisch Gladbach, Germany) was used. The protocol provides a differentiation in 7 days: on day 0, iPSC was seeded in different numbers for the 3 sheets (according to the instructions provided by the company) and according to the plate of interest (for details, see Appendix E) in the presence of a specific volume of the medium for the 3 germ layers (added with ROCK inhibitor at the final concentration of 10 μM). During the following 6 days after the seeding, the medium was changed according to the instruction:

- Endoderm: the day after seeding (day 1) medium was not changed, while starting from day 2 until day 6 medium it was changed with the StemMACS EndoDiff Medium every 24 hours after washing with PBS-Ca^{2+}/Mg^{2+};
- Mesoderm: after 24 h from seeding (day 1) medium was replaced with the StemMACS MesoDiff Medium I, and changed with the StemMACS MesoDiff Medium II on days 4, 5 and 6;
- Ectoderm: medium was changed with the StemMACS Trilineage EctoDiff Medium every 24 h (from day 1 to day 6).

8 Statistical analysis

All the results were expressed as mean ± standard errors of the mean (SE) of at least three independent experiments.
Depending on the biological assays, data were analysed by one- or two-way analysis of variance (ANOVA) and Bonferroni post-test, or by the Student's t-test, using GraphPad Prism software version 6. Significant differences were considered for $p < 0.05$. EC_{50} values were calculated by variable slope (four-parameter) non-linear regression at a statistical confidence interval of 95%, using the GraphPad Prism version 6. The heat map and clustering analysis were obtained using the Rstudio software.

Results

1 Evaluation of the cytotoxic effect of PLTX on iPSC

The cytotoxic effects induced by PLTX on the iPSC 253G1 line were evaluated by means of mitochondrial activity measured by the MTT reduction test after 4 h exposure to the toxin ($1.0x10^{-14}$-$1.0x10^{-7}$ M) and compared to the cytotoxic effects on a non-stem cell line (i.e., human HaCaT keratinocytes) (fig. 33).

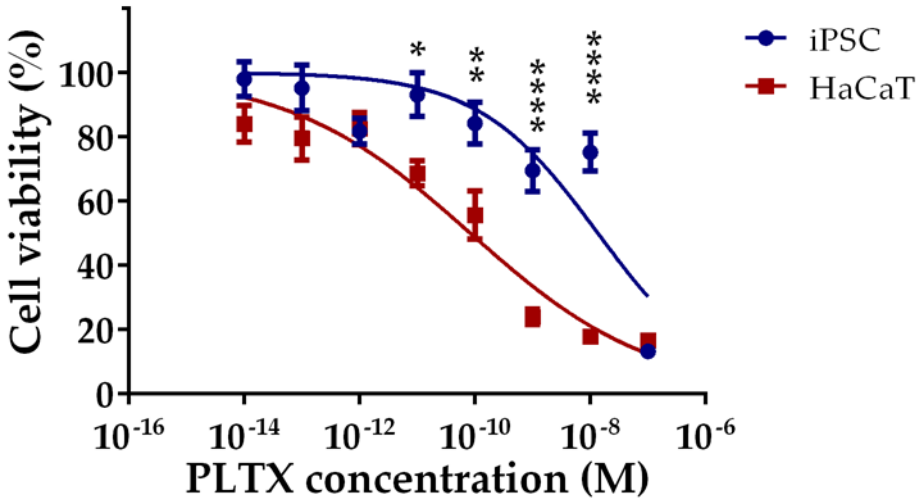

*Figure 33. Cytotoxic effect of PLTX on iPSC and HaCaT cells after 4 h exposure evaluated by the MTT test. Data are expressed as % of reduction of cell viability compared to untreated controls (100% viability) and are the mean ± SE of three independent experiments. Statistical analysis: *, $p < 0.05$; **, $p < 0.01$; ****, $p < 0.0001$ (two-way ANOVA and Bonferroni's post-test).*

PLTX induced a concentration-dependent cell viability reduction in both the cell lines tested after 4 h of exposure. The two concentration-response curves were statistically different ($p < 0.0001$, two-way ANOVA) and iPSC resulted more resistant to the toxin effect (fig. 33), with an EC_{50} value of $1.3x10^{-8}$ M (C.I. 95%= 0.5-$3.8x10^{-8}$ M), about 2 orders of magnitude higher ($p < 0.0001$) as compared to the EC_{50} value calculated for HaCaT cells, equal to $8.3x10^{-11}$ M (C.I. 95%= 0.4-$1.9x10^{-10}$ M). Cytotoxicity data obtained on other somatic cell lines (i.e., Caco-2 enterocytes, PANC-1 pancreatic cells and HepG2 hepatocytes) confirmed the lower sensitivity of iPSC to PLTX effects in comparison to non-stem cells (data not shown).

2 Evaluation of binding affinity of PLTX on iPSC

The different cytotoxicity of PLTX on iPSC as compared to the non-stem cell line leads to hypothesize a different binding affinity of the toxin. For this reason, a cell-based ELISA assay was performed (fig. 34): cells of both lines were exposed to scalar concentrations of PLTX ($5.1x10^{-13}$–$1.0x10^{-8}$ M) for 10 minutes and the binding of the toxin was detected as reported in Materials and methods.

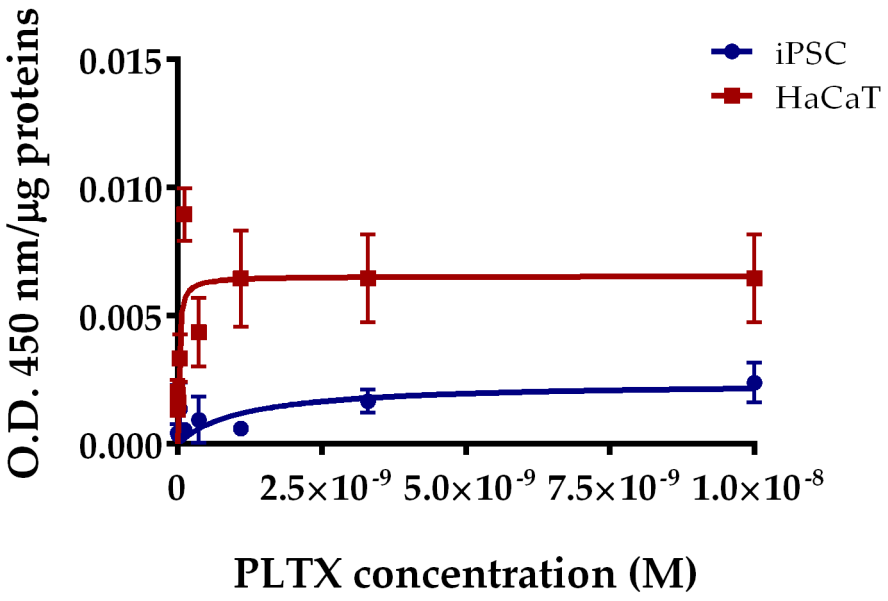

Figure 34. Saturation curves of PLTX binding on iPSC and HaCaT cell lines, detected by a cell-based ELISA binding assay. The optical density values obtained were normalized on the µg of proteins of each sample. Data are represented as mean ± SE of three independent experiments.

Figure 34 shows the saturation curves of PLTX binding to the two cell lines, reporting the absorbance (O.D.) values measured at 450 nm, normalized on the proteins amount in each sample. From each curve, the dissociation constant (Kd), index of the concentration of toxin necessary to saturate 50% of the binding sites, and the maximum binding (Bmax) of the toxin, index of the total binding sites present, were calculated. The graph shows that iPSC were characterized by a significantly lower binding affinity than that found in the somatic cell line (HaCaT). Indeed, a Kd equal to $1.1x10^{-9}$ M (C.I. 95%= 1.0-$4.1x10^{-9}$ M) was calculated, about two orders of magnitude higher ($p < 0.0001$) than that calculated for HaCaT cells (Kd= $1.9x10^{-11}$ M; C.I. 95%= 1.0-$4.2x10^{-11}$ M). Similarly, Bmax value in iPSC was equal to 0.0024 (C.I. 95%= 0.0005-0.0043), significantly lower ($p < 0.0001$) than that calculated for HaCaT cells (Bmax= 0.0065; C.I. 95%= 0.0052-0.0079).

3 Evaluation of Na^+/K^+ ATPase genes expression in iPSC

To understand the reason behind the different cytotoxicity and binding affinity of the toxin between the two cell lines, the isoforms of the Na^+/K^+ ATPase pump, the molecular target of PLTX, were analysed in terms of gene expression. Indeed, literature data suggests that different expression of isoforms of the α and β subunits are correlated to a different *in vitro* sensitivity to the toxin effects[299]. Specifically, in iPSC and HaCaT cells not exposed to the toxin, gene expression of four isoforms of the α subunit and three of the β subunit, were analysed by q-PCR (fig. 35).

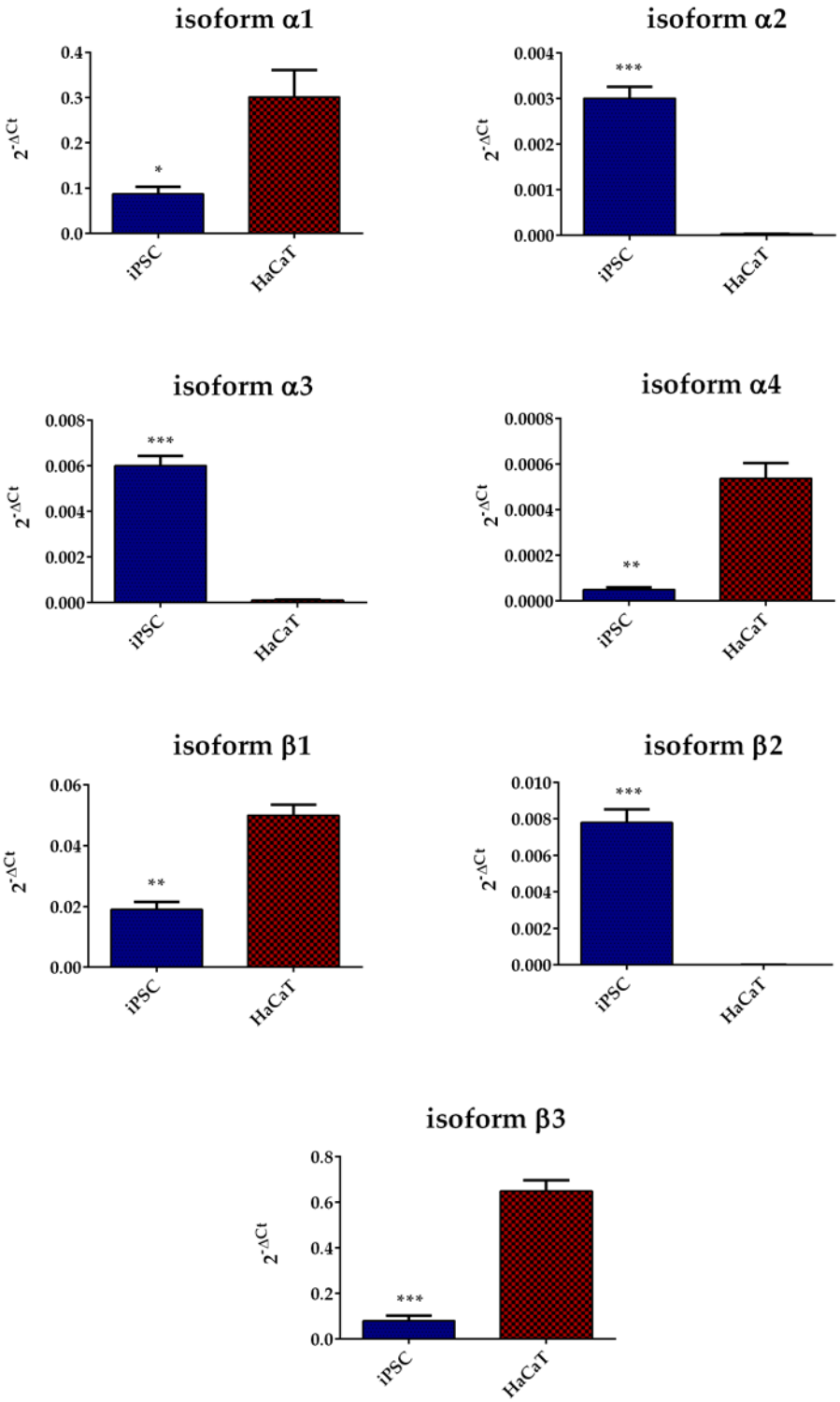

*Figure 35. Gene expression of the isoforms of the α and β subunits of Na^+/K^+ ATPase, molecular target of PLTX, in iPSC compared to HaCaT cells. Data are the mean± SE of three independent experiments and are reported as $2^{-\Delta Ct}$ versus the housekeeping ACTB gene. Statistical analysis (iPSC vs HaCaT): *, p <0.05; **, p < 0.01; ***, p < 0.001; ****, p < 0.0001 (Student's t-test).*

As reported in figure 35, in iPSC, isoforms of the α subunit were differentially expressed, with the following order: α1 (relative expression: 0.0870 fold change) > α3 (relative expression: 0.0060 fold change) > α2 (relative expression: 0.0030 fold change) > α4 (relative expression: 0.00005 fold change). Similarly, also the isoforms of the β subunit were differentially expressed in iPSC, and in particular with the following order: β3 (relative expression: 0.0798 fold change) > β1 (relative expression: 0.0190 fold change) > β2 (relative expression: 0.0078 fold change).
This expression pattern was significantly different from that observed in HaCaT cells. Regarding α subunit, in HaCaT cells isoforms were differently expressed with the following order: α1 (relative expression: 0.3009 fold change) > α4 (relative expression: 0.0005 fold change) > α3 (relative expression: 0.00009 fold change) > α2 (relative expression: 0.00003 fold change). Regarding β subunit, in HaCaT cells isoforms were differently expressed with the following order: β3 (relative expression: 0.649 fold change) > β1 (relative expression: 0.05 fold change) > β2 (relative expression: 0.00001 fold change). In addition, the α2 ($p < 0.001$), α3 ($p < 0.001$) and β2 ($p < 0.001$) isoforms were significantly more expressed in iPSC than in HaCaT cells; the α1 isoforms ($p < 0.05$), α4 ($p < 0.01$), β1 ($p < 0.01$) and β3 ($p < 0.001$) were statistically less expressed in stem cells than in keratinocytes. The differences in the expression of α2, α3 and β2 isoforms are particularly evident, which are significantly expressed in stem cells but whose expression in keratinocytes is almost negligible.

4 Evaluation of the cytotoxic effect of PLTX on iPSC up to 96 h

Considering the resistance of iPSC to cytotoxic effects induced by PLTX, the time of exposure to the toxin was increased up to 96 h in the iPSC line. Cell viability was analysed by the MTT reduction assay in iPSC exposed to PLTX ($1.0x10^{-17}$-$1.0x10^{-7}$ M) for 24, 72 and 96 h. In addition, after 24 h of exposure to the same concentration range of the toxin, cell medium was replaced with toxin-free medium for a further 48 or 72 h (recovery condition) to study the reversibility of the damage (fig. 36).

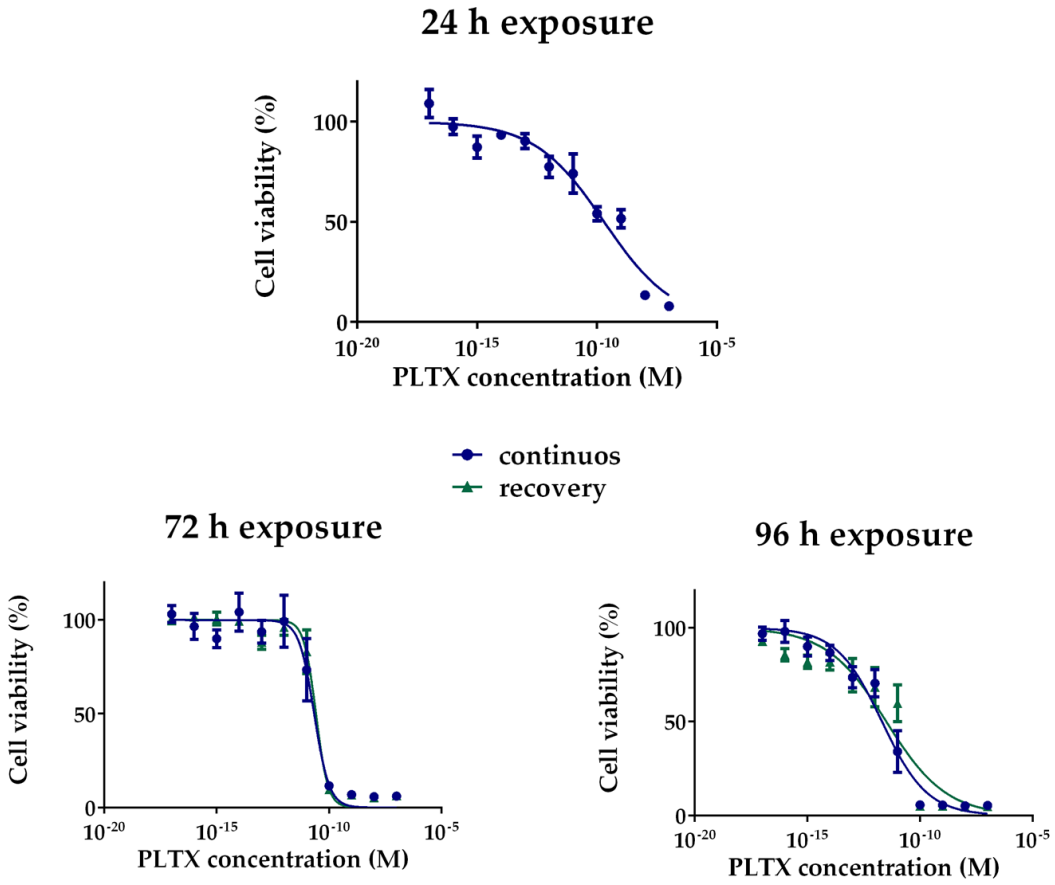

Figure 36. Cytotoxic effect of PLTX on iPSC after A) 24 h B) 72h of continuous exposure or under the relevant recovery condition (24 h of treatment followed by 48 h in toxin-free medium) and C) 96 h of continuous exposure or under the relevant recovery condition (24 h of treatment followed by 72 h in toxin-free medium), evaluated by the MTT assay. Data are expressed as % of cell viability compared to untreated controls (100% viability) and are the mean ± SE of three independent experiments. Statistical analysis: two-way ANOVA and Bonferroni's post-test.

The graphs represented in figure 36 shows that the cytotoxic effect induced by PLTX was concentration- and time-dependent. Specifically, reduction of cell viability was induced with EC_{50} values of $1.9x10^{-10}$ M (C.I. 95%= 0.9-4.6x10^{-10} M), $2.2x10^{-11}$ M (C.I. 95%= 1.3-3.7x10^{-11} M) and $2.1x10^{-12}$ M (C.I. 95% = 1.1-3.7x10^{-12} M) after 24, 72 and 96 h exposure, respectively.

In addition, comparing the results obtained after PLTX continuous exposure with those obtained under the relevant recovery conditions, no significant differences, either in the concentration-response curves (two-way ANOVA) or in the EC_{50} values (Student's t-test),

were found for both the exposure times considered (72 and 96 h). This observation suggests that the cytotoxic effect induced by the toxin on iPSC seems to be irreversible.

5 Evaluation of the effect of PLTX on iPSC stemness

On the basis of the above reported cytotoxicity data, a concentration of PLTX equal to $1.0x10^{-11}$ M was selected to analyse the effects of PLTX after 24, 72 and 96 h on stemness perturbation. To this aim, markers of stemness and markers of differentiation into the 3 germ layers (endoderm, mesoderm and ectoderm) was evaluated in terms of gene and protein expression.

5.1 Gene expression levels

In the case of gene analysis, the expression of a panel of 13 genes, five for stemness (*OCT4*, *C-MYC*, *KLF4*, *SOX2* and *NANOG*) and eight differentiation markers of the 3 germ layers (*SOX17*, *AFP* and *FOXA2* for endoderm; *ACTA2*, *BRACHYURY* and *CXCR4* for mesoderm; *PAX6* and *SOX1* for ectoderm) was quantified by q-PCR analysis. The negative differentiation control is represented by control iPSC (not exposed to the toxin) while the positive differentiation controls (endoderm, mesoderm and ectoderm) were obtained by differentiating iPSC into the three germ layers individually using a commercial kit (see chapter 7 in Materials and methods). Gene expression levels of each sample, calculated as $2^{-\Delta Ct}$ (i.e., normalized with respect to housekeeping *ACTB*), were represented as a heat map and a clustering analysis was performed to better understand the effect of PLTX on stemness (fig. 37).

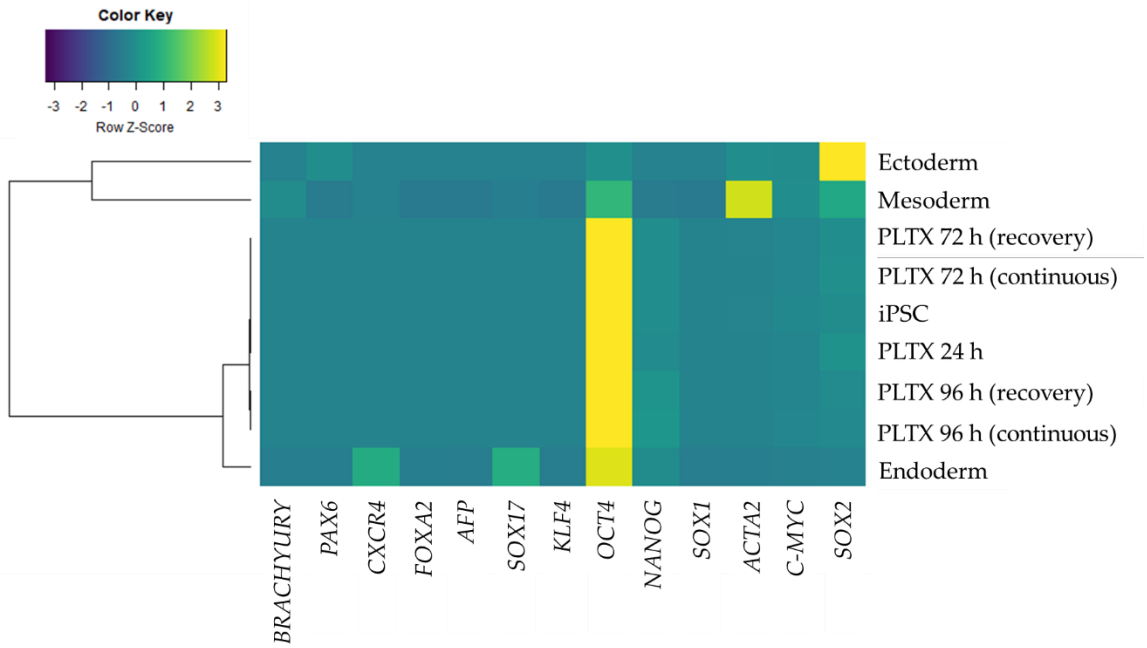

Figure 37. Heat map and clustering analysis of gene expression of stemness and differentiation markers in iPSC exposed to PLTX following 24, 72 and 96 h of continuous exposure or 24 h of toxin exposure, followed by 48 or 72 h recovery in toxin-free medium. The reported data are expressed as $2^{-\Delta Ct}$ and are the mean ± SE of three experiments.

Figure 37 shows that all the samples exposed to PLTX, regardless the exposure times, were grouped in a single high-affinity cluster together with iPSC not exposed to the toxin (iPSC used as a negative control of stemness). The dendrogram represents this cluster with extremely short interconnecting arms, indicating a very tight relationship. The clustering analysis also shown a secondary grouping of the samples exposed to PLTX with only one of the positive differentiation controls, namely the endoderm. The clustering analysis, therefore, suggested that on the basis of the gene expression patterns of all the markers, the treatment with the toxin seems to maintain iPSC in a stem state, possibly directed – in a secondary and non-exclusive way – to a slight differentiation towards the endoderm germ layer.

5.2 Protein expression levels

Protein expression levels of OCT4, SOX17, BRACHYURY and PAX6 were analysed in iPSC protein lysates under the same conditions reported for gene expression: iPSC of negative controls; 3 positive differentiation controls (endoderm, mesoderm and ectoderm) and iPSC exposed to PLTX ($1.0x10^{-11}$ M) for 24, 72 and 96 h (fig. 38). In the latter condition, however, the two timing of exposure to PLTX under recovery conditions were not considered because they did not show any differences compared to the continuous condition, both in terms of cytotoxicity (fig. 36) and gene expression (fig. 37)

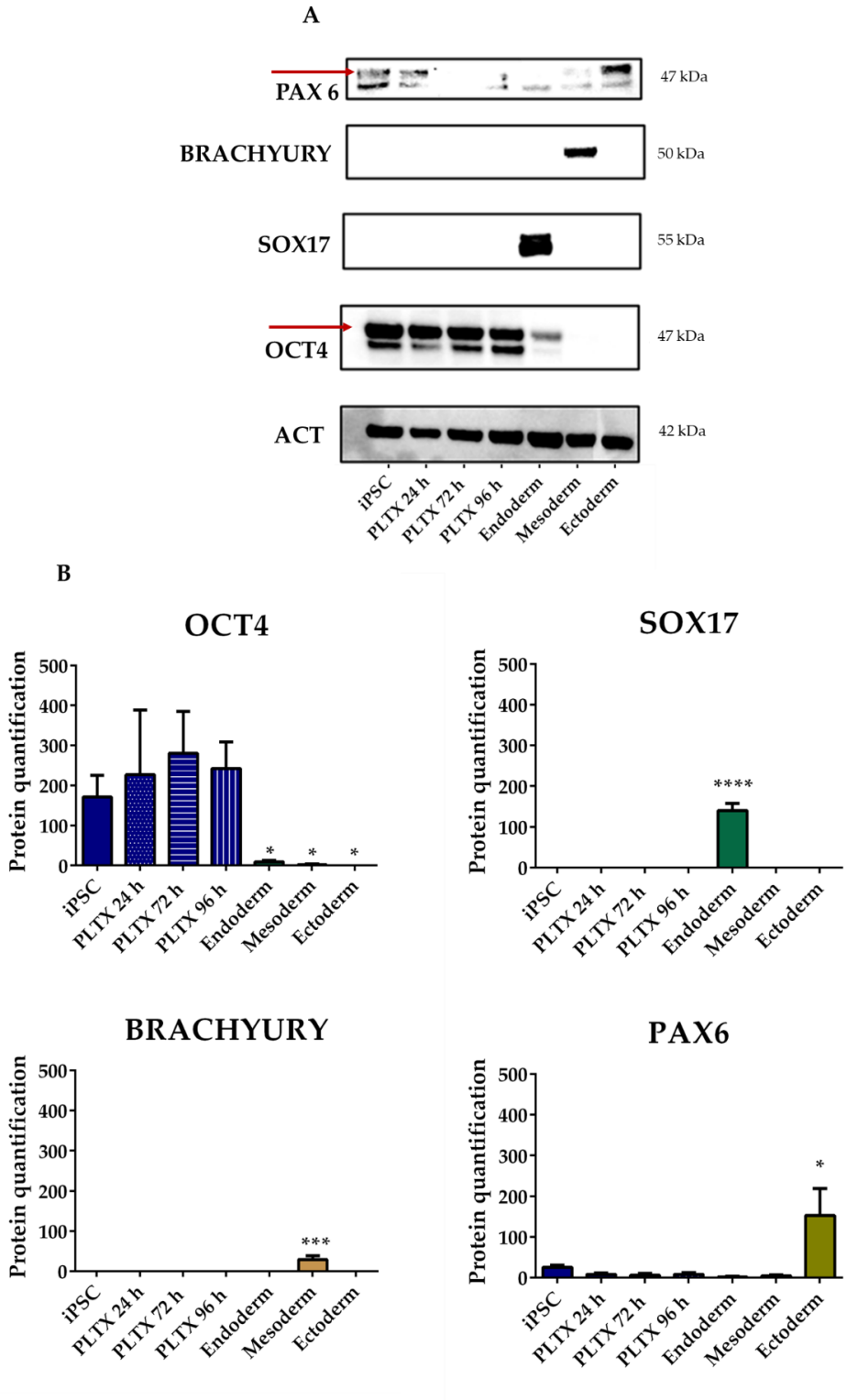

*Figure 38. A) Representative images of Western blot analysis reporting protein expression of OCT4, SOX17, BRACHYURY and PAX6 and of the reference protein (ACT) and B) relative quantification of the corresponding protein levels expressed as % with respect to the reference protein (ACT), represented as the mean ± SE of three experiments. Statistical analysis: *, $p < 0.05$; ***, $p < 0.001$; ****, $p < 0.0001$ (one-way ANOVA and Bonferroni's post-test).*

Western blot analysis and the relative quantification of protein expression levels, represented in figure 38, shows that in both untreated iPSC (negative control of stemness) and PLTX-exposed iPSC (exposed to PLTX for 24, 72 and 96 h) the proteins SOX17 and BRACHYURY (marker respectively of endoderm and mesoderm) were not detected, while PAX6 (marker of ectoderm) was detected in a significant lesser extent with respect to the positive control ectoderm. On the contrary, OCT4 (marker of stemness) was expressed in a comparable manner among untreated iPSC and PLTX-exposed iPSC, but significantly less expressed (or even not detected) in the three positive controls. These observations confirm the results obtained by the genetic analysis, suggesting that PLTX exposure do not seem to alter stemness properties of iPSC.

6 Evaluation of PLTX effects on iPSC differentiation

To evaluate the effects of PLTX during the differentiation of iPSC into the three germ layers, the concentration of $1.0x10^{-11}$ M was selected as reported above. iPSC were exposed to PLTX and simultaneously induced to individually differentiate into the three germ layers. The effect of the toxin on iPSC differentiation was analysed in terms of gene and protein expression of stemness and differentiation markers.

6.1 Gene expression levels

The analysis of gene expression level was carried out similarly to what reported above. The negative control is represented by control iPSC not exposed to the toxin and the positive differentiation controls are endoderm, mesoderm and ectoderm, obtained in the same way as reported above. Gene expression levels of each sample, calculated as $2^{-\Delta Ct}$ (i.e., normalized with respect to housekeeping *ACTB*), were represented as a heat map and a clustering analysis was performed (fig. 39).

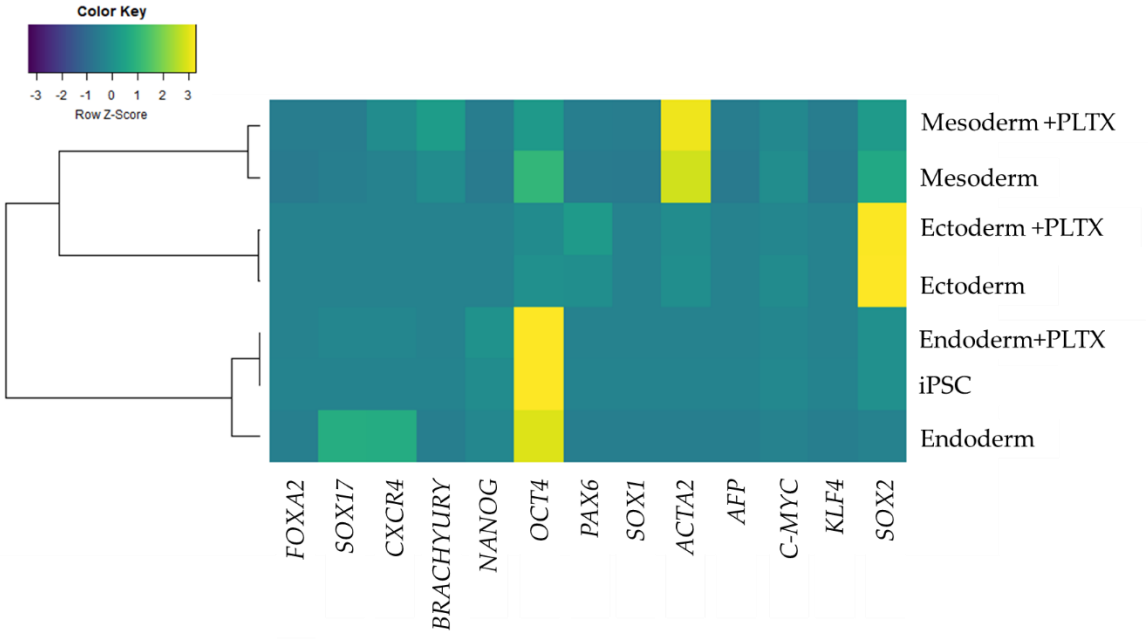

Figure 39. Heat map and clustering analysis of gene expression of stemness and differentiation markers in iPSC exposed to PLTX (1.0x10^{-11} M) and simultaneously differentiated into the three germ layers (endoderm, mesoderm and ectoderm) using a commercial kit. Data are the mean ± SE of three experiments and are expressed as $2^{-\Delta Ct}$.

The clustering analysis reported in figure 39 shows that iPSC exposed to PLTX (1.0x10^{-11}M) during their differentiation towards endoderm cells grouped firstly with iPSC (i.e., the negative control) with a high affinity clustering as shown by the extremely short length of the connecting arm. Only secondly, this group clustered with endoderm (positive control of this germ layer) with a lower affinity. This did not happen for the other two germ layers, since iPSC exposed to the toxin and differentiated into mesoderm or ectoderm clustered only with the respective positive control. This data suggests a selective negative impact of PLTX on iPSC differentiation towards the endoderm germ layer.

6.2 Protein expression levels

To confirm gene expression analysis in iPSC samples exposed to PLTX (1.0x10^{-11} M) and simultaneously induced to differentiate into the three germ layers, protein lysates were collected and western blot analysis was performed evaluating the protein expression levels of OCT4, SOX17, BRACHYURY and PAX6 using ACT as reference protein (fig. 40).

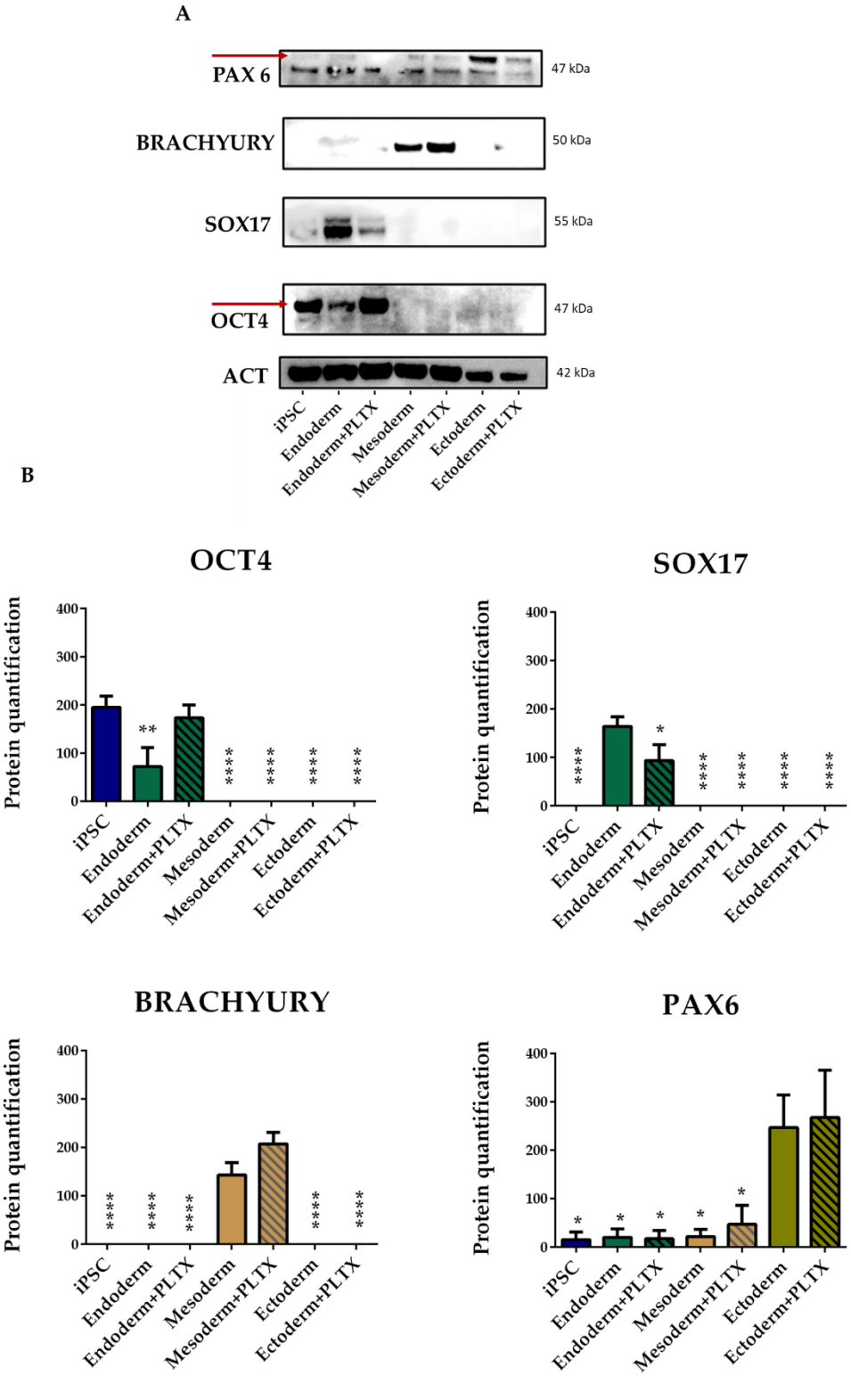

*Figure 40. A) Representative images of western blot analysis showing protein expression of OCT4, SOX17, BRACHYURY, PAX6 and of the reference protein (ACT) and B) relative quantification of the protein levels expressed as % with respect to the reference protein (ACT); results are the mean ± SE of three experiments. Statistical analysis vs the relevant positive control: *, p <0.05; **, p <0.01; ****, p <0.0001 (one-way ANOVA and Bonferroni's post-test).*

Protein expression analysis confirmed gene expression results reported above. Indeed, OCT4, marker of stemness, was expressed in a similar way between iPSC and iPSC exposed to PLTX during the endoderm differentiation (endoderm+PLTX) as demonstrated by both the western blot image (fig. 40 A) and the relevant quantification of the protein level (fig. 40 B). Furthermore, SOX17 protein (endoderm marker) appears less expressed in endoderm+PLTX samples as compared to the positive control of endoderm differentiation ($p < 0.05$). For the other two embryonic layers, mesoderm and ectoderm, as expected, the expression of OCT4 significantly decreased compared to the negative control (iPSC), but the presence of PLTX during the selective differentiation process, did not affect protein expression of the respective markers (BRACHYURY and PAX6).

7 PLTX effects on iPSC viability during differentiation

To evaluate if the alteration of the correct iPSC differentiation towards endoderm induced by PLTX ($1.0x10^{-11}$ M) could be due to a cytotoxic effect of the toxin, cell viability was analysed using the MTT assay in iPSC exposed to PLTX during the differentiation process (for a total of 6 days exposure). As reported in figure 41, cell viability was not reduced by the presence of PLTX during differentiation for any of the 3 germ layers.

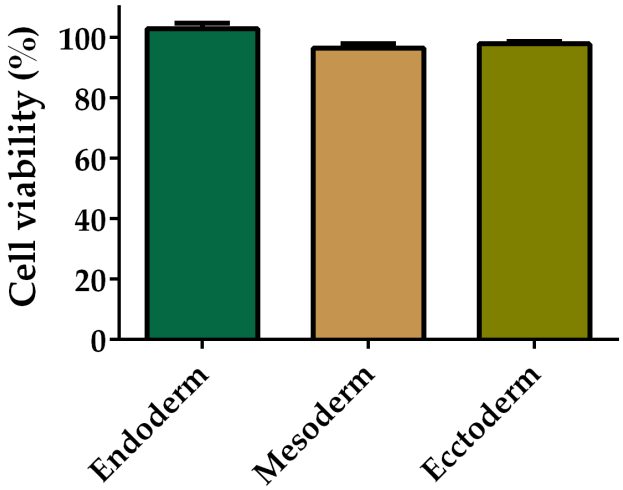

Figure 41. Cell viability of iPSC exposed to PLTX ($1.0x10^{-11}$ M) during the differentiation process into the three germ layers evaluated by the MTT assay at the end of the differentiation (6 days). Data are expressed as % of reduction of cell viability compared to the relevant positive differentiation controls (100% viability) and are the mean ± SE of at least three independent experiments. Statistical analysis: one-way ANOVA and Bonferroni's post-test.

8 PLTX cytotoxicity on the three germ layers

As a last step of the study, the cytotoxic effect induced by the toxin on the three differentiated germ layers was evaluated using the MTT test. In this case, iPSC were firstly differentiated into endoderm, mesoderm or ectoderm and subsequently exposed to three selected concentrations ($1.0x10^{-11}$, $1.0x10^{-9}$ and $1.0x10^{-7}$ M) of PLTX for 24 h (fig. 42).

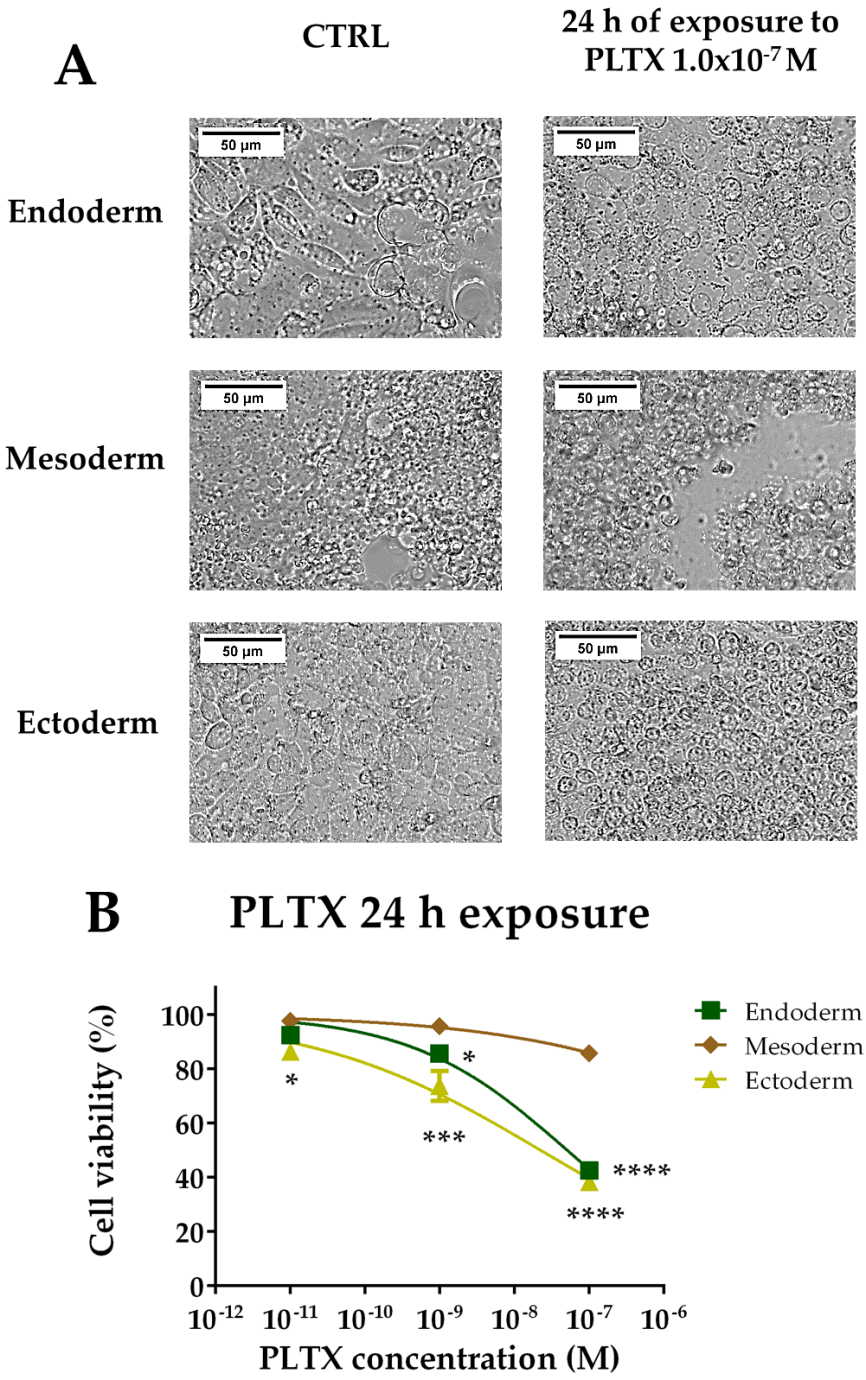

*Figure 42. A) Representative image of iPSC differentiated selectively into the three germ layers and subsequently exposed to PLTX ($1.0x10^{-7}$ M) for 24 h in comparison to the negative control (CTRL; iPSC differentiated not exposed to the toxin). Photos were obtained with an inverted microscope (Leica Microsystems) with 20X objective magnification. B) Cytotoxic effect induced by 24 h exposure to PLTX ($1.0x10^{-11}$, $1.0x10^{-9}$ and $1.0x10^{-7}$ M) on iPSC differentiated into the germ layers, evaluated by the MTT test. Data are expressed as % of cell viability compared to the relevant positive differentiation controls (100% viability) and are the mean ± SE of at least three independent experiments. Statistical analysis vs mesoderm (the less sensitive germ layer): *: $p < 0.05$; ***: $p < 0.001$; ****: $p < 0.0001$ (two-way ANOVA and Bonferroni's post-test).*

Figure 42 B shows that the cytotoxic effect induced by PLTX was higher in the endoderm and ectoderm germ layers, whereas in mesoderm cells, viability was only slightly and not significantly reduced by the toxin. The effects were induced with EC_{50}s of $5.1x10^{-8}$ M (C.I. 95%= 2.0-11.0 $x10^{-8}$ M), $2.2x10^{-8}$ M (C.I. 95%= 0.7-7.4$x10^{-8}$ M) in endoderm and ectoderm cells, respectively. For the mesoderm, given the extremely low effect induced by the toxin, it was not possible to calculate an EC_{50} value.
Morphological analysis performed by light microscopy (fig. 42 A) showed that at the highest concentration ($1.0x10^{-7}$ M), PLTX induced morphological changes only in endoderm and ectoderm cells, while morphology of mesoderm cells was similar to that of control cells (CTRL; mesoderm cells not exposed to PLTX).

9 Evaluation of Na^+/K^+ ATPase genes expression in the three germ layers

To investigate if the different sensitivities towards PLTX cytotoxicity of the three germ layers could be correlated to different expression patterns of the isoforms of the Na^+/K^+ ATPase α and β subunit, gene expression analysis was carried out using q-PCR on differentiated iPSC into the 3 germ layers (fig. 43).

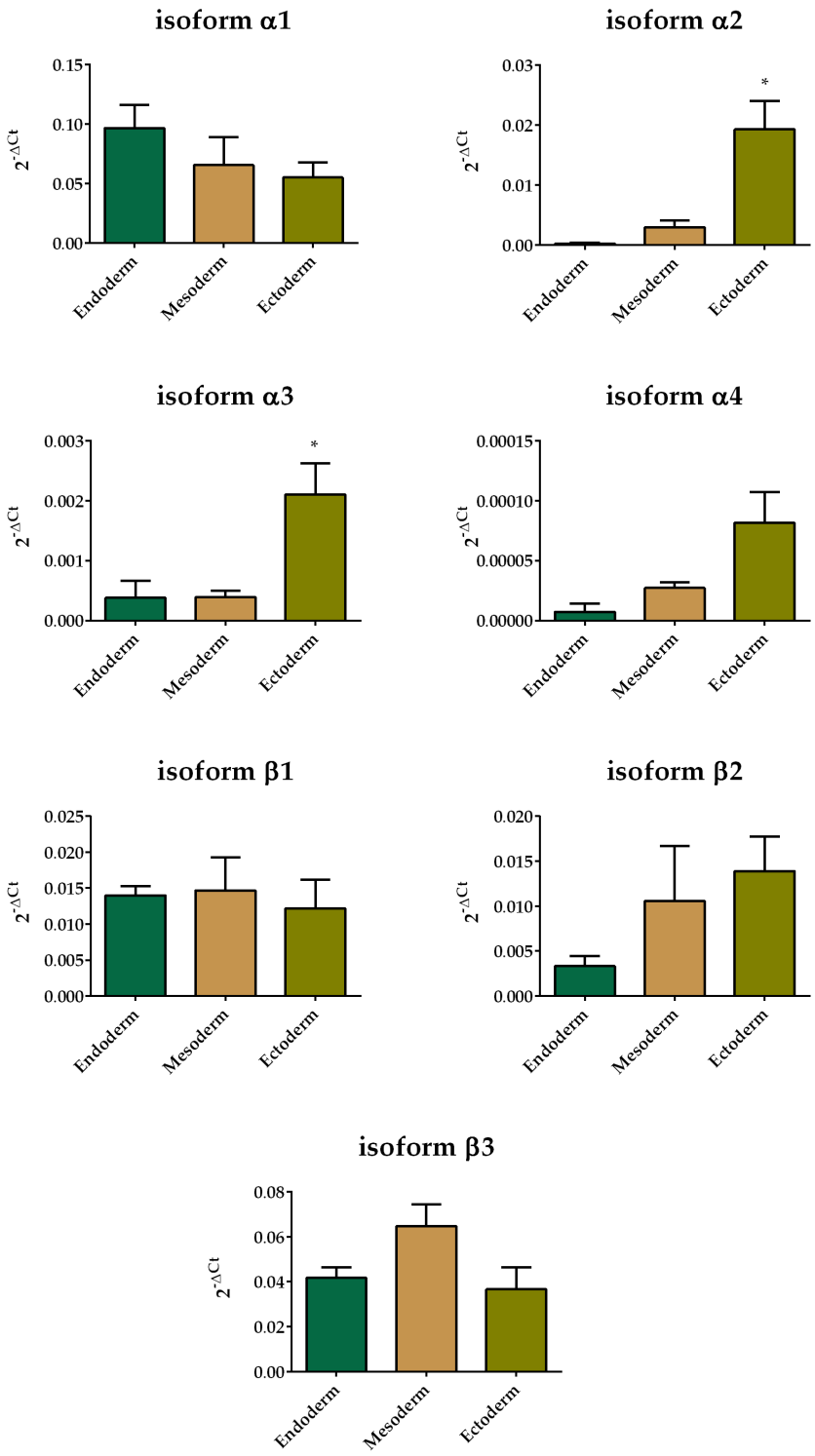

*Figure 43. Gene expression of the isoforms of the α and β subunit of Na^+/K^+ ATPase in iPSC selectively differentiated into the three embryonic layers. Data are reported as $2^{-\Delta Ct}$ (vs the housekeeping ACTB gene) and are the mean of three independent experiments ± SE. Statistical analysis vs mesoderm: *, $p < 0.05$ (one-way ANOVA and Bonferroni's post-test).*

As shown in figure 43, all the β subunits were not differently expressed at the gene level in a significant manner between iPSC differentiated into the 3 germ layers. Only regarding the α subunits significant differences were found, $\alpha 2$ and $\alpha 3$ being more expressed only in ectoderm in comparison to the mesoderm ($p < 0.05$), the most resistant germ layer to the cytotoxic effect of PLTX (fig. 42 B).

Discussion and conclusion

From a toxicological point of view, the effects of PLTX have been extensively studied both *in vivo* and *in vitro*. However, an under-evaluated aspect is its embryotoxic potential. In fact, previously published studies have shown a possible embryotoxic potential of PLTX through a teratogenic test on *Xenopus laevis* embryos. The study highlighted a significant mortality of the embryo exposed to the toxin, with malformations and growth retardation[128], probably associated with altered gene expression patterns[129]. Therefore, to better elucidate the potential embryotoxicity of PLTX, the section B of this thesis was conducted on human induced pluripotent stem cells (iPSC, cell line 253G1), analysing the effects of PLTX in three consecutive stages of the embryonic development. In particular, iPSC is a fruitful *in vitro* model used in different pharmacological and toxicological studies, including embryotoxicity analysis, being able to mimic stem cells of the inner part of blastocyst with pluripotent properties at the basis of their differentiation potential into the three germ layers[287,288].

In the first part of the study, the effect of PLTX on undifferentiated iPSC was analysed using the MTT test, which measures cell viability by means of mitochondrial activity. The obtained results were compared with data obtained on a non-stem cell line, the HaCaT cell line. HaCaT cells are spontaneously immortalized human keratinocytes on which the toxic effects of PLTX have been extensively studied[52,79,242,243]. This cell model was chosen on the basis of literature data, showing that this cell line is one of the most sensitive to PLTX cytotoxic effects[292]. The toxin reduced cell viability of iPSC with an EC_{50} of $1.3x10^{-8}$ M, more than two orders of magnitude higher than that calculated for keratinocytes ($8.3x10^{-11}$ M), thus suggesting a lower sensitivity of iPSC to the cytotoxic effects of PLTX as compared to somatic cells. This phenomenon could be ascribable to a lower binding affinity of PLTX for iPSC as compared with keratinocytes. Indeed, the Kd value for stem cells ($1.1x10^{-9}$ M), was two orders of magnitude higher than that reported for HaCaT ($1.9x10^{-11}$ M). A possible explanation of this lower binding affinity could rely on the different expression patterns of the isoforms of the Na^+/K^+ ATPase, the molecular target of the toxin, observed in the two cell models. The pump is a protein complex consisting of different subunits (α and β), each present in different isoforms, the expression of which is species- and tissue-specific[63]. Furthermore, previous data have shown that the expression of these isoforms is characterized by a high interindividual variability and each of them has different affinities and sensitivities to cardioactive glycosides[300–302]. In addition, as previously reported, the cytotoxic potency of PLTX appears to be related to the individual expression pattern of the

different genetic variants of Na^+/K^+ ATPase[299]. In this thesis, the expression levels of the four isoforms for the α subunit and of the three isoforms for the β subunit were analysed. The data obtained showed that all the isoforms analysed are differentially expressed between stem cells and HaCaT cells. In particular, the isoforms $\alpha 2$, $\alpha 3$ and $\beta 2$ are significantly more expressed in stem cells than in HaCaT cells, where their expression is negligible. On the basis of the relative gene expression data of each isoform, the gene expression ratios of these isoforms were calculated for both iPSC and HaCaT cell: in particular, the $\alpha 1/\alpha 3$ expression ratio appeared higher in HaCaT cells (expression ratio of 14.5 in iPSC and 3167.3 in HaCaT), while the $\alpha 3/\beta 3$ (0.07 in iPSC and 0.00015 in HaCaT) and $\alpha 3/\beta 1$ (0.3 in iPSC and 0.002 in HaCaT) expression ratios was higher in iPSC.

These observations are consistent with that previously reported on monocytes collected from healthy volunteers in which a negative correlation between EC_{50}s and the $\alpha 1$ and $\alpha 3$ expression ratio as well as a positive correlation between EC_{50}s and the $\alpha 3/\beta 3$ and $\alpha 3/\beta 1$ expression ratios were reported[299]. On the whole, these data corroborate the hypothesis that specific gene expression patterns of the single isoforms of α and β subunits of the molecular target of PLTX may be associated with a lower sensitivity towards the toxin.

However, despite this lower sensitivity, the toxin still appears to significantly reduce the viability of iPSC in a concentration- and time-dependent manner, suggesting a cytotoxic potential also on this model. Furthermore, by exposing iPSC to PLTX for 24 h to the toxin followed by 48 or 72 h in toxin-free medium, the calculated EC_{50}s and the concentration-response curves obtained were not statistically different with respect to the relevant continuous exposure of cells (72 and 96 h, respectively). These results suggest that PLTX-induced cytotoxicity was irreversible on iPSC, an important aspect that should be taken in consideration.

As a further step of the study, the embryotoxic potential of the toxin was evaluated by means of altered stemness properties of iPSC. As previously reported, in fact, literature data show that PLTX is capable of interfering with gene expression in *Xenopus laevis* embryos with consequent impact on embryos growth and development[128,129]. Initially, the effect of PLTX on stemness was analysed in terms of gene expression of a panel of 13 genes: five stemness markers (*OCT4*, *C-MYC*, *KLF4*, *SOX2*, and *NANOG*) and eight differentiation markers of the three germ layers (*SOX17*, *AFP* and *FOXA2* for endoderm; *ACTA2*, *BRACHYURY* and *CXCR4* for mesoderm; *PAX6* and *SOX1* for ectoderm). The data, expressed as $2^{-\Delta Ct}$ (normalized with respect to housekeeping *ACTB*) were represented as a heat map and a clustering analysis showed that PLTX maintains the stemness properties of iPSC regardless of time (24, 72 or 96 h) and type of exposure (continuous or recovery). Indeed, PLTX-treated iPSC were grouped with iPSC not exposed to the toxin in a high-affinity cluster. This result was confirmed by western blotting analysis, showing

that OCT4 (stem cell marker) was expressed in all PLTX-treated samples in a similar way with respect to iPSC not exposed to the toxin. In addition, the relevant markers of iPSC differentiation into the three germ layers were not detected in the former.

In the next step of the study, the ability of the toxin to induce any perturbation of the correct differentiation of stem cells into the three germ layers was evaluated. In this case, PLTX ($1.0x10^{-11}$ M) did not induce any cytotoxic effect in the three germ layers, but negatively influenced the differentiation of iPSC into endoderm cells, as can be seen from the clustering analysis of gene expression and protein analysis. In fact, PLTX exposure during iPSC differentiation towards endoderm seem to inhibit this process, maintaining iPSC at a stemness status. On the contrary, the differentiation towards the other two layers (mesoderm and ectoderm) seems to be not affected by the presence of PLTX. Intriguingly, on iPSC selectively differentiated into the three germ layers and exposed to PLTX for 24 h after completing the differentiation process, different sensitivities of the three germ layers were evidenced towards the toxin: endoderm and ectoderm were the most sensitive to the cytotoxic effect of PLTX; conversely, the mesoderm was almost insensitive to PLTX. Also in this case, the different sensitivity seems to be related to a different gene expression of some Na^+/K^+ ATPase isoforms, being $\alpha 2$ and $\alpha 3$ the most differently expressed in the ectoderm germ layer. However, in this case, the different cytotoxicity of PLTX was not clearly associated with the expression of the isoforms of the molecular target, for this reason further studies are necessary to clarify this aspect.

In conclusion, using an iPSC model, section B of this thesis highlighted the potential embryotoxic effect of PLTX during the early phases of embryo development, an aspect still under-evaluated in literature. In particular, even though stem cells appear to be less sensitive to the toxin effects in comparison to somatic cells, PLTX is still able to induce significant irreversible concentration- and time-dependent cytotoxic effects. It should be noted that these effects were recorded at nanomolar and sub-nanomolar concentrations, usually used in literature to study the *in vitro* effects of the toxin. However, given the lack of epidemiological data showing the actual human exposure during PLTX poisonings, it is unfeasible to estimate a possible embryo exposure to the toxin. Some speculations can be made by the evaluation of PLTX release by *O.* cf. *ovata* cells, to which humans could be exposed accidentally by different exposure routes, or by *Palythoa* corals during human poisonings. For instance, Guerrini et al. quantified 6.13×10^{-6} g/L (around $2x10^{-9}$ M)[206] of PLTX released by cultured *O. ovata* collected in the Tyrrhenian Sea in 2006. More recently, around 41 μg/mL (equal to about $1x10^{-5}$ M) were detected in the water of an aquarium containing *Palythoa* corals during a poisoning episode[100]. These levels are higher than the toxin concentrations inducing significant cytotoxic effects on iPSC. However, given the

lack of toxicokinetic data on PLTX, it is impossible to predict the entity of embryo exposure to this toxin.

Notwithstanding, the ability of very low toxin concentrations (i.e. $1x10^{-11}$ M) to induce a perturbation on the correct differentiation of stem cells towards endoderm represents an important finding at the basis of an incorrect embryo development. However, considering that iPSC represent a simple *in vitro* model of the early phases of embryo development, further studies are necessary to understand the actual embryotoxic potential of PLTX, also considering the subsequent developmental phases.

General conclusions

The increased incidence, frequency and geographical distribution of the phenomenon called Harmful Algal Bloom (HAB) represent an emergent sanitary problem also in the Mediterranean Sea. The algal species associated with this phenomenon can produce potent biotoxins, with negative consequences both at the ecosystem level and on human health, with a potential negative socio-economic impact.

The present thesis was divided in two parts, covering both ecotoxicological and human toxicology aspects. In the first part of the study, the ecotoxicological impact of four marine toxins frequently identified in last decades also in the Mediterranean Sea (PLTX, OA, DTX1 and DTX2) was assessed on *Artemia franciscana*, a model organism for ecotoxicological studies. This is the first study on the effects of these pure toxins on different developmental stages of an *Artemia* species, considering not only the organism's mortality (the main evaluated parameter reported in literature) but also analysing some biochemical parameters, such as the induction of oxidative stress. Exposure of *A. franciscana* to these toxins induced a different pattern of variations in ROS levels and antioxidant enzymes, suggesting differences in the mechanisms of toxicity. All the toxins exerted toxic effects on *A. franciscana* at concentrations higher than those detected at the environmental level, so far. However, it has to be considered that the incidence and frequency of HABs, as well as the geographic expansion of the toxins' producers are constantly increasing and could lead to higher environmental toxins concentrations. The toxic effects on *A. franciscana* suggest a potential ecotoxicological impact of these toxins due to a possible reduction of *Artemia* population. Being *Artemia* spp. significant components of the marine zooplankton, which is at the basis of the marine food web, a reduction of this micro-crustacean population at the environmental level could have negative impacts also on organisms at higher trophic level. Among the four investigated toxins, PLTX resulted the most lethal compound (followed by DTX1 > OA = DTX2; based on the calculated LC_{50}s).

For this reason, in the second part of the study, PLTX was investigated also for its effects on humans, considering the still under-evaluated embryotoxic potential. This is the first study on this aspect using a human induced pluripotent stem cell (iPSC) line as an *in vitro* model. Although iPSC were more resistant to the cytotoxic effects of PLTX than somatic cells, the toxin impaired their correct differentiation towards the endoderm. Considering the effect on cells differentiated toward the three germ layers, it exerted the highest cytotoxicity toward endoderm, which suggests a potential embryotoxic effect due to an impaired embryo development. However, it has to be considered that these effects were

observed at very low concentrations, and the level of a possible embryo exposure to PLTX cannot be estimated due to the lack of PLTX toxicokinetic data. Moreover, since iPSC are a simple *in vitro* model of the early stages of embryonic development, further studies are needed to assess the effects of PLTX at subsequent embryonic differentiation steps, aimed at completely understanding its potential embryotoxicity.

In conclusion, this thesis increased the knowledge on the toxic effects of PLTX, OA and two its analogues at environmental level and in humans, also in the perspective of a future increase of exposure to these toxins due to the diffusion of their producers during the globally expanding HAB phenomenon.

References

1. Anderson, D. M. Approaches to monitoring, control and management of harmful algal blooms (HABs). *Ocean & Coastal Management* **52**, 342–347 (2009).
2. Patel, S. S., Lovko, V. J. & Lockey, R. F. Red Tide: Overview and Clinical Manifestations. *J Allergy Clin Immunol Pract* **8**, 1219–1223 (2020).
3. Zaccaroni, A. & Scaravelli, D. Toxicity of Sea Algal Toxins to Humans and Animals. in *Algal Toxins: Nature, Occurrence, Effect and Detection* (eds. Evangelista, V., Barsanti, L., Frassanito, A. M., Passarelli, V. & Gualtieri, P.) 91–158 (Springer Netherlands, 2008).
4. Grattan, L. M., Holobaugh, S. & Morris, J. G. Harmful Algal Blooms and Public Health. *Harmful Algae* **57**, 2–8 (2016).
5. Kouakou, C. R. C. & Poder, T. G. Economic impact of harmful algal blooms on human health: a systematic review. *Journal of Water and Health* **17**, 499–516 (2019).
6. Sanseverino, I., Conduto, Diana, Pozzoli, Luca, Dobricic, Srdan & Lettieri, Teresa. *Algal bloom and its economic impact - Publications Office of the EU*. EUR 27905 EU (2016).
7. Todd, E.C:D. Estimated costs of paralytic shellfish, diarrhetic. in *Harmful Marine Algal Blooms* 831–834 (Lavoisier, 1995).
8. Pretty, J.N. *et al.* Environmental Costs of Freshwater Eutrophication in England and Wales | Environmental Science & Technology. *Environ. Sci. Technol.* **37**, 201–208 (2003).
9. Lipton, D.W. Pfiesteria's Economic Impact on Seafood Industry Sales & Recreational Fishing. in *Proceedings of the Workshop on the Economics of Policy Options for Nutrient Management and Pfiesteria* 35–38 (B. L. Gardner and L. Koch (eds.), 1999).
10. Dodds, W., K. *et al.* Eutrophication of U.S. Freshwaters: Analysis of Potential Economic Damages. *Environ Sci Technol* **43**, 12–19 (2009).
11. Anderson, D. M., Andersen, P., Bricelj, V. M., Cullen, J. J. & Rensel, J. J. *Monitoring and management strategies for harmful algal blooms in coastal waters*. (APEC #201-MR-01.1, Asia Pacific Economic Program, Singapore, and Intergovernmental Oceanographic Commission Technical Series No. 59, 2001).
12. Zingone, A. *et al.* Toxic marine microalgae and noxious blooms in the Mediterranean Sea: A contribution to the Global HAB Status Report. *Harmful Algae* **102** 101843 (2021).
13. Neves, R. A. F., Nascimento, S. M. & Santos, L. N. Harmful algal blooms and shellfish in the marine environment: an overview of the main molluscan responses, toxin dynamics, and risks for human health. *Environ Sci Pollut Res* **28**, 55846–55868 (2021).

14. Faggio, C., Torre, A., Lando, G., Sabatino, G. & Trischitta, F. Carbonate precipitates and bicarbonate secretion in the intestine of sea bass, Dicentrarchus labrax. *J Comp Physiol B* **181**, 517–525 (2011).

15. Parsaeimehr, A., Lutzu, G. A., Rahman Shah, M. & Parra Saldivar, R. Detection to treatment and global impacts of algal toxins. *Front Biosci (Schol Ed)* **11**, 214–235 (2019).

16. *Report of the Joint FAO/IOC/WHO ad hoc ExpertConsultation on Biotoxins in Bivalve Molluscs*. (2004).

17. Morabito, S., Silvestro, S. & Faggio, C. How the marine biotoxins affect human health. *Nat Prod Res* **32**, 621–631 (2018).

18. McCabe, R. M. *et al.* An unprecedented coastwide toxic algal bloom linked to anomalous ocean conditions. *Geophys Res Lett* **43**, 10366–10376 (2016).

19. Tillmann, U., Elbrächter, M., Krock, B., John, U. & Cembella, A. Azadinium spinosum gen. et sp. nov. (Dinophyceae) identified as a primary producer of azaspiracid toxins. *European Journal of Phycology* **44**, 63–79 (2009).

20. Landsberg, J. H. The Effects of Harmful Algal Blooms on Aquatic Organisms. *Reviews in Fisheries Science* **10**, 113–390 (2002).

21. Moore, R. E. & Scheuer, P. J. Palytoxin: A New Marine Toxin from a Coelenterate. *Science* **172**, 495–498 (1971).

22. Walsh, G. E. & Bowers, R. L. A review of Hawaiian zoanthids with descriptions of three new species. *Zoological Journal of the Linnean Society* **50**, 161–180 (1971).

23. Oku, N., Sata, N. U., Matsunaga, S., Uchida, H. & Fusetani, N. Identification of palytoxin as a principle which causes morphological changes in rat 3Y1 cells in the zoanthid Palythoa aff. margaritae. *Toxicon* **43**, 21–25 (2004).

24. Quinn, R. J., Kashiwagi, M., Moore, R. E. & Norton, T. R. Anticancer activity of zoanthids and the associated toxin, palytoxin, against Ehrlich ascites tumor and P-388 lymphocytic leukemia in mice. *J Pharm Sci* **63**, 257–260 (1974).

25. Béress, L., Zwick, J., Kolkenbrock, H. J., Kaul, P. N. & Wassermann, O. A method for the isolation of the caribbean palytoxin (C-PTX) from the coelenterate (zooanthid) Palythoa caribaeorum. *Toxicon* **21**, 285–290 (1983).

26. Gleibs, S. & Mebs, D. Distribution and sequestration of palytoxin in coral reef animals. *Toxicon* **37**, 1521–1527 (1999).

27. Hashimoto, Y., Fusetani, N. & Kimura, S. Aluterin: a Toxin of Filefish, Alutera scripta, Probably Originating from a Zoantharian, Palythoa tuberculosa. *J-stage* **35**, 1086–1093 (1969).

28. Deeds, J. R., Handy, S. M., White, K. D. & Reimer, J. D. Palytoxin found in Palythoa sp. zoanthids (Anthozoa, Hexacorallia) sold in the home aquarium trade.
PLoS ONE **6**, e18235 (2011).

29. Gleibs, S., Mebs, D. & Werding, B. Studies on the origin and distribution of palytoxin in a Caribbean coral reef. *Toxicon* **33**, 1531–1537 (1995).
30. Ukena, T. *et al.* Structure elucidation of ostreocin D, a palytoxin analog isolated from the dinoflagellate Ostreopsis siamensis. *Bioscience, Biotechnology, and Biochemistry* **65**, 2585–2588 (2001).
31. Lenoir, S. *et al.* First evidence of palytoxin analogues from an Ostreopsis mascarenensis (Dinophyceae) benthic bloom in southwestern Indian ocean. *J. Phycol.* **40**, 1042–1051.
32. Ciminiello, P. *et al.* Complex palytoxin-like profile of Ostreopsis ovata. Identification of four new ovatoxins by high-resolution liquid chromatography/mass spectrometry. *Rapid Communications in Mass Spectrometry* **24**, 2735–2744 (2010).
33. Kerbrat, A. S. *et al.* First Evidence of Palytoxin and 42-Hydroxy-palytoxin in the Marine Cyanobacterium Trichodesmium. *Mar Drugs* **9**, 543–560 (2011).
34. Uemura, D., Hirata, Y., Iwashita, T. & Naoki, H. Studies on palytoxins. *Tetrahedron* **41**, 1007–1017 (1985).
35. Moore, R. E., Helfrich, P. & Patterson, G. M. L. The deadly seaweed of Hana [Palythoa toxica, coelenterates, Hawaii]. *Oceanus* **25**, 54–63 (1982).
36. Carballeira, N. M. *et al.* Fatty acid composition of bacteria associated with the toxic dinoflagellate Ostreopsis lenticularis and with Caribbean Palythoa species. *Lipids* **33**, 627–632 (1998).
37. Seeman, P., Gernert, C., Schmitt, S., Mebs, D. & Hentschel, U. Detection of hemolytic bacteria from Palythoa caribaeorum (Cnidaria, Zoantharia) using a novel palytoxin-screening assay. *Antonie van Leeuwenhoek* **96**, 405–411 (2009).
38. Frolova, G. M., Kuznetsova, T. A., Mikhailov, V. V. & Elyakov, G. B. An enzyme linked immunosorbent assay for detecting palytoxin-producing bacteria. *Russ J Bioorg Chem* **26**, 285–289 (2000).
39. Ramos, V. & Vasconcelos, V. Palytoxin and analogs: biological and ecological effects. *Mar Drugs* **8**, 2021–2037 (2010).
40. Pelin, M., Brovedani, V., Sosa, S. & Tubaro, A. Palytoxin-Containing Aquarium Soft Corals as an Emerging Sanitary Problem. *Mar Drugs* **14**, E33 (2016).
41. Moore, R. E. & Bartolini, G. Structure of palytoxin. *Jurnal of American Chemical Society* **103**, 2491–2494 (1981).
42. Uemura, D., Ueda, K., Hirata, Y., Naoki, H. & Iwashita, T. Further studies on palytoxin. II. structure of palytoxin. *Tetrahedron Letters* **22**, 2781–2784 (1981).
43. Patocka, J., Nepovimova, E., Wu, Q. & Kuca, K. Palytoxin congeners. *Arch Toxicol* **92**, 143–156 (2018).

44. Tubaro, A., Sosa, S. & Hungerford, J. Toxicology and diversity of marine toxins. in *Veterinary Toxicology* 896–934 (Academic Press, 2012).
45. Tartaglione, L. *et al.* Chemical, molecular, and eco-toxicological investigation of Ostreopsis sp. from Cyprus Island: structural insights into four new ovatoxins by LC-HRMS/MS. *Anal Bioanal Chem* **408**, 915–932 (2016).
46. Pelin, M., Sosa, S. & Tubaro, A. Palytoxins: Toxicological Profile. in *Marine and Freshwater Toxins* (eds. Gopalakrishnakone, P., Haddad Jr., V., Tubaro, A., Kim, E. & Kem, W. R.) 129–145 (Springer Netherlands, 2016).
47. Ciminiello, P. *et al.* Stereostructure and biological activity of 42-hydroxy-palytoxin: a new palytoxin analogue from Hawaiian Palythoa subspecies. *Chem Res Toxicol* **22**, 1851-1859 (2009).
48. Tubaro, A. *et al.* Acute oral toxicity in mice of a new palytoxin analog: 42-hydroxy-palytoxin. *Toxicon* **57**, 755–763 (2011).
49. Ciminiello, P. *et al.* Stereoisomers of 42-hydroxy palytoxin from Hawaiian Palythoa toxica and P. tuberculosa: stereostructure elucidation, detection, and biological activities. *J Nat Prod* **77**, 351–357 (2014).
50. Ito, E. & Yasumoto, T. Toxicological studies on palytoxin and ostreocin-D administered to mice by three different routes. *Toxicon* **54**, 244–251 (2009).
51. Poli, M. *et al.* Toxicity and pathophysiology of palytoxin congeners after intraperitoneal and aerosol administration in rats. *Toxicon* **150**, 235–250 (2018).
52. Pelin, M. *et al.* Pro-inflammatory effects of palytoxin: an in vitro study on human keratinocytes and inflammatory cells. *Toxicol Res (Camb)* **5**, 1172–1181 (2016).
53. Rhodes, L. World-wide occurrence of the toxic dinoflagellate genus Ostreopsis Schmidt. *Toxicon* **57**, 400–407 (2011).
54. Redondo, J., Fiedler, B. & Scheiner-Bobis, G. Palytoxin-induced Na+ influx into yeast cells expressing the mammalian sodium pump is due to the formation of a channel within the enzyme. *Molecular pharmacology* **49**, 49–57 (1996).
55. Chhatwal, G. S., Hessler, H. J. & Habermann, E. The action of palytoxin on erythrocytes and resealed ghosts. *Naunyn-Schmiedeberg's Archives of Pharmacology* **323**, 261-268 (1983).
56. Böttinger, H., Béress, L. & Habermann, E. Involvement of (Na+ + K+)-ATPase in binding and actions of palytoxin on human erythrocytes. *Biochimica et Biophysica Acta (BBA) - Biomembranes* **861**, 165–176 (1986).
57. Scheiner-Bobis, G., zu Heringdorf, D. M., Christ, M. & Habermann, E. Palytoxin induces K+ efflux from yeast cells expressing the mammalian sodium pump. *Molecular pharmacology* **45**, 1132–1136 (1994).

58. Artigas, P. & Gadsby, D. C. Ion Occlusion/Deocclusion Partial Reactions in Individual Palytoxin-Modified Na/K Pumps. *Annals of the new york academy of sciences* **986**, 116–126 (2006).

59. Guennoun, S. & Horisberger, J. D. Structure of the 5th transmembrane segment of the Na,K-ATPase α subunit: a cysteine-scanning mutagenesis study. *FEBS Letters* **482**, 144-148 (2000).

60. Cornelius, F. Rate Determination in Phosphorylation of Shark Rectal Na,K-ATPase by ATP: Temperature Sensitivity and Effects of ADP. *Biophysical Journal* **77**, 934–942 (1999).

61. Rakowski, R. F., Gadsby, D. C. & De Weer, P. Stoichiometry and voltage dependence of the sodium pump in voltage-clamped, internally dialyzed squid giant axon. *J Gen Physiol* **93**, 903–941 (1989).

62. Lingrel, J. B. & Kuntzweiler, T. Na+,K(+)-ATPase. *J Biol Chem* **269**, 19659–19662 (1994).

63. Vale, C. & Ares, I. R. Biochemistry of Palytoxins and Ostreocins. in *Phycotoxins: Chemistry and Biochemistry* 95–118 (John Wiley & Sons, Ltd, 2007).

64. Glorioso, N. *et al.* Association of ATP1A1 and dear single-nucleotide polymorphism haplotypes with essential hypertension: sex-specific and haplotype-specific effects. *Circ Res* **100**, 1522–1529 (2007).

65. Scarrone, S. *et al.* Sex differences in human lymphocyte Na,K-ATPase as studied by labeled ouabain binding. *Int J Neurosci* **117**, 275–285 (2007).

66. Rodrigues, A. M., Almeida, A.-C. G., Infantosi, A. F. C., Teixeira, H. Z. & Duarte, M. A. Model and simulation of Na+/K+ pump phosphorylation in the presence of palytoxin. *Comput Biol Chem* **32**, 5–16 (2008).

67. Ikeda, M., Mitani, K. & Ito, K. Palytoxin induces a nonselective cation channel in single ventricular cells of rat. *Naunyn Schmiedebergs Arch Pharmacol* **337**, 591–593 (1988).

68. Muramatsu, I., Nishio, M., Kigoshi, S. & Uemura, D. Single ionic channels induced by palytoxin in guinea-pig ventricular myocytes. *Br J Pharmacol* **93**, 811–816 (1988).

69. Artigas, P. & Gadsby, D. C. Large diameter of palytoxin-induced Na/K pump channels and modulation of palytoxin interaction by Na/K pump ligands. *J Gen Physiol* **123**, 357–376 (2004).

70. Habermann, E. Palytoxin acts through Na+,K+-ATPase. *Toxicon* **27**, 1171-1187 (1989).

71. picture of sodium potassium pump. https://www.pinterest.cl/pin/30680841184793976/.

72. Rossini, G. P. & Bigiani, A. Palytoxin action on the Na+,K+-ATPase and the disruption of ion equilibria in biological systems. *Toxicon* **57**, 429–439 (2011).

73. Vale, C., Alfonso, A., Suñol, C., Vieytes, M. R. & Botana, L. M. Modulation of calcium entry and glutamate release in cultured cerebellar granule cells by palytoxin. *J Neurosci Res* **83**, 1393–1406 (2006).
74. Wu, C. H. Palytoxin: membrane mechanisms of action. *Toxicon* **54**, 1183–1189 (2009).
75. Kockskämper, J. *et al.* Palytoxin disrupts cardiac excitation-contraction coupling through interactions with P-type ion pumps. *Am J Physiol Cell Physiol* **287**, C527-538 (2004).
76. Del Favero, G. *et al.* Sanitary problems related to the presence of Ostreopsis spp. in the Mediterranean Sea: a multidisciplinary scientific approach. *Ann Ist Super Sanita* **48**, 407–414 (2012).
77. Bellocci, M., Sala, G. L. & Prandi, S. The cytolytic and cytotoxic activities of palytoxin. *Toxicon* **57**, 449–459 (2011).
78. Louzao, M. C., Ares, I. R. & Cagide, E. Marine toxins and the cytoskeleton: a new view of palytoxin toxicity. *FEBS J* **275**, 6067–6074 (2008).
79. Pelin, M., Sosa, S., Pacor, S., Tubaro, A. & Florio, C. The marine toxin palytoxin induces necrotic death in HaCaT cells through a rapid mitochondrial damage. *Toxicol Lett* **229**, 440–450 (2014).
80. EFSA Panel on Contaminants in the Food Chain (CONTAM). Scientific Opinion on marine biotoxins in shellfish – Palytoxin group. *EFSA Journal* **7**, 1393 (2009).
81. Amzil, Z. *et al.* Ovatoxin-a and palytoxin accumulation in seafood in relation to Ostreopsis cf. ovata blooms on the French Mediterranean coast. *Mar Drugs* **10**, 477–496 (2012).
82. Alcala, A. C., Alcala, L. C., Garth, J. S., Yasumura, D. & Yasumoto, T. Human fatality due to ingestion of the crab Demania reynaudii that contained a palytoxin-like toxin. *Toxicon* **26**, 105–107 (1988).
83. Onuma, Y. *et al.* Identification of putative palytoxin as the cause of clupeotoxism. *Toxicon* **37**, 55–65 (1999).
84. Taniyama, S. *et al.* Occurrence of a food poisoning incident by palytoxin from a serranid Epinephelus sp. in Japan. *J Nat Toxins* **11**, 277–282 (2002).
85. Wu, M.-L., Yang, C.-C., Deng, J.-F. & Wang, K.-Y. Hyperkalemia, hyperphosphatemia, acute kidney injury, and fatal dysrhythmias after consumption of palytoxin-contaminated goldspot herring. *Ann Emerg Med* **64**, 633–636 (2014).
86. Tubaro, A. *et al.* Case definitions for human poisonings postulated to palytoxins exposure. *Toxicon* **57**, 478–495 (2011).
87. Kasuhara, K. *et al.* Rhabdomyolysis induced by ostraciid fish poisoing. *Nihon Naika Gakkai Zasshi* **94**, 750–752 (2005).
88. Deeds, J. R. & Schwartz, M. D. Human risk associated with palytoxin exposure. *Toxicon* **56**, 150–162 (2010).

89. Okano, H. *et al.* Rhabdomyolysis and myocardial damage induced by palytoxin, a toxin of blue humphead parrotfish. *Internal Medicine (Tokyo, Japan)* **37**, 330–333 (1998).
90. Llewellyn, L. E. Human fatalities in Vanuatu after eating a crab (Daira perlata). *Med J Aust* **175**, 343–344 (2001).
91. Shinzato, T. *et al.* Cowfish (Umisuzume, Lactoria diaphana) poisoning with rhabdomyolysis. *Intern Med* **47**, 853–856 (2008).
92. Taniyama, S. *et al.* Survey of food poisoning incidents in Japan due to ingestion of marine boxfish and their toxicity. *Shokuhin Eiseigaku Zasshi* **50**, 270–277 (2009).
93. Hoffmann, K. *et al.* A case of palytoxin poisoning due to contact with zoanthid corals through a skin injury. *Toxicon* **51**, 1535–1537 (2008).
94. Nordt, S. P., Wu, J., Zahller, S., Clark, R. F. & Cantrell, F. L. Palytoxin poisoning after dermal contact with zoanthid coral. *J Emerg Med* **40**, 397–399 (2011).
95. Durando, P. *et al.* Ostreopsis ovata and human health: epidemiological and clinical features of respiratory syndrome outbreaks from a two-year syndromic surveillance, 2005-06, in north-west Italy. *Euro Surveill* **12**, E070607.1 (2007).
96. Tichadou, L. *et al.* Health impact of unicellular algae of the Ostreopsis genus blooms in the Mediterranean Sea: experience of the French Mediterranean coast surveillance network from 2006 to 2009. *Clin Toxicol (Phila)* **48**, 839–844 (2010).
97. Honsell, G. *et al.* Harmful dinoflagellate Ostreopsis cf. ovata Fukuyo: detection of ovatoxins in field samples and cell immunolocalization using antipalytoxin antibodies. *Environ Sci Technol* **45**, 7051–7059 (2011).
98. Wieringa, A. *et al.* Respiratory impairment in four patients associated with exposure to palytoxin containing coral. *Clin Toxicol (Phila)* **52**, 150–151 (2014).
99. Hamade, A. K. *et al.* Suspected Palytoxin Inhalation Exposures Associated with Zoanthid Corals in Aquarium Shops and Homes - Alaska, 2012-2014. *MMWR Morb Mortal Wkly Rep* **64**, 852–855 (2015).
100. Tartaglione, L. *et al.* An aquarium hobbyist poisoning: Identification of new palytoxins in Palythoa cf. toxica and complete detoxification of the aquarium water by activated carbon. *Toxicon* **121**, 41–50 (2016).
101. Rumore, M. M. & Houst, B. M. Palytoxin poisoning via inhalation in pediatric siblings. *IJCRI* **5**, 501 (2014).
102. Bernasconi, M., Berger, D., Tamm, M. & Stolz, D. Aquarism: an innocent leisure activity? Palytoxin-induced acute pneumonitis. *Respiration* **84**, 436–439 (2012).
103. Sud, P., Su, M. K., Greller, H. A., Majlesi, N. & Gupa, A. Case series: inhaled coral vapor -- toxicity in a tank. *J Med Toxicol.* **9**, 282–286 (2013).

104. Ruiz, Y., Fuchs, J., Beuschel, R., Tschopp, M. & Goldblum, D. Dangerous reef aquaristics: Palytoxin of a brown encrusting anemone causes toxic corneal reactions. *Toxicon* **106**, 42–45 (2015).

105. Ciminiello, P. *et al.* First finding of Ostreopsis cf. ovata toxins in marine aerosols. *Environ Sci Technol* **48**, 3532–3540 (2014).

106. Shears, N. T. & Ross, P. M. Blooms of benthic dinoflagellates of the genus Ostreopsis; an increasing and ecologically important phenomenon on temperate reefs in New Zealand and worldwide. *Harmful Algae* **8**, 916–925 (2009).

107. Moshirfar, M., Khalifa, Y. M., Espandar, L. & Mifflin, M. D. Aquarium coral keratoconjunctivitis. *Arch Ophthalmol* **128**, 1360–1362 (2010).

108. Kermarec, F. *et al.* Health risks related to Ostreopsis ovata in recreational waters. *Environnement, Risques & Santé* **7**, 357–363 (2008).

109. Ciminiello, P. *et al.* The Genoa 2005 outbreak. Determination of putative palytoxin in Mediterranean Ostreopsis ovata by a new liquid chromatography tandem mass spectrometry method. *Anal Chem* **78**, 6153–6159 (2006).

110. Sansoni, G. *et al.* Fioriture algali di Ostreopsis ovata (Gonyaulacales: Dinophyceae): un problema emergente. *Biologia Ambientale* **17**, 17–23 (2003).

111. Aligizaki, K., Katikou, P., Milandri, A. & Diogène, J. Occurrence of palytoxin-group toxins in seafood and future strategies to complement the present state of the art. *Toxicon* **57**, 390–399 (2011).

112. Morton, B. E., Fraser, C. F., Thenawidjaja, M., Albagli, L. & Rayner, M. D. Potent inhibition of sperm motility by palytoxin. *Exp Cell Res* **140**, 261–265 (1982).

113. Totti, C., Accoroni, S., Cerino, F., Cucchiari, E. & Romagnoli, T. Ostreopsis ovata bloom along the Conero Riviera (northern Adriatic Sea): Relationships with environmental conditions and substrata. *Harmful Algae* **9**, 233–239 (2010).

114. Gorbi, S. *et al.* Biological effects of palytoxin-like compounds from Ostreopsis cf. ovata: a multibiomarkers approach with mussels Mytilus galloprovincialis. *Chemosphere* **89**, 623–632 (2012).

115. Accoroni, S. & Totti, C. The toxic benthic dinoflagellates of the genus Ostreopsis in temperate areas: a review. *Adv Ocean Limnol* **7**, (2016).

116. Faimali, M. *et al.* Toxic effects of harmful benthic dinoflagellate Ostreopsis ovata on invertebrate and vertebrate marine organisms. *Marine Environmental Research* **76**, 97–107 (2012).

117. Neves, R. A. F., Contins, M. & Nascimento, S. M. Effects of the toxic benthic dinoflagellate Ostreopsis cf. ovata on fertilization and early development of the sea urchin Lytechinus variegatus. *Mar. Environ. Res.* **135**, 11–17 (2018).

118. Pagliara, P. & Caroppo, C. Toxicity assessment of Amphidinium carterae, Coolia cfr. monotis and Ostreopsis cfr. ovata (Dinophyta) isolated from the northern Ionian Sea (Mediterranean Sea). *Toxicon* **60**, 1203–1214 (2012).

119. Privitera, D. *et al.* Toxic effects of Ostreopsis ovata on larvae and juveniles of Paracentrotus lividus. *Harmful Algae* **18**, 16–23 (2012).

120. Gorbi, S. *et al.* Effects of harmful dinoflagellate Ostreopsis cf. ovata exposure on immunological, histological and oxidative responses of mussels Mytilus galloprovincialis. *Fish Shellfish Immunol.* **35**, 941–950 (2013).

121. Louzao, M. C. *et al.* Cytotoxic effect of palytoxin on mussel. *Toxicon* **56**, 842–847 (2010).

122. Cen, J. *et al.* Effects of palytoxins extracted from Ostreopsis ovata on the oxidative stress and immune responses in Pacific white shrimp Litopenaeus vannamei. *Fish Shellfish Immunol.* **95**, 670–678 (2019).

123. Pezzolesi, L. *et al.* Influence of temperature and salinity on Ostreopsis cf. ovata growth and evaluation of toxin content through HR LC-MS and biological assays. *Water Research* **46**, 82–92 (2012).

124. Neves, R. A. F., Fernandes, T., dos Santos, L. N. & Nascimento, S. M. Toxicity of benthic dinoflagellates on grazing, behavior and survival of the brine shrimp Artemia salina. *PLoS One* **12**, (2017).

125. Rhodes, L., Adamson, J., Suzuki, T., Briggs, L. & Garthwaite, I. Toxic marine epiphytic dinoflagellates, Ostreopsis siamensis and Coolia monotis (Dinophyceae), in New Zealand. *New Zealand Journal of Marine and Freshwater Research* **34**, 371–383 (2000).

126. Anne-Sophie, P. *et al.* Effects of the toxic dinoflagellate Ostreopsis cf. ovata on survival, feeding and reproduction of a phytal harpacticoid copepod. *Journal of Experimental Marine Biology and Ecology* **516**, 103–113 (2019).

127. Guppy, R., Ackbarali, C. & Ibrahim, D. Toxicity of crude organic extracts from the zoanthid Palythoa caribaeorum: A biogeography approach. *Toxicon* **167**, 117–122 (2019).

128. Franchini, A., Casarini, L. & Ottaviani, E. Toxicological effects of marine palytoxin evaluated by FETAX assay. *Chemosphere* **73**, 267–271 (2008).

129. Franchini, A., Casarini, L., Malagoli, D. & Ottaviani, E. Expression of the genes siamois, engrailed-2, bmp4 and myf5 during Xenopus development in presence of the marine toxins okadaic acid and palytoxin. *Chemosphere* **77**, 308–312 (2009).

130. Tachibana, K. *et al.* Okadaic acid, a cytotoxic polyether from two marine sponges of the genus Halichondria. *Jurnal of American Chemical Society* **103**, 2469–2471 (1981).

131. Reguera, B. *et al.* Dinophysis toxins: causative organisms, distribution and fate in shellfish. *Mar Drugs* **12**, 394–461 (2014).

132. Yasumoto, T., Seino, N., Murakami, Y. & Murata, M. Toxins Produced by Benthic Dinoflagellates. *Biological Bulletin* **172**, 128–131 (1987).
133. Sosa, S. & Tubaro, A. Okadaic Acid and Other Diarrheic Toxins: Toxicological Profile. in *Marine and Freshwater Toxins* 147–168 (2016).
134. Murata, M., Shimatani, M., Sugitani, H., Oshima, Y. & Yasumoto, T. Isolation and structural elucidation of the causative toxin of the diarrhetic shellfish poisoning. *Bulletin of the Japanese Society of Scientific Fisheries* **48**, 549–552 (1982).
135. Hu, T. *et al.* Isolation of a new diarrhetic shellfish poison from Irish mussels. *J. Chem. Soc., Chem. Commun.* **1**, 39–41 (1992).
136. Yasumoto, T. *et al.* Diarrhetic shellfish toxins. *Tetrahedron* **41**, 1019–1025 (1985).
137. Suzuki, T. & Mitsuya, T. Comparison of dinophysistoxin-1 and esterified dinophysistoxin-1 (dinophysistoxin-3) contents in the scallop Patinopecten yessoensis and the mussel Mytilus galloprovincialis. *Toxicon* **39**, 905–908 (2001).
138. Hu, T., Curtis, J., Walter, J. & Wright, J. L. C. Identification of DTX-4, a new water-soluble phosphatase inhibitor from the toxic dinoflagellate Prorocentrum lima. *Journal of the Chemical Society, Chemical Communications* **5**, 597 (1995).
139. Hu, T., Curtis, J. M., Walter, J. A., McLachlan, J. L. & Wright, J. L. C. Two new water-soluble dsp toxin derivatives from the dinoflagellate prorocentrum maculosum: possible storage and excretion products. *Tetrahedron Letters* **36**, 9273–9276 (1995).
140. Konoki, K. *et al.* In Vitro Acylation of Okadaic Acid in the Presence of Various Bivalves' Extracts. *Mar Drugs* **11**, 300–315 (2013).
141. Murata, M., Legrand, A., Ishibashi, Y., Fukui, M. & Yasumoto, T. Structures and Configurations of Ciguatoxin from the Moray Eel Gymnothorax javanicus and Its Likely Precursor from the Dinoflagellate Gambierdiscus toxicus. *JACS* **112**, 4380–4386 (1990).
142. Honkanen, R. E., Codispoti, B. A., Tse, K., Boynton, A. L. & Honkanan, R. E. Characterization of natural toxins with inhibitory activity against serine/threonine protein phosphatases. *Toxicon* **32**, 339–350 (1994).
143. Takai, A. *et al.* Inhibitory effect of okadaic acid derivatives on protein phosphatases. A study on structure-affinity relationship. *Biochem J* **284 (Pt 2)**, 539–544 (1992).
144. Twiner, M. J. *et al.* Structure-Activity Relationship Studies Using Natural and Synthetic Okadaic Acid/Dinophysistoxin Toxins. *Mar Drugs* **14**, E207 (2016).
145. Cohen, P., Holmes, C. F. & Tsukitani, Y. Okadaic acid: a new probe for the study of cellular regulation. *Trends Biochem Sci* **15**, 98–102 (1990).
146. Louzao, M. C., Vieytes, M. R. & Botana, L. M. Effect of okadaic acid on glucose regulation. *Mini Rev Med Chem* **5**, 207–215 (2005).
147. Xing, Y. *et al.* Structure of protein phosphatase 2A core enzyme bound to tumor-inducing toxins. *Cell* **127**, 341–353 (2006).

148. Suganuma, M. *et al.* Okadaic acid: an additional non-phorbol-12-tetradecanoate-13-acetate-type tumor promoter. *Proc Natl Acad Sci U S A* **85**, 1768–1771 (1988).
149. Garibo, D., de la Iglesia, P., Diogène, J. & Campàs, M. Inhibition equivalency factors for dinophysistoxin-1 and dinophysistoxin-2 in protein phosphatase assays: applicability to the analysis of shellfish samples and comparison with LC-MS/MS. *J Agric Food Chem* **61**, 2572–2579 (2013).
150. Bialojan, C. & Takai, A. Inhibitory effect of a marine-sponge toxin, okadaic acid, on protein phosphatases. Specificity and kinetics. *Biochem J* **256**, 283–290 (1988).
151. Aquatic (marine and freshwater) biotoxins. in *Environmental health criteria (EHC) 37* (World Health Orgnization, 1984).
152. Hamano, Y., Kinoshita, Y. & Yasumoto, T. Enteropathogenicity of Diarrhetic Shellfish Toxins in Intestinal Models (Studies on Diarrhetic Shellfish Toxins. I). *Food Hygiene and Safety Science (Shokuhin Eiseigaku Zasshi)* **27**, 375 (1986).
153. Linee guida applicative del regolamento (ce) n. 853/2004 del parlamento europeo e del consiglio sull'igiene dei prodotti di origine animale.
154. Valdiglesias, V., Prego-Faraldo, M. V., Pásaro, E., Méndez, J. & Laffon, B. Okadaic acid: more than a diarrheic toxin. *Mar Drugs* **11**, 4328–4349 (2013).
155. Valdiglesias, V., Laffon, B., Pásaro, E. & Méndez, J. Okadaic acid induces morphological changes, apoptosis and cell cycle alterations in different human cell types. *J Environ Monit* **13**, 1831–1840 (2011).
156. Costa, A. P. *et al.* Neuroglial alterations in rats submitted to the okadaic acid-induced model of dementia. *Behav Brain Res* **226**, 420–427 (2012).
157. Valdiglesias, V. *et al.* Induction of oxidative DNA damage by the marine toxin okadaic acid depends on human cell type. *Toxicon* **57**, 882–888 (2011).
158. Leira, F., Louzao, M. C., Vieites, J. M., Botana, L. M. & Vieytes, M. R. Fluorescent microplate cell assay to measure uptake and metabolism of glucose in normal human lung fibroblasts. *Toxicol In Vitro* **16**, 267–273 (2002).
159. Valdiglesias, V. *et al.* Assessment of okadaic acid effects on cytotoxicity, DNA damage and DNA repair in human cells. *Mutat Res* **689**, 74–79 (2010).
160. Fujiki, H. & Suganuma, M. Carcinogenic aspects of protein phosphatase 1 and 2A inhibitors. *Prog Mol Subcell Biol* **46**, 221–254 (2009).
161. Kamat, P. K., Rai, S., Swarnkar, S., Shukla, R. & Nath, C. Molecular and cellular mechanism of okadaic acid (OKA)-induced neurotoxicity: a novel tool for Alzheimer's disease therapeutic application. *Mol Neurobiol* **50**, 852–865 (2014).

162. Flórez-Barrós, F., Prado-Alvarez, M., Méndez, J. & Fernández-Tajes, J. Evaluation of genotoxicity in gills and hemolymph of clam Ruditapes decussatus fed with the toxic dinoflagellate Prorocentrum lima. *J Toxicol Environ Health A* **74**, 971–979 (2011).
163. Carvalho Pinto-Silva, C. R. *et al.* Micronucleus induction in mussels exposed to okadaic acid. *Toxicon* **41**, 93–97 (2003).
164. Pinto-Silva, C. R. C., Creppy, E. E. & Matias, W. G. Micronucleus test in mussels Perna perna fed with the toxic dinoflagellate Prorocentrum lima. *Arch Toxicol* **79**, 422–426 (2005).
165. Escoffier, N. *et al.* Toxicity to medaka fish embryo development of okadaic acid and crude extracts of Prorocentrum dinoflagellates. *Toxicon* **49**, 1182–1192 (2007).
166. *Artemia: Basic and Applied Biology*. (Springer Netherlands, 2002). doi:10.1007/978-94-017-0791-6.
167. Asem, A. Historical record on brine shrimp Artemia more than one thousand years ago from Urmia Lake, Iran. *Journal of Biological Research-Thessaloniki* **9**, 113–114 (2008).
168. Asem, A., Rastegar-Pouyani, N. & Ríos-Escalante, P. D. L. The genus Artemia Leach, 1819 (Crustacea: Branchiopoda). I. True and false taxonomical descriptions. *Lat. Am. J. Aquat. Res.* **38**, 501–506 (2010).
169. Triantaphyllidis, G., Abatzopoulos, T. & Sorgeloos, P. Review of the biogeography of the genus Artemia (Crustacea, Anostraca). *Journal of Biogeography* **25**, 213–226 (1998).
170. Triantaphyllidis, G., Criel, G., Abatzopoulos, T. & Sorgeloos, P. International study on Artemia. LIII. Morphological study of Artemia with emphasis to Old World strains. I. Bisexual populations. *Hydrobiologia* **357**, 139–153 (1997).
171. Browne, R. A. *Artemia Biology*. (CRC Press, 2017). doi:10.1201/9781351069892.
172. Sorgeloos, P. The use of the brine shrimp Artemia in aquaculture. *The brine shrimp Artemia* **3**, 25–46 (1980).
173. Dhont, J. & Sorgeloos, P. Applications of Artemia. in *Artemia: Basic and Applied Biology* (eds. Abatzopoulos, Th. J., Beardmore, J. A., Clegg, J. S. & Sorgeloos, P.) 251–277 (Springer Netherlands, 2002). doi:10.1007/978-94-017-0791-6_6.
174. Lavens, P. & Sorgeloos, P. *Manual on the Production and Use of Live Food for Aquaculture*. (Food and Agriculture Organization of the United Nations, 1996).
175. Léger, P., Bengtson, D. A., Simpson, K. L. & Sorgeloos, P. The use and nutritional value of Artemia as a food source. (2000).
176. Cooper, S. D., Winkler, D. W. & Lenz, P. H. The Effect of Grebe Predation on a Brine Shrimp Population. *Journal of Animal Ecology* **53**, 51–64 (1984).
177. Kellogg, V. L. A new Artemia and its life conditions. *Science* **24**, 594–596 (1906).

178. Ruebhart, D. R., Cock, I. E. & Shaw, G. R. Brine shrimp bioassay: Importance of correct taxonomic identification of Artemia (Anostraca) species. *Environmental Toxicology* **23**, 555–560 (2008).
179. Sheir, S. K., Galal-Khallaf, A., Mohamed, A. H. & Mohammed-Geba, K. Morphological and molecular clues for recording the first appearance of Artemia franciscana in Egypt. *Heliyon* **4**, e01110 (2018).
180. Clegg, J. S. & Trotman, C. N. A. Physiological and Biochemical Aspects of Artemia Ecology. in *Abatzopoulos T.J., Beardmore J.A., Clegg J.S., Sorgeloos P. (eds) Artemia: Basic and Applied Biology* vol. 1 129–170 (Springer, Dordrecht, 2002).
181. Gajardo, G. M. & Beardmore, J. A. The brine shrimp artemia: adapted to critical life conditions. *Front Physiol* **3**, 185 (2012).
182. Ogello, E., Kembenya, E., Githukia, C., Nyonje, B. & Munguti, J. The occurrence of the brine shrimp, Artemia franciscana (Kellog 1906) in Kenya and the potential economic impacts among Kenyan coastal communities. *International Journal of Fisheries and Aquatic Studies* **1**, 151–156 (2014).
183. Van Stappen, G. Introduction, biology and ecology of Artemia. in *Manual on the production and use of live food for aquaculture* vol. 361 79–106 (FAO, 1996).
184. Criel, G. & Macrae, T. H. Reproductive Biology of Artemia. in *In: Abatzopoulos T.J., Beardmore J.A., Clegg J.S., Sorgeloos P. (eds) Artemia: Basic and Applied Biology* vol. 1 39–128 (Springer, Dordrecht, 2002).
185. Lavens, P. & Sorgeloos, P. The cryptobiotic state of Artemia cysts, its diapause deactivation and hatching: a review. in *Artemia Research and its Applications* vol. 3 556 (Universa Press, Wetteren, Belgium., 1987).
186. Sorgeloos, P., Lavens, P., Léger, P., Tackaert, W. & Versichele, D. Manual for the culture and use of brine shrimp Artemia in aquaculture. *Belgium, Artemia Reference Center, Faculty of Agriculture, State University Ghent*, 319 (1986).
187. Vanhaecke, P., Tackaert, W. & Sorgeloos, P. *The biogeography of Artemia: an updated review. Artemia research and its applications, Vol. 1. Morphology, genetics, strain characterization, toxicology*. (Universa Press, Wetteren, Belgium, 1987).
188. Gajardo, G. M. & Beardmore, J. A. Electrophoretic evidence suggests that the Artemia found in the Salar de Atacama, Chile, is A. franciscana Kellogg | SpringerLink. *Hydrobiologia* **257**, 65–71 (1993).
189. Freires, I. A., Sardi, J. de C. O., de Castro, R. D. & Rosalen, P. L. Alternative Animal and Non-Animal Models for Drug Discovery and Development: Bonus or Burden? *Pharm Res* **34**, 681–686 (2017).
190. Low, C. F. & Chong, C. M. Peculiarities of innate immune memory in crustaceans. *Fish Shellfish Immunol* **104**, 605–612 (2020).

191. Lenormand, T. *et al.* Resurrection ecology in Artemia. *Evol Appl* **11**, 76–87 (2018).
192. Persoone, G. & Wells, P. G. Artemia in aquatic toxicology: a review. *Artemia research and its applications* **1**, 259–275 (1987).
193. Soto-Jiménez, M. F. *et al.* Biological responses of a simulated marine food chain to lead addition. *Environmental Toxicology and Chemistry* **30**, 1611–1617 (2011).
194. Nunes, B. S., Carvalho, F. D., Guilhermino, L. M. & Van Stappen, G. Use of the genus Artemia in ecotoxicity testing. *Environ. Pollut.* **144**, 453–462 (2006).
195. Mackie, J. A. & Geller, J. Experimental parameters affecting quantitative PCR of Artemia franciscana: a model for a marine zooplanktonic target in natural plankton samples. *Limnology and Oceanography: Methods* **8**, 337–347 (2010).
196. Rodd, A. L. *et al.* Effects of surface-engineered nanoparticle-based dispersants for marine oil spills on the model organism Artemia franciscana. *Environ. Sci. Technol.* **48**, 6419–6427 (2014).
197. Libralato, G., Prato, E., Migliore, L., Cicero, A. M. & Manfra, L. A review of toxicity testing protocols and endpoints with Artemia spp. *Ecological Indicators* **69**, 35–49 (2016).
198. Xu, X. *et al.* Toxic Assessment of Triclosan and Triclocarban on Artemia salina. *Bull Environ Contam Toxicol* **95**, 728–733 (2015).
199. Migliore, L., Civitareale, C., Brambilla, G. & Delupis, G. D. D. Toxicity of several important agricultural antibiotics to Artemia. *Water Research* **31**, 1801–1806 (1997).
200. Beattie, K. A. *et al.* Comparative effects and metabolism of two microcystins and nodularin in the brine shrimp Artemia salina. *Aquat. Toxicol.* **62**, 219–226 (2003).
201. Cavion, F. *et al.* Ecotoxicological impact of graphene oxide: toxic effects on the model organism Artemia franciscana. *Environmental Science: Nano* **7**, 3605–3615 (2020).
202. Venkateswara Rao, J., Kavitha, P., Jakka, N. M., Sridhar, V. & Usman, P. K. Toxicity of organophosphates on morphology and locomotor behavior in brine shrimp, Artemia salina. *Arch Environ Contam Toxicol* **53**, 227–232 (2007).
203. Brix, K. V., Cardwell, R. D. & Adams, W. J. Chronic toxicity of arsenic to the Great Salt Lake brine shrimp, Artemia franciscana. *Ecotoxicol Environ Saf* **54**, 169–175 (2003).
204. Manfra, L., Savorelli, F., Pisapia, M., Magaletti, E. & Cicero, A. M. Long-term lethal toxicity test with the crustacean Artemia franciscana. *J Vis Exp* e3790 10.3791/3790 (2012).
205. Pane, L., Chiara, A., Giacco, E., Alessandra, S. & Mariottini, G. Utilization of Marine Crustaceans as Study Models: A New Approach in Marine Ecotoxicology for European (REACH) Regulation. in *Ecotoxicology* vol. 5 (2012).
206. Guerrini, F. *et al.* Comparative growth and toxin profile of cultured Ostreopsis ovata from the Tyrrhenian and Adriatic Seas. *Toxicon* **55**, 211–220 (2010).

207. Accoroni, S. *et al.* Ostreopsis cf. ovata bloom in the northern Adriatic Sea during summer 2009: ecology, molecular characterization and toxin profile. *Mar. Pollut. Bull.* **62**, 2512–2519 (2011).

208. Ninčević Gladan, Ž. *et al.* Massive Occurrence of the Harmful Benthic Dinoflagellate Ostreopsis cf. ovata in the Eastern Adriatic Sea. *Toxins (Basel)* **11**, 300 (2019).

209. Brissard, C. *et al.* Complex Toxin Profile of French Mediterranean Ostreopsis cf. ovata Strains, Seafood Accumulation and Ovatoxins Prepurification. *Mar Drugs* **12**, 2851-2876 (2014).

210. Casabianca, S. *et al.* Quantification of the Toxic Dinoflagellate Ostreopsis spp. by qPCR Assay in Marine Aerosol. *Environ. Sci. Technol.* **47**, 3788–3795 (2013).

211. Dahlmann, J., Budakowski, W. R. & Luckas, B. Liquid chromatography–electrospray ionisation-mass spectrometry based method for the simultaneous determination of algal and cyanobacterial toxins in phytoplankton from marine waters and lakes followed by tentative structural elucidation of microcystins. *Journal of Chromatography A* **994**, 45–57 (2003).

212. Leonardo, S. *et al.* Self-assembled monolayer-based immunoassays for okadaic acid detection in seawater as monitoring tools. *Marine Environmental Research* **133**, 6–14 (2018).

213. Contreras, H. R. & García, C. Inter-species variability of okadaic acid group toxicity in relation to the content of fatty acids detected in different marine vectors. *Food Additives & Contaminants: Part A* **36**, 464–482 (2019).

214. Liu, Y. *et al.* Sediment as a Potential Pool for Lipophilic Marine Phycotoxins with the Case Study of Daya Bay of China. *Mar Drugs* **17**, 623 (2019).

215. Giménez-Campillo, C. *et al.* Determination of Cyanotoxins and Phycotoxins in Seawater and Algae-Based Food Supplements Using Ionic Liquids and Liquid Chromatography with Time-Of-Flight Mass Spectrometry. *Toxins (Basel)* **11**, 610 (2019).

216. He, X. *et al.* Occurrence, distribution, source, and influencing factors of lipophilic marine algal toxins in Laizhou Bay, Bohai Sea, China. *Mar Pollut Bull* **150**, 110789 (2020).

217. He, X. *et al.* Distribution Characteristics and Environmental Control Factors of Lipophilic Marine Algal Toxins in Changjiang Estuary and the Adjacent East China Sea. *Toxins (Basel)* **11**, E596 (2019).

218. Wu, D. *et al.* Distribution, partitioning, and seasonal variation of lipophilic marine algal toxins in aquatic environments of a typical semi-closed mariculture bay. *Environ Pollut* **255**, 113299 (2019).

219. Zulkifli, S. Z., Aziz, F. Z. A., Ajis, S. Z. M. & Ismail, A. Nauplii of Brine Shrimp (Artemia salina) as a Potential Toxicity Testing Organism for Heavy Metals Contamination. in *From Sources to Solution* (eds. Aris, A. Z., Tengku Ismail, T. H., Harun,

R., Abdullah, A. M. & Ishak, M. Y.) 233–237 (Springer, 2014). doi:10.1007/978-981-4560-70-2_43.

220. Zhu, S., Luo, F., Chen, W., Zhu, B. & Wang, G. Toxicity evaluation of graphene oxide on cysts and three larval stages of Artemia salina. *Sci. Total Environ.* **595**, 101–109 (2017).

221. Brandt, R. & Keston, A. S. Synthesis of diacetyldichlorofluorescin: A stable reagent for fluorometric analysis. *Analytical Biochemistry* **11**, 6–9 (1965).

222. Gomes, A., Fernandes, E. & Lima, J. L. F. C. Fluorescence probes used for detection of reactive oxygen species. *Journal of Biochemical and Biophysical Methods* **65**, 45–80 (2005).

223. LeBel, C. P., Ischiropoulos, H. & Bondy, S. C. Evaluation of the probe 2′,7′-dichlorofluorescin as an indicator of reactive oxygen species formation and oxidative stress. *Chemical research in toxicology* **5**, 227–231 (1992).

224. Boyland, E. & Chasseaud, L. F. The Role of Glutathione and Glutathione S-Transferases in Mercapturic Acid Biosynthesis. in *Advances in Enzymology - and Related Areas of Molecular Biology* (ed. Nord, F. F.) 173–219 (John Wiley & Sons, Inc., 2006). doi:10.1002/9780470122778.ch5.

225. Zhao, Z., Tepperman, K., Dorsey, J. G. & Elder, R. C. Determination of cisplatin and some possible metabolites by ion-pairing chromatography with inductively coupled plasma mass spectrometric detection. *Journal of Chromatography B: Biomedical Sciences and Applications* **615**, 83–89 (1993).

226. Habig, W. H., Pabst, M. J. & Jakoby, W. B. Glutathione S-Transferases: THE FIRST ENZYMATIC STEP IN MERCAPTURIC ACID FORMATION. *Journal of Biological Chemistry* **249**, 7130–7139 (1974).

227. Vehovszky, A., Szabó, H., Acs, A., Gyori, J. & Farkas, A. Effects of rotenone and other mitochondrial complex I inhibitors on the brine shrimp Artemia. *Acta. Biol. Hung.* **61**, 401–410 (2010).

228. Wang, Y., Branicky, R., Noe, A. & Hekimi, S. Superoxide dismutases: Dual roles in controlling ROS damage and regulating ROS signaling | Journal of Cell Biology | Rockefeller University Press. *J Cell Biol* **217**, 1915–1928 (2017).

229. Zhao, S., Wang, Y. & Duo, L. Biochemical toxicity, lysosomal membrane stability and DNA damage induced by graphene oxide in earthworms. *Environ Pollut* **269**, 116225 (2021).

230. Zhang, J., Chen, R., Yu, Z. & Xue, L. Superoxide Dismutase (SOD) and Catalase (CAT) Activity Assay Protocols for Caenorhabditis elegans. *Bio-protocol* **7**, e2505–e2505 (2017).

231. Chelikani, P., Fita, I. & Loewen, P. C. Diversity of structures and properties among catalases. *Cell Mol Life Sci* **61**, 192–208 (2004).

232. Wilson, I. B. Mechanism of enzymic hydrolysis. I. Role of the acidic group in the esteratic site of acetylcholinesterase. *Biochim Biophys Acta* **7**, 466–470 (1951).
233. Badawy, M. E. I. & El-Aswad, A. F. Bioactive Paper Sensor Based on the Acetylcholinesterase for the Rapid Detection of Organophosphate and Carbamate Pesticides. *International Journal of Analytical Chemistry* **2014**, e536823 (2014).
234. Jemec, A. *et al.* Biochemical biomarkers in chronically metal-stressed daphnids. *Comp. Biochem. Physiol. C Toxicol. Pharmacol.* **147**, 61–68 (2008).
235. Granéli, E., Vidyarathna, N. K., Funari, E., Cumaranatunga, P. R. T. & Scenati, R. Can increases in temperature stimulate blooms of the toxic benthic dinoflagellate Ostreopsis ovata? *Harmful Algae* **10**, 165–172 (2011).
236. Larsson, M. E., Laczka, O. F., Suthers, I. M., Ajani, P. A. & Doblin, M. A. Hitchhiking in the East Australian Current: rafting as a dispersal mechanism for harmful epibenthic dinoflagellates. *Marine Ecology Progress Series* **596**, 49–60 (2018).
237. Casabianca, S. *et al.* Plastic-associated harmful microalgal assemblages in marine environment. *Environ. Pollut.* **244**, 617–626 (2019).
238. Masó, M., Garcés, E., Pagès, F. & Camp, J. Drifting plastic debris as a potential vector for dispersing Harmful Algal Bloom (HAB) species. *Scientia Marina* **67**, 107–111 (2003).
239. Papadopoulos, A. I., Lazaridou, E., Mauridou, G. & Touraki, M. Glutathione S-transferase in the branchiopod Artemia salina. *Marine Biology* **144**, 295–301 (2004).
240. Livingstone, D. R. Organic Xenobiotic Metabolism in Marine Invertebrates. in *Advances in Comparative and Environmental Physiology: Volume 7* (eds. Houlihan, D. F., Livingstone, D. R. & Lee, R. F.) 45–185 (Springer, 1991). doi:10.1007/978-3-642-75897-3_2.
241. Barata, C. *et al.* Changes in antioxidant enzyme activities, fatty acid composition and lipid peroxidation in Daphnia magna during the aging process. *Comp Biochem Physiol B Biochem Mol Biol* **140**, 81–90 (2005).
242. Pelin, M. *et al.* Effects of the marine toxin palytoxin on human skin keratinocytes: Role of ionic imbalance. *Toxicology* **282**, 30–38 (2011).
243. Pelin, M. *et al.* Oxidative stress induced by palytoxin in human keratinocytes is mediated by a H+-dependent mitochondrial pathway. *Toxicology and Applied Pharmacology* **266**, 1–8 (2013).
244. Schieber, M. & Chandel, N. S. ROS Function in Redox Signaling and Oxidative Stress. *Current Biology* **24**, R453–R462 (2014).
245. Ott, M., Gogvadze, V., Orrenius, S. & Zhivotovsky, B. Mitochondria, oxidative stress and cell death. *Apoptosis* **12**, 913–922 (2007).
246. Olsen, T., Ellerbeck, L., Fisher, T., Callaghan, A. & Crane, M. Variability in acetylcholinesterase and glutathione S-transferase activities in Chironomus riparius

Meigen deployed in situ at uncontaminated field sites. *Environ. Toxicol. Chem.* **20**, 1725-1732 (2001).
247. Ajuzie, C. C. Palatability and fatality of the dinoflagellate Prorocentrum lima to Artemia salina. *J Appl Phycol* **19**, 513–519 (2007).
248. Gong, Y. *et al.* Molecular mechanisms of zooplanktonic toxicity in the okadaic acid-producing dinoflagellate Prorocentrum lima. *Environ Pollut* **279**, 116942 (2021).
249. Koukaras, K., Baxevanis, A., Vasdekis, C., Abatzopoulos, T. J. & Nikolaidis, G. Detection of Dinophysis cells toxicity by using parthenogenetic and clonal Artemia. in Steidinger, K. A., J. H. Landsberg, C. R. Tomas, and G. A. Vargo (Eds.), (2004).
250. Zhang, Y. T. *et al.* Comparison of Short-Term Toxicity of 14 Common Phycotoxins (Alone and in Combination) To The Survival of Brine Shrimp Artemia Salina. *Ecotoxicology* **A preprint**, (2021).
251. Aune, T. *et al.* Relative toxicity of dinophysistoxin-2 (DTX-2) compared with okadaic acid, based on acute intraperitoneal toxicity in mice. *Toxicon* **49**, 1–7 (2007).
252. Huhn, J. *et al.* A structural basis for the reduced toxicity of dinophysistoxin-2. *Chem Res Toxicol* **22**, 1782–1786 (2009).
253. Chen, J. *et al.* Occurrence and distribution of marine natural organic pollutants: Lipophilic marine algal toxins in the Yellow Sea and the Bohai Sea, China. *Sci Total Environ* **612**, 931–939 (2018).
254. Wang, J. *et al.* Simple determination of six groups of lipophilic marine algal toxins in seawater by automated on-line solid phase extraction coupled to liquid chromatography-tandem mass spectrometry - PubMed. *Chemosphere* **262**, 128374 (2021).
255. Kavyasudha, C. *et al.* Clinical Applications of Induced Pluripotent Stem Cells - Stato Attuale. *Adv Exp Med Biol* **1079**, 127–149 (2018).
256. Kim, T.-W., Che, J.-H. & Yun, J.-W. Use of stem cells as alternative methods to animal experimentation in predictive toxicology. *Regul Toxicol Pharmacol* **105**, 15–29 (2019).
257. Takahashi, K. & Yamanaka, S. Induction of pluripotent stem cells from mouse embryonic and adult fibroblast cultures by defined factors. *Cell* **126**, 663–676 (2006).
258. Masui, S. *et al.* Pluripotency governed by Sox2 via regulation of Oct3/4 expression in mouse embryonic stem cells. *Nat Cell Biol* **9**, 625–635 (2007).
259. Niwa, H., Ogawa, K., Shimosato, D. & Adachi, K. A parallel circuit of LIF signalling pathways maintains pluripotency of mouse ES cells. *Nature* **460**, 118–122 (2009).
260. Yoshida, Y. & Yamanaka, S. Induced Pluripotent Stem Cells 10 Years Later: For Cardiac Applications. *Circ Res* **120**, 1958–1968 (2017).
261. Zakrzewski, W., Dobrzyński, M., Szymonowicz, M. & Rybak, Z. Stem cells: past, present, and future. *Stem Cell Res Ther* **10**, 68 (2019).

262. Genova, E. *et al.* Induced pluripotent stem cells for therapy personalization in pediatric patients: Focus on drug-induced adverse events. *World J Stem Cells* **11**, 1020–1044 (2019).
263. Hoffman, G. E., Schrode, N., Flaherty, E. & Brennand, K. J. New considerations for hiPSC-based models of neuropsychiatric disorders. *Mol Psychiatry* **24**, 49–66 (2019).
264. Hawkins, K., Joy, S. & McKay, T. Cell signalling pathways underlying induced pluripotent stem cell reprogramming. *World J Stem Cells* **6**, 620–628 (2014).
265. Armstrong, L. *et al.* Human induced pluripotent stem cell lines show stress defense mechanisms and mitochondrial regulation similar to those of human embryonic stem cells. *Stem Cells* **28**, 661–673 (2010).
266. Chin, M. H. *et al.* Induced pluripotent stem cells and embryonic stem cells are distinguished by gene expression signatures. *Cell Stem Cell* **5**, 111–123 (2009).
267. Deng, J. *et al.* Targeted bisulfite sequencing reveals changes in DNA methylation associated with nuclear reprogramming. *Nat Biotechnol* **27**, 353–360 (2009).
268. Puri, M. C. & Nagy, A. Concise review: Embryonic stem cells versus induced pluripotent stem cells: the game is on. *Stem Cells* **30**, 10–14 (2012).
269. Stadtfeld, M. & Hochedlinger, K. Induced pluripotency: history, mechanisms, and applications. *Genes Dev* **24**, 2239–2263 (2010).
270. Dimos, J. T. *et al.* Induced pluripotent stem cells generated from patients with ALS can be differentiated into motor neurons. *Science* **321**, 1218–1221 (2008).
271. Byers, B., Lee, H. & Reijo Pera, R. Modeling Parkinson's disease using induced pluripotent stem cells. *Curr Neurol Neurosci Rep* **12**, 237–242 (2012).
272. Ferreira, L. M. R. & Mostajo-Radji, M. A. How induced pluripotent stem cells are redefining personalized medicine. *Gene* **520**, 1–6 (2013).
273. Chun, Y. S., Byun, K. & Lee, B. Induced pluripotent stem cells and personalized medicine: current progress and future perspectives. *Anat Cell Biol* **44**, 245–255 (2011).
274. Liu, W., Deng, Y., Liu, Y., Gong, W. & Deng, W. Stem cell models for drug discovery and toxicology studies. *J Biochem Mol Toxicol* **27**, 17–27 (2013).
275. Phillips, B. W. & Crook, J. M. Pluripotent human stem cells: A novel tool in drug discovery. *BioDrugs* **24**, 99–108 (2010).
276. Estevan, C., Romero, A. C., Pamies, D., Vilanova, E. & Sogorb, M. A. Embryonic Stem Cells in Toxicological Studies. in *Embryonic Stem Cells Basic- Biology to Bioengineering* 492 (IntechOpen, 2011).
277. Moore, K., Persaud, T. V. N. & Torchia, M. *The Developing Human- Clinically Oriented Embryology*. (ELSEVIER, 2018).
278. Ghimire, S., Mantziou, V., Moris, N. & Martinez Arias, A. Human gastrulation: The embryo and its models. *Dev Biol* **474**, 100–108 (2021).

279. Serio, R. N. & Gudas, L. J. Modification of stem cell states by alcohol and acetaldehyde - PubMed. *Chem Biol Interact.* **316**, 108919 (2019).
280. Tachikawa, S., Nishimura, T., Nakauchi, H. & Ohnuma, K. Thalidomide induces apoptosis in undifferentiated human induced pluripotent stem cells. *In Vitro Cell. Dev. Biol. Anim.* **53**, 841–851 (2017).
281. Davidsen, N., Rosenmai, A. K., Lauschke, K., Svingen, T. & Vinggaard, AM. Developmental effects of PFOS, PFOA and GenX in a 3D human induced pluripotent stem cell differentiation model. *Chemosphere* **279**, 130624 (2021).
282. Adler, S., Lindqvist, J., Uddenberg, K., Hyllner, J. & Strehl, R. Testing potential developmental toxicants with a cytotoxicity assay based on human embryonic stem cells. *Altern Lab Anim* **36**, 129–140 (2008).
283. Hübner, D. *et al.* Infection of iPSC Lines with Miscarriage-Associated Coxsackievirus and Measles Virus and Teratogenic Rubella Virus as a Model for Viral Impairment of Early Human Embryogenesis. *ACS Infect Dis* **3**, 886–897 (2017).
284. Claus, C., Jung, M. & Hübschen, J. M. Pluripotent Stem Cell-Based Models: A Peephole into Virus Infections during Early Pregnancy. *Cells* **9**, E542 (2020).
285. Aikawa, N. A novel screening test to predict the developmental toxicity of drugs using human induced pluripotent stem cells. *J Toxicol Sci* **45**, 187–199 (2020).
286. Luz, A. L. & Tokar, E. J. Pluripotent Stem Cells in Developmental Toxicity Testing: A Review of Methodological Advances. *Toxicol Sci* **165**, 31–39 (2018).
287. Fan, Y. *et al.* Generation of human blastocyst-like structures from pluripotent stem cells. *Cell Discov* **7**, 1–14 (2021).
288. Sozen, B. *et al.* Reconstructing aspects of human embryogenesis with pluripotent stem cells. *Nat Commun* **12**, 5550 (2021).
289. Boukamp, P. *et al.* Normal keratinization in a spontaneously immortalized aneuploid human keratinocyte cell line. *J Cell Biol* **106**, 761–771 (1988).
290. Riss, T. L. *et al.* Cell Viability Assays. in *Assay Guidance Manual* (eds. Markossian, S. et al.) (Eli Lilly & Company and the National Center for Advancing Translational Sciences, 2004).
291. Mosmann, T. Rapid colorimetric assay for cellular growth and survival: application to proliferation and cytotoxicity assays. *J Immunol Methods* **65**, 55–63 (1983).
292. Pelin, M. *et al.* A Novel Sensitive Cell-Based Immunoenzymatic Assay for Palytoxin Quantitation in Mussels. *Toxins (Basel)* **10**, E329 (2018).
293. Pelin, M. *et al.* Characterization of palytoxin binding to HaCaT cells using a monoclonal anti-palytoxin antibody. *Mar Drugs* **11**, 584–598 (2013).
294. TRIzol Reagent, USER GUIDE by Invitrogen (https://tools.thermofisher.com/content/sfs/manuals/trizol_reagent.pdf).

295. Interpretation of Nucleic Acid 260/280 (T123-TECHICAL BULLET) by Thermo SCIENTIFIC (http://tools.thermofisher.com/content/sfs/brochures/T123-NanoDrop-Lite-Interpretation-of-Nucleic-Acid-260-280-Ratios.pdf).
296. NanoDrop (T042-TECHNICAL BULLET) by Thermo SCIENTIFIC (http://hpc.ilri.cgiar.org/beca/training/IMBB_2015/lectures/NanoDrop.pdf).
297. High-Capacity RNA-to-cDNA™ Kit by appliedbiosystems, Thermofisher SCIENTIFIC (https://tools.thermofisher.com/content/sfs/manuals/cms_047249.pdf).
298. Kubista, M. *et al.* The real-time polymerase chain reaction. *Mol Aspects Med* **27**, 95-125 (2006).
299. Pelin, M., Stocco, G., Florio, C., Sosa, S. & Tubaro, A. In Vitro Cell Sensitivity to Palytoxin Correlates with High Gene Expression of the Na+/K+-ATPase β2 Subunit Isoform. *Int J Mol Sci* **21**, E5833 (2020).
300. Hauck, C. *et al.* Isoform specificity of cardiac glycosides binding to human Na+,K+-ATPase alpha1beta1, alpha2beta1 and alpha3beta1. *Eur J Pharmacol* **622**, 7–14 (2009).
301. Katz, A. *et al.* Selectivity of digitalis glycosides for isoforms of human Na,K-ATPase. *J Biol Chem* **285**, 19582–19592 (2010).
302. Cherniavsky Lev, M., Karlish, S. J. D. & Garty, H. Cardiac glycosides induced toxicity in human cells expressing α1-, α2-, or α3-isoforms of Na-K-ATPase. *Am J Physiol Cell Physiol* **309**, C126-135 (2015).

Appendices

Appendix A

Effects of EtOH (PLTX solvent, 0.25-15.00%) on *Artemia franciscana* cysts hatching after 96 h of exposure (A), viability of nauplii Instar I (B) and adults (C) after 8, 24, 48 and 72 h of exposure. Red arrows indicate the concentration of EtOH (0.5%) used during the exposure to PLTX and used as a negative control.

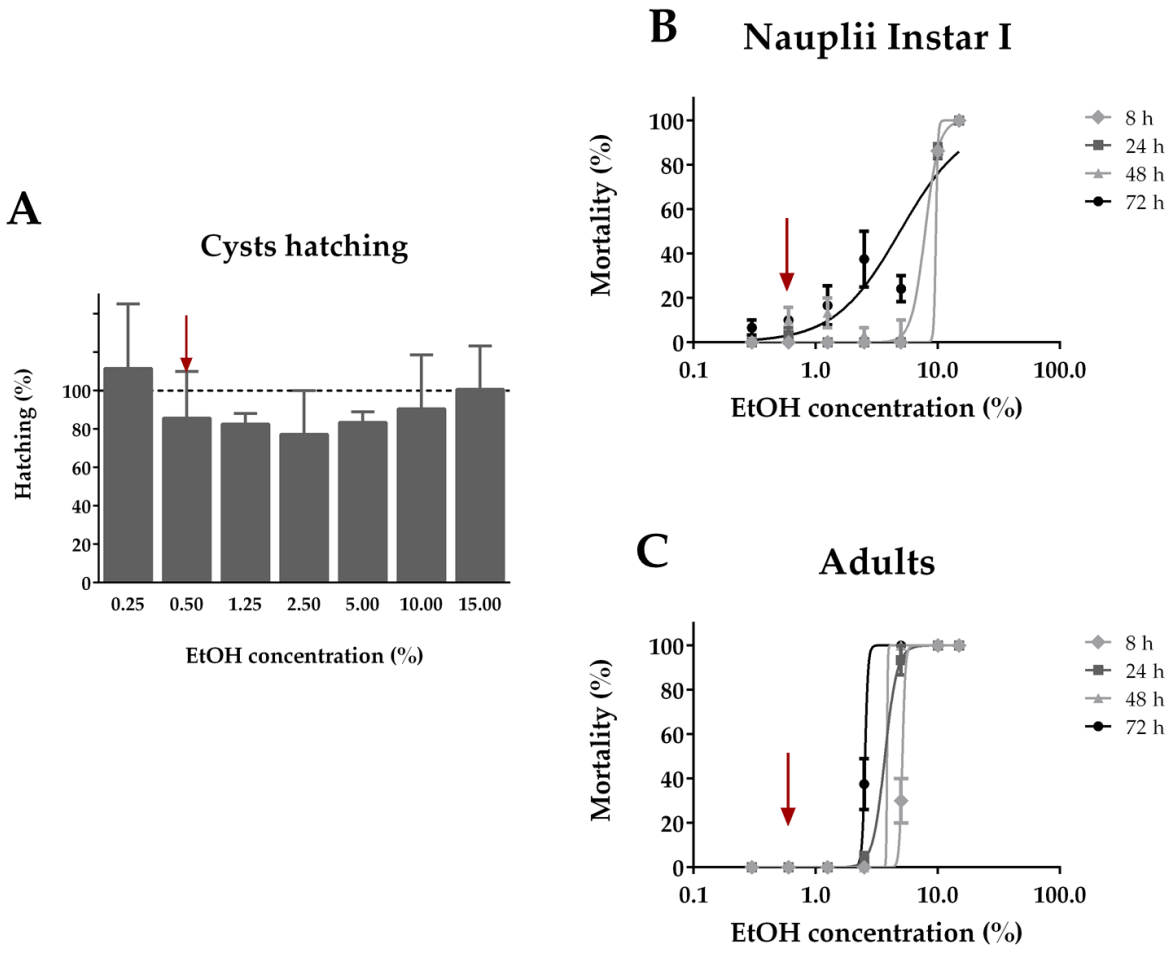

Appendix B

Effects of MeOH (OA and DTXs solvent, 0.07-25.00%) on *Artemia franciscana* cysts hatching after 96 h of exposure (A), viability of nauplii Instar I (B) and adults (C) after 24, 48 and 72 h of exposure. Red arrows indicate the concentration of MeOH used during the exposure to OA and DTXs (0.1%) and used as a negative control.

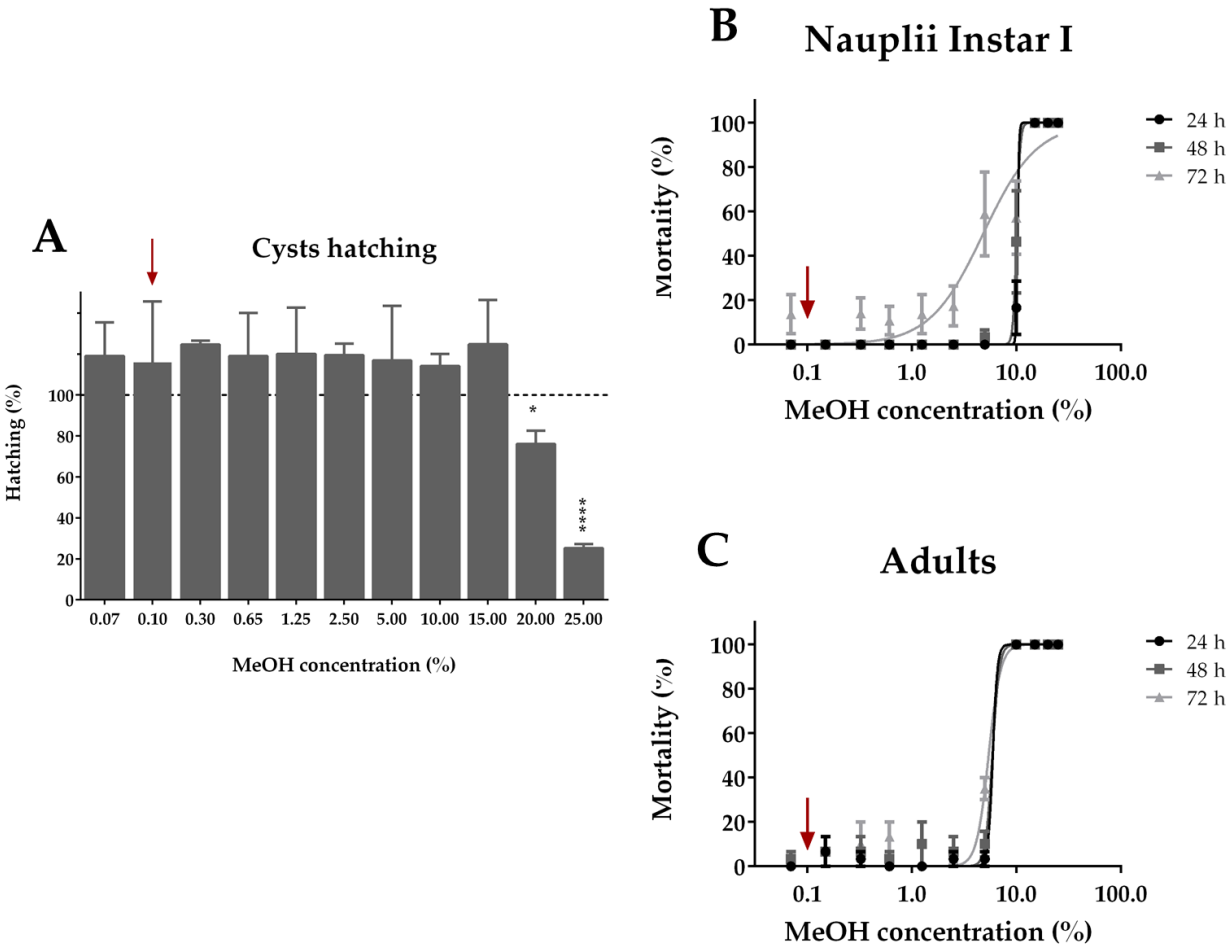

Appendix C

Characteristics of the primer used for the gene expression analysis of the Na^+/K^+ ATPase isoform.

Gene	Primer	Sequence of primer 5′→3′	Amplicon lenght (pb)
ACTB (housekeeping)	forward	GACGACATGGAGAAAATCTG	131
	reverse	ATGATCTGGGTCATCTTCTC	
A1	forward	GTGTCTTTCTTCATCCTTTCTC	184
	reverse	CCACAGCTTCTAAGTTCTTC	
A2	forward	TCAAGAACATGGTACCTCAG	153
	reverse	TACAGCCATGAGAAGAGATG	
A3	forward	ATCTGCTCAGATAAGACAGG	175
	reverse	AACTCTTGTCAAATGAGGTC	
A4	forward	TCCCTACAGTATTCTCATCTTC	193
	reverse	CTAGTGTCTCAGATGTTGTG	
B1	forward	AAAGTACAAAGATTCAGCCC	95
	reverse	CATGATTAAAGTCTCCTCGTTC	
B2	forward	CTCATGTACTTCCCCTACTATG	116
	reverse	ATGCGACATTCTACATTCAC	
B3	forward	GCCAAGGATAGATTGTGTTTC	185
	reverse	CTGTTACTTCTTTCCCAGTG	

Appendix D

Characteristics of the primer used for the gene expression analysis of genes marker of stemness and the differentiation in the three germ layers.

	Gene	Primer	Sequence of primer 5′→3′	Amplicon lenght (pb)
houskeeping	*ACTB*	forward	GACGACATGGAGAAAATCTG	131
		reverse	ATGATCTGGGTCATCTTCTC	
Marker of stemness	*SOX2*	forward	ATAATAACAATCATCGGCGG	90
		reverse	AAAAAGAGAGAGGCAAACTG	
	OCT4	forward	GATCACCCTGGGATATACAC	198
		reverse	GCTTTGCATATCTCCTGAAG	
	KLF4	forward	TCTTGAGGAAGTGCTGAG	147
		reverse	ATGAGCTCTTGGTAATGGAG	
	NANOG	forward	CCAGAACCAGAGAATGAAATC	120
		reverse	TGGTGGTAGGAAGAGTAAAG	
	C-MYC	forward	TGAGGAGGAACAAGAAGATG	86
		reverse	ATCCAGACTCTGACCTTTTG	
Marker of ectoderm	*PAX6*	forward	AGAGAATACCAACTCCATCAG	152
		reverse	GATAATGGGTTCTCTCAAACTC	
	SOX1	forward	TGCTTGTTCTGTTAACTCAC	100
		reverse	AAAGAACCTCAGAGAGAGTC	
Marker of endoderm	*FOXA2*	forward	CGAGTTAAAGTATGCTGGG	143
		reverse	CATGTACGTGTTCATGCC	
	SOX17	forward	ATCTCTTTACACTCCTCGAC	92
		reverse	CCTTTATCTTAAACCCAGCG	
	AFP	forward	GATCCCACTTTTCCAAGTTC	79
		reverse	TTTGTTCATGAATGTCTCCC	
Marker of mesoderm	*ACTA2*	forward	AGATCAAGATCATTGCCCC	116
		reverse	TTCATCGTATTCCTGTTTGC	
	BRACHYURY	forward	GAATCCACATAGTGAGAGTTG	169
		reverse	TCACTTCTTTCCTTTGCATC	
	CXCR4	forward	AACTTCAGTTTGTTGGCTG	120
		reverse	GTGTATATACTGATCCCCTCC	

Appendix E

Summary of the differentiation kit protocol

	plate	Day 0 (iPSC seeding)	Day 1	Day 2	Day 3	Day 4	Day 5	Day 6
Endoderm	6-well plate	600 000 cells/well in 2 mL of iPSC medium	X	2 mL of TC StemMACS EndoDiff Medium after washing with 4 mL of PBS-Ca^{2+}/Mg^{2+}	2 mL of TC StemMACS EndoDiff Medium after washing with 4 mL of PBS-Ca^{2+}/Mg^{2+}	2 mL of TC StemMACS EndoDiff Medium after washing with 4 mL of PBS-Ca^{2+}/Mg^{2+}	2 mL of TC StemMACS EndoDiff Medium after washing with 4 mL of PBS-Ca^{2+}/Mg^{2+}	2 mL of TC StemMACS EndoDiff Medium after washing with 4 mL of PBS-Ca^{2+}/Mg^{2+}
	96-well plate	20 000 cells/well in 100 µL of iPSC medium	X	100 µL of TC StemMACS EndoDiff Medium after washing with 200 µL di PBS-Ca^{2+}/Mg^{2+}	100 µL of TC StemMACS EndoDiff Medium after washing with 200 µL di PBS-Ca^{2+}/Mg^{2+}	100 µL of TC StemMACS EndoDiff Medium after washing with 200 µL di PBS-Ca^{2+}/Mg^{2+}	100 µL of TC StemMACS EndoDiff Medium after washing with 200 µL di PBS-Ca^{2+}/Mg^{2+}	100 µL of TC StemMACS EndoDiff Medium after washing with 200 µL di PBS-Ca^{2+}/Mg^{2+}
Mesoderm	6 well plate	380 000 cells/well in 2 mL of iPSC medium	6 mL of TC StemMACS MesoDiff Medium I	X	X	4 mL of TC StemMACS MesoDiff Medium II	4 mL of TC StemMACS MesoDiff Medium II	4 mL of TC StemMACS MesoDiff Medium II
	96 well plate	12 000 cells/well in 100 µL of iPSC medium	300 µL of TC StemMACS MesoDiff Medium I	X	X	200 µL of TC StemMACS MesoDiff Medium II	200 µL of TC StemMACS MesoDiff Medium II	200 µL of TC StemMACS MesoDiff Medium II
Ectoderm	6-well plate	500 000 cells/well in 2 mL of TC StemMACS Trilineage EctoDiff Medium	2 mL of TC StemMACS Trilineage EctoDiff Medium	2 mL of TC StemMACS Trilineage EctoDiff Medium	2 mL of TC StemMACS Trilineage EctoDiff Medium	2 mL of TC StemMACS Trilineage EctoDiff Medium	2 mL of TC StemMACS Trilineage EctoDiff Medium	2 mL of TC StemMACS Trilineage EctoDiff Medium
	96-well plate	15 000 cells/well in 100 µL of TC StemMACS Trilineage EctoDiff Medium	100 µL of TC StemMACS Trilineage EctoDiff Medium	100 µL of TC StemMACS Trilineage EctoDiff Medium	100 µL of TC StemMACS Trilineage EctoDiff Medium	100 µL of TC StemMACS Trilineage EctoDiff Medium	100 µL of TC StemMACS Trilineage EctoDiff Medium	100 µL of TC StemMACS Trilineage EctoDiff Medium
iPSC (negative control)	6-well plate	15 000 cells/well in 2 mL of iPSC medium	2 mL of iPSC medium	X	X	2 mL of iPSC medium	X	X
	96-well plate	500 cells/well in 100 µL of iPSC medium	100 µL of iPSC medium	X	X	100 µL of iPSC medium	X	X